Controlled Release of Antimalarial Artemisone by Macromolecular Structures

DISSERTATION

zur Erlangung des akademischen Grades eines Doktors der
Naturwissenschaften (Dr. rer. nat.)
in der Bayreuther Graduiertenschule für Mathematik und
Naturwissenschaften (BayNAT)
der Universität Bayreuth

vorgelegt von

Amir Reza Bagheri

aus *Teheran, Iran*

Bayreuth, 2020

Die vorliegende Arbeit wurde von September 2013 bis Oktober 2017 am Lehrstuhl der Makromolekularen Chemie II (MCII) der Fakultät für Biologie, Chemie und Geowissenschaften an der Universität Bayreuth, unter der Betreuung von Professor Dr. Andreas Greiner angefertigt.

Vollständiger Abdruck der von der Bayreuther Graduiertenschule für Mathematik und Naturwissenschaften (BayNAT) der Universität Bayreuth genehmigten Dissertation zur Erlangung des akademischen Grades eines Doktors der Naturwissenschaften (Dr. rer. nat.).

Dissertation eingereicht am: 21.10.2020

Zulassung durch das Leitungsgremium: 18.11.2020

Wissenschaftliches Kolloquium: 30.06.2021

Amtierender Direktor: Prof. Dr. Markus Lippitz

Prüfungsausschuss:

Prof. Dr. Andreas Greiner	(Gutachter)
Prof. Dr. Ruth Freitag	(Gutachterin)
Prof. Dr. Matthias Breuning	(Vorsitz)
Prof. Dr. Birgit Weber	

Our greatest weakness lies in giving up. The most certain way to succeed is always to try just one more time.

Thomas A. Edison

List of Publications

Parts of this work were previously published:

1. <u>A. R. Bagheri</u>, J. Golenser, A. Greiner, Controlled and Manageable Release of Antimalarial Artemisone by Encapsulation in Biodegradable Carriers, *European Polymer Journal* **2020,** *129,* Article 109625.

2. <u>A. R. Bagheri</u>, S. Agarwal, J. Golenser, A. Greiner, Unlocking Nanocarriers for the Programmed Release of Antimalarial Drugs, *Global Challenges* **2017,** *1,* 1600011.

3. G. Duan, <u>A. R. Bagheri</u>, S. Jiang, J. Golenser, S. Agarwal, A. Greiner, Exploration of Macroporous Polymeric Sponges as Drug Carriers, *Biomacromolecules* **2017,** *18,* 3215.

4. J. Golenser, V. Buchholz, <u>A. R. Bagheri</u>, A. Nasereddin, R. Dzikowski, J. Guo, N. H. Hunt, S. Eyal, N. Vakruk, A. Greiner, *Parasites & Vectors* **2017,** *10,* 117.

5. <u>A. R. Bagheri</u>, C. Laforsch, A. Greiner, S. Agarwal, Fate of So-Called Biodegradable Polymers in Seawater and Freshwater, *Global Challenges* **2017,** *1,* 1700048.

Abbreviation

µl: microliters

µm: micrometers

3D: Three dimensional

ACTs: Artemisinins

ART: Artemisone

CM: Cerebral Malaria

CVD: Chemical vapor deposition:

DDS: Drug delivery carriers and systems

EDX: Energy-dispersive X-ray spectroscopy

FDA: (US) Food and Drug Administration

g: gram

GPC: Gel permeation chromatography

h: hour

HPLC: High-performance liquid chromatography

ml: milliliters

MPEG: α-methoxy-ω-hydroxy-poly (ethylene glycol)

NFN: nanofiber nonwovens

nm: nanometers

NMR: Nuclear magnetic resonance spectroscopy

ºC: Celsius grade

PCL: Polycaprolactone

PPX: Poly(p-xylylene)

RSD: relative standard deviation

SEM: Scanning electron microscopy

SLS: Sodium lauryl sulfate

Table of Contents

Chapter 1

Introduction and aim of the work

Controlled Release of Antimalarial Artemisone by Macromolecular Structures

1 Introduction and aim of the work

In this dissertation, different kinds of macromolecular structures have been considered as the carrier for the delivery of artemisone (ART) as an effective antimalarial substance. In different clinical studies, ART could demonstrate its effectiveness against P. falciparum successfully. One of the challenges in the practical use of artemisinins (ACTs) as hydrophobic drugs, is the dosage that should be optimal for efficacy and lack of toxicity. In all research works that have been reported in this thesis, different types of carriers could be applied to produce the programmed/controlled drug release systems, which could be a solution for maintaining the optimal dosage of ART for more extended periods. The time-dependent release of a drug with or without external stimuli is referred to as a controlled release in general literature.

In an ideal case, a delivery system should provide immediate initial therapeutic drug concentration (burst dose) and then maintain this concentration for an extended period (sustained dose) depending upon the requirement. Further, the rate of sustained release of therapeutic concentration should match the rate of the absorption by the body in order not to exceed the toxic level. This gets more complicated as physiological conditions, and therefore the rate of drug absorption varies from person to person. An ideal controlled release system for diseases like malaria should provide imminent release of one or more drugs, according to personal requirements. This should be independent of the environmental influence, in a reproducible manner, accessible and usable even under rural conditions, not requiring complicated technology, and also programmable according to the type and status of the infection.

In this thesis, different classifications of materials based on electrospun nanofibers, polymeric films, 3D structures, and particles could be successfully applied to carry the ART. Drug molecules could be efficiently immobilized in these materials, and the drug release from these carriers could be adequately studied. Effectively, the kinetics of the ART release from macromolecular carriers could be adjusted by modification of the carrier.

The primary target of this Ph.D. work was the establishment of not only a scientific study for delivery of an antimalarial but also a fundamental study to focus on the polymeric structures as the drug carrier with focusing on the advantage and disadvantage of each system for delivery of mainly hydrophobic drugs with low water solubility. Today, nanotechnology is considered as an exciting opportunity for the delivery of hydrophobic drugs which have low bioavailability.

Furthermore, the real application of such polymeric carrier in the real world was one of the main concerns. Therefore, besides the real in vivo experiments (implantation of ART loaded scaffolds in mice), we tried to introduce another administration route based on the setting up of a delivery system based on the infusion system. We suggest that the combination of the advantage of precise and reproducible programmed release from nanofiber nonwovens (NFN) in vitro with the drug delivery infusion system is very beneficial. In our system, the control over drug release is achieved outside the physiological environment by placing ART-loaded NFN in the drip chamber of an infusion system, which can flexibly release ART.

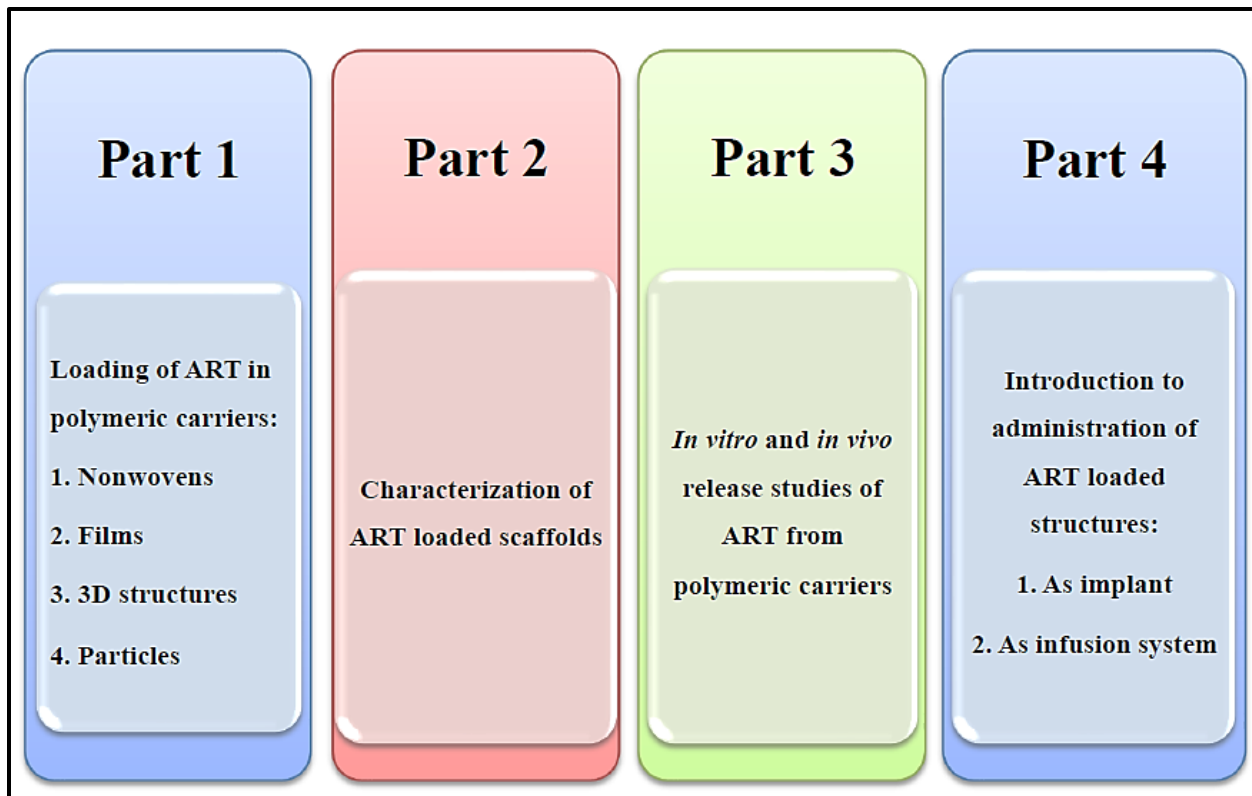| Part 1	Part 2	Part 3	Part 4
Loading of ART in polymeric carriers: 1. Nonwovens 2. Films 3. 3D structures 4. Particles	Characterization of ART loaded scaffolds	*In vitro* and *in vivo* release studies of ART from polymeric carriers	Introduction to administration of ART loaded structures: 1. As implant 2. As infusion system

Figure 1 The studied levels during this Ph.D. work

Chapter 2

Theoretical background

2 Theoretical background and overview of the literature

2.1 Drug delivery carriers and systems (DDS)

DDS are designed to consistently introduce therapeutic agents into the body at a required dose level and rate [1-5]. Maybe, one of the first attempts to set up the DDS was reported in the 1960s when Folkman circulated rabbit blood inside a silicone rubber and found out that if he opened the tubing to anesthetic gases on the outside, the rabbits would fall asleep. It was then offered that such short, sealed segments of such a system containing a drug could be placed and could become a constant rate drug delivery device [6]. Drug delivery systems can be fabricated to adjust the pharmaceutical parameters like the pharmacokinetics and the distribution of related medicines to the utility as the drug carriers [7]. The pharmacological characteristics of conventional medicines can be improved through the application of DDS. Drug delivery systems are supporting us in gaining the novel therapeutically curative ways for the successful treatment of diseases due to their benefits. The main advantages of DDS involve increasing drug solubility, reduction in toxicity, protection of the drug from rapid decomposition and degradation, and finally, reduction in side effects in patients, especially in non-target tissues. The controlled release systems or controlled drug delivery systems for different types of medicines have been widely fabricated due to their advantages. Among different classifications of the carriers, the polymeric (macromolecular) carriers play significant roles.
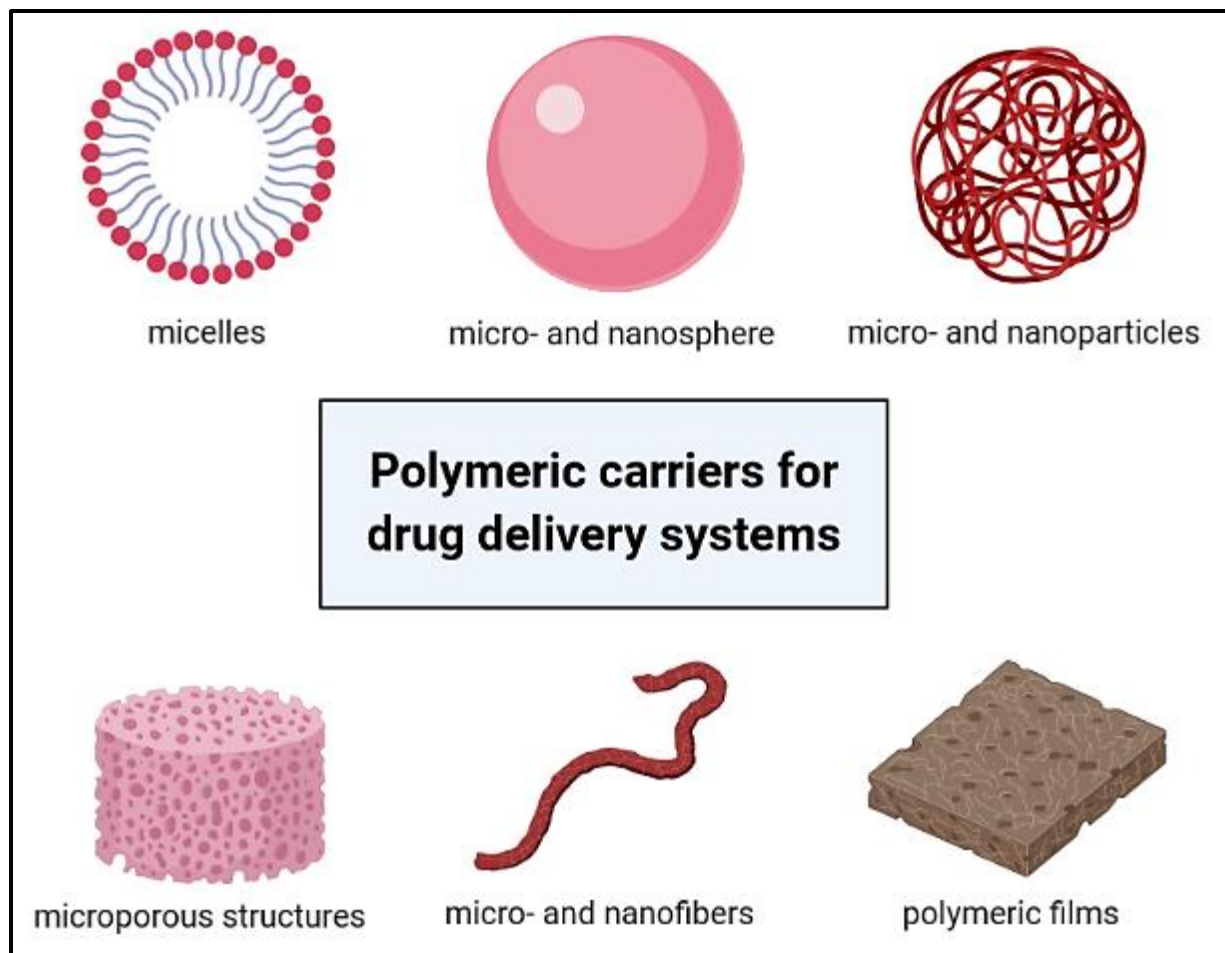
Figure 2 Different types of polymeric carriers used as delivery vehicles for targeted drug delivery

Various benefits of DDS compared to other methods of drug administration routes have been reported [8-9]. These advantages involve a reduction in the side effects of systemic administration by local administration from a controlled release system, improved drug administration in areas where proper medical supervision is not available, continuous release of small quantities of drug instead of harmful or toxic large doses, and improvement of patient compliance [10-11]. In order to reach these goals, several parameters should be considered in a controlled drug delivery system or a drug carrier;

such as the nature of delivery carrier materials, the drug properties, route of administration, mechanism of drug release, the ability of targeting, and biocompatibility (Fig. 3).

Figure 3 Stimuli-responsive targeted delivery of therapeutic agents; Schematic illustration of stimuli-responsive DDS [7] *[Permission: this is an open article distributed under the terms of the creative commons CC BY license, which permits unrestricted use, distribution, and reproduction in any medium, provided the original work is properly cited.]*
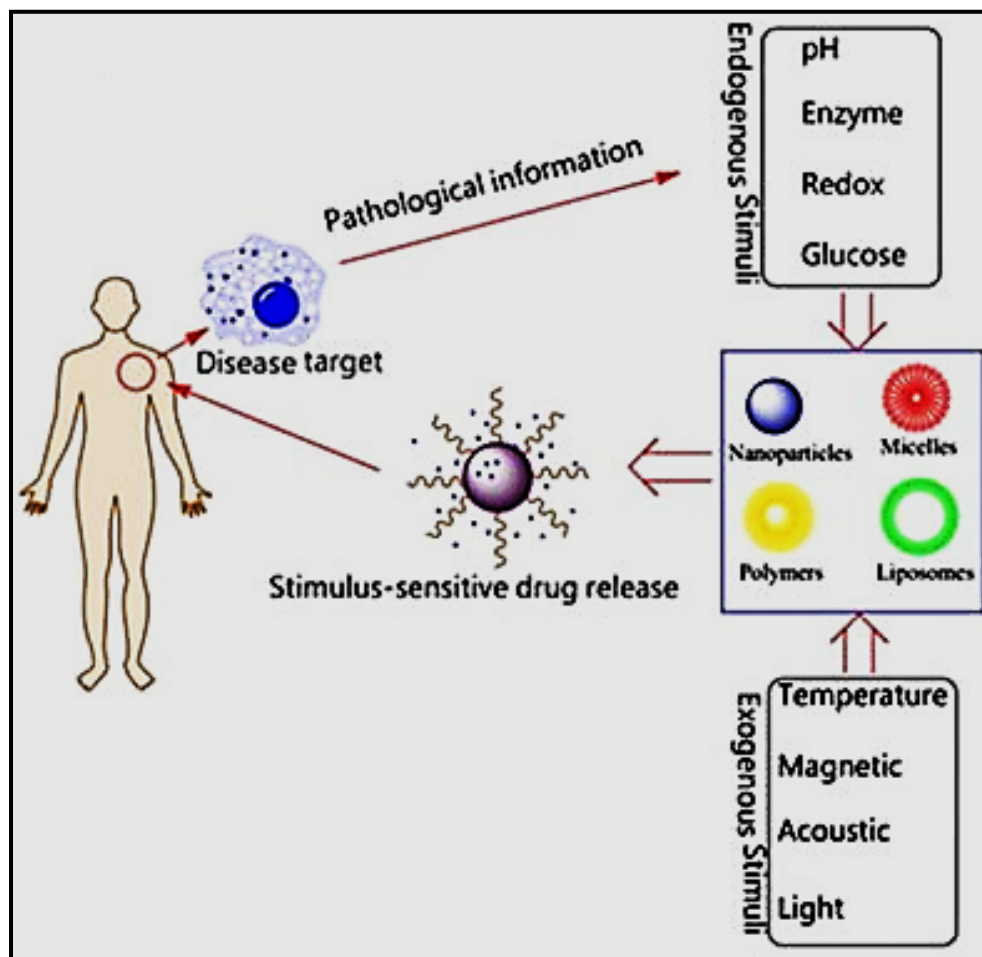
In the past years, a variety of biocompatible DDS has been prepared with improved properties. It was demonstrated that when a pharmaceutical agent or molecule is encapsulated within, or attached to a carrier, drug efficacy and safety may be improved. The concept facilitates active researches for the design of biocompatible and biodegradable materials as drug delivery systems. Recent research works have led to the development and improvement of a new approach in the field of controlled drug delivery or controlled drug release system with the creation of nano-sized biodegradable polymeric drug delivery systems [12-14]. The critical requirement of a controlled drug release system is to allow sustained release of the active agent continuously over an extended period of time to obtain a consistent therapeutic drug release profile which duration of delivery, route of administration, drug properties, mechanism of drug release, biocompatibility, the nature of the delivery ability to the targeting results in extended therapeutic advantages throughout action by reducing problems associated with multiple dosing [15-16].

2.1.1 Controlled DDS by electrospun structures

Nanofibers have attracted much attention for various medical applications [17-20]. The advantages of nanofibers are derived from their high specific surface area and the formation of the highly porous surface [21-23]. Medical applications of nanofibers are included to fabricate wound dressings [24-25] tissue engineering scaffolds [26-27] and nanofibrous drug (pharmaceutical agent) delivery systems [28-30]. There are different techniques to fabricate nanofibers, including phase separation, melt-blown, self-assembly, phase template, and electrospinning [31-32].

Electrospinning is a state-of-the-art method of making porous nanofibrous structures, and it has received much and much attention because it is a versatile, adaptable and straightforward technique to fabricate nanofibrous membranes from a broad wide range of polymers in a relatively easy and straightforward way [33-35]. The setup for electrospinning consists of three major components: 1. a high-voltage power supply, 2. a spinneret (a metallic needle), and 3. a collector (Fig. 4). The spinning mechanism is partly complicated due to complex electro-fluid mechanical forces involved. In the process of electrospinning, the polymer solution housed in a syringe is fed through the spinneret at a constant and controllable rate. The electrostatic field exists in the space of the electrospinning device when a high voltage is applied. The electrostatic field charges the solution drop at the nozzle of a spinneret and the induced charges are evenly distributed over the surface. Under the action of electrostatic interactions, the drop is distorted into a sharp object that is called a "Taylor cone." The electrified jet can be attracted by the collectors, and it is directed towards the collector with the opposite electrical charge.

As it travels to the collector, the solvent is evaporated, and the solid polymer nanofiber is deposited as a nonwoven mat on the surface of the collector.
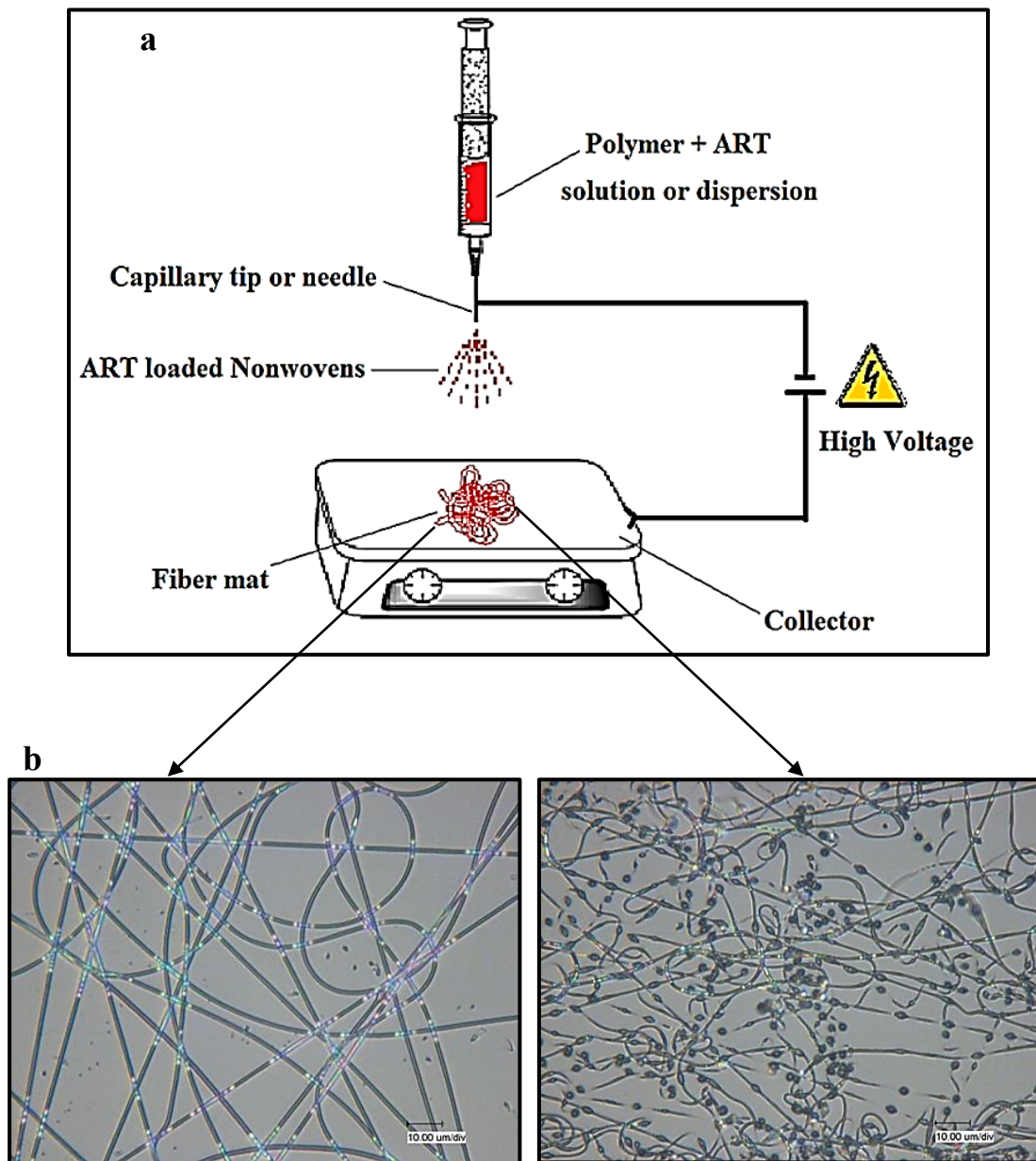

Figure 4 a) A schematic structure of an electrospinning process. b) Microscopic structures of nanofibers without and with beads.

2.1.2 Controlled DDS by polymeric films

Drug delivery by polymeric films using a film, something like a tablet to administer drugs via absorption in the mouth (buccally or sublingually), via the small intestines (enterically) or for subcutaneous applications like implantation offers many advantages for controlled DDS system [36-37]. The process of fabrication of such carriers is technically very straightforward and procurable. Pharmaceutical scientists around the world are trying to explore the polymeric films as the novel DDS tool. Films have played an essential role as an alternative approach to conventional dosage forms. Such films have been considered to be convenient to swallow, self-administrable, and fast dissolving dosage form, all of which make it a versatile platform for drug delivery. This drug delivery system has been used for both systemic and local action via several routes such as oral, buccal, sublingual, ocular, and transdermal routes. The design of these effective drug-loaded films needs a comprehensive knowledge of the pharmacological and pharmaceutical properties of drugs and polymers, along with an appropriate selection of manufacturing processes.

A film can be prepared either by applying hydrophilic polymers that rapidly dissolve on the tongue, transferring the drug to the systemic circulation via dissolution when contact with the liquid is present or by application of hydrophobic polymeric carriers which support the retarded drug release [38-39]. Currently, a significant amount of original works in literature, but there is still a need for extensive studies to optimize the performance of drug-loaded films accurately. The lack of appropriate guidance for the manufacture, characterization, and quality control of such drug-loaded films has absorbed the need of adequate studies in this area from the pharmaceutical aspects.

.

Figure 5 A fabricated film based on heat-press technique containing 2 mg antimalaria drug, artemisone.

2.1.3 Controlled DDS by 3D structures

Drug delivery systems achieved from 3-dimensional (3D) structures is a rapidly growing area of research studies. It is essential to achieve structures in what drug stability is ensured; the drug loading capacity is suitable, and the desired controlled release profile can be gained. It should be considered that the development of appropriate fabrication that allows 3D drug delivery systems (DDS) to be fabricated in a simple, reliable, and reproducible manner. The range of production methods at the moment being used to form 3D DDS involving electrospinning (in the form of solution or melt), wet-spinning, and 3D-printing. The application of these techniques enables the production of DDS from the macro-scale down even to the nanoscale [40,41]. There is an increasing interest in the fabrication of three dimensional (3D) macro-, micro- or nanoscale systems prepared from polymeric (macromolecular) structures that may find potential applications in tissue engineering scaffolds and drug delivery systems. Drug delivery by 3D structures is gaining growing attention in pharmaceutical formulation development as a practical path

to overcome many challenges of conventional pharmaceutical formulations. For instance, the standard manufacturing involving milling, mixing, granulation, and compression can result in different qualities of the final products regarding drug loading, the kinetics of the drug release, the stability of the drug, and the stability of the pharmaceutical dosage form. DDS fabricated from 3D structures have enabled flexibility in the design and production of complex carriers, which can be used in controlled and programmable pharmaceutics. Among 3D structures, porous materials have attracted a great deal of attention due to their low density, high surface area, and large porosity and have been widely applied for drug delivery purposes. The ordered open pore structure, the high surface area, and the high porosity are essential for optimum loading and controlled release. The large surface area leads to the high drug adsorption, which can be stored and released from meso and micropores on the surface or in bulk. A novel class of polymeric three-dimensional (3D) sponges made from short electrospun fibers have attracted growing interest. The capacity of these sponges for the uptake of liquids was found to be as high as 100× the mass of the sponge itself. Such sponges could be an ideal macroporous carrier for drugs, with high loading and intrinsic mechanical compressibility and multiple potential uses. This would allow the implantation of the drug-loaded sponge.
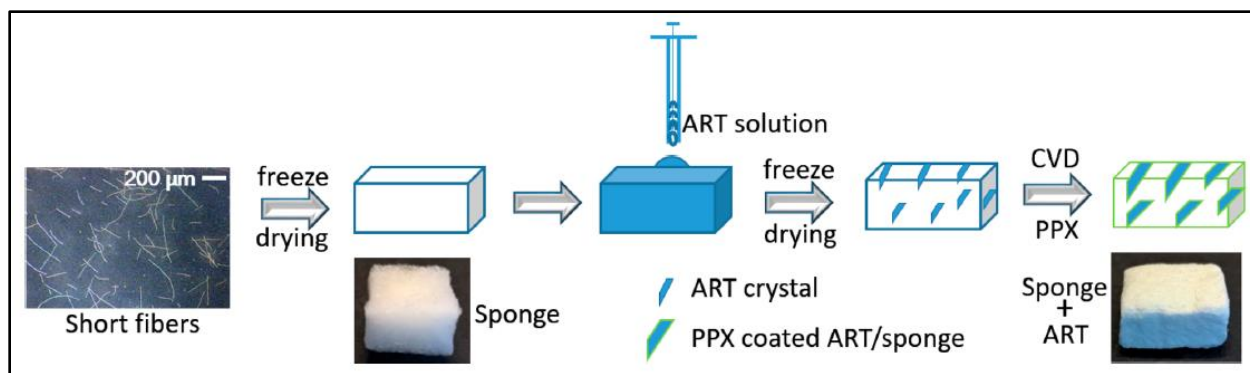
Figure 6 Schematic imagination of a 3D structure (ultralight and ultra-porous material loaded by antimalarial artemisone [42]; *[Permission has been granted.]*

2.1.4 Controlled DDS by particulate systems

Many solid dosage formulations in the pharmaceutical industries are based generally on particles, especially microparticles. Dried powders are inhaled into the lung, transferred to the nose, filled into capsules, or pressed in the form of tablets for oral applications, or even delivered transdermally. In the past, microparticles were often considered merely as carriers, usually micronized dry material, without sophisticated attributes [43-44]. The primary purposes of the micronization and drying processes were to obtain suitable particle size and remove the main content of the solvent. This point of view has changed as novel drug delivery strategies were developed and improved. The advanced therapeutic approaches have established complex requirements for dosage forms, which can only be obtained by particles that are purposed for a range of functions such as stabilization of the active agent, transport and targeting of the dose, or release management. The particle is no longer observed as a passive carrier, but rather as an essential part of the drug delivery system [45-46].

Attempts to realize and control particle formation processes were increased in the last years, corresponding with the development of pulmonary therapeutics that were commonly given by injection. The pulmonary route was found mainly to be viable for the systemic delivery of proteins and peptides, for example insulin, triggering the development of diverse administration systems and particle engineering strategies. Microparticles can be fabricated by many different processing methods. Wet chemistry and phase separation treatments and alternative drying processes such as spray freeze drying, or supercritical fluid technologies, have also been applied widely for particle fabrication purposes.

Spray-drying is a rapid, continuous, cost-effective, and reproducible process for the fabrication of dry powders from a fluid material by atomization through an atomizer into a hot drying gas medium (usually air). Often spray-drying is considered only as a dehydration process. However, it can be applied for the encapsulation of hydrophilic or hydrophobic active compounds within different carriers without substantial thermal degradation as well, even of heat-sensitive (active) substances due to fast drying (in seconds or milliseconds) and relatively short exposure time to heat. The gained solid particles present relatively narrow size distribution at the submicron-to-micron scale [47,48].
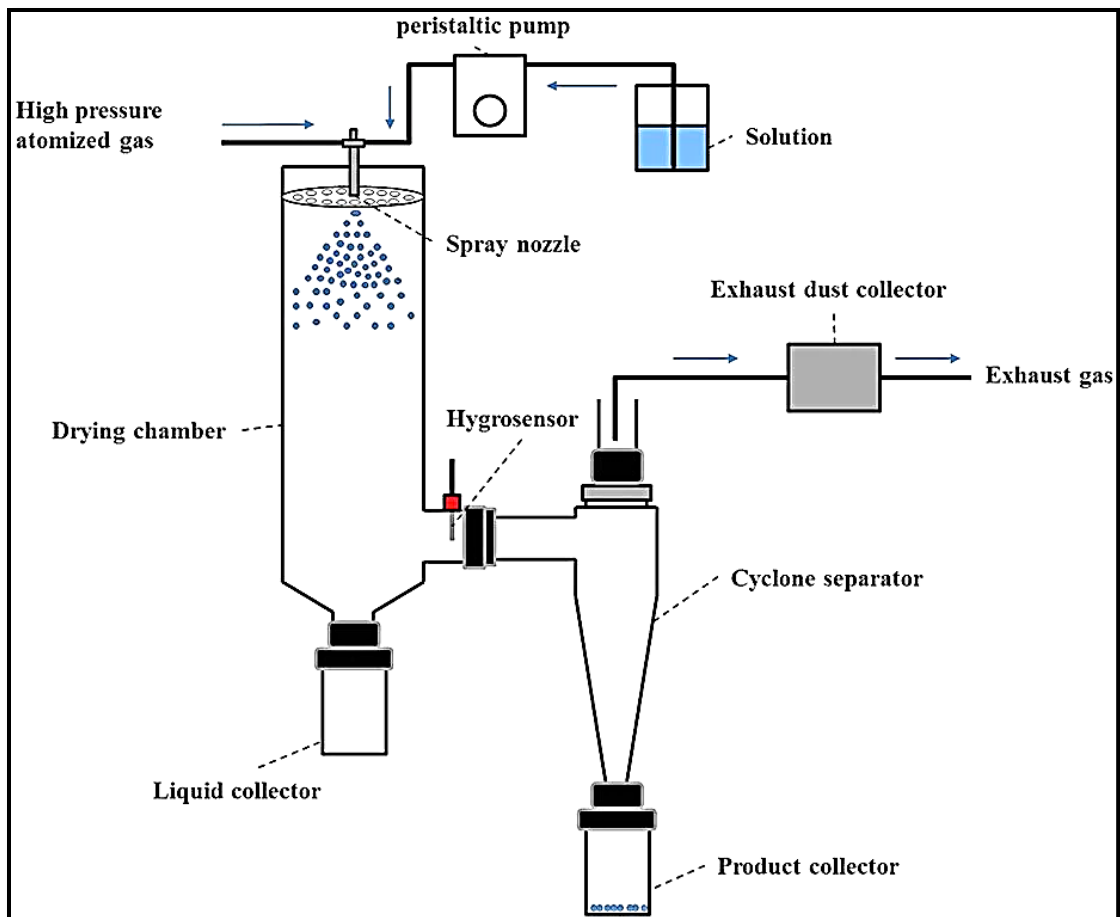
Figure 7 Mechanism of a spray-drying process [49]; *[Permission: this is an open article distributed under the terms of the creative commons CC BY license, which permits unrestricted use, distribution, and reproduction in any medium, provided the original work is properly cited.]*

2.2 Controlled drug release from polymeric carries

Controlled drug delivery technology introduces one of the most rapidly advancing areas of science and technology in which chemists and pharmacists are contributing to human health care. Such delivery systems offer various benefits comparing to conventional dosage forms, including improved efficacy, decreased toxicity, and increased patient compliance and comfort. Such systems often employ synthetic polymers as carriers for the drugs. All controlled drug delivery and release systems aim to improve the effectiveness of drug therapy. This refinement can take the form of improving therapeutic activity comparing to the intensity of side effects, minimization of the number of drug

administrations required during treatment, or eliminating the need for specialized drug administration (e.g., repeated several injections) [50-52].

The drug-release mechanism can be physical or chemical in nature. Diffusion is always revolved for non-biodegradable matrix and membrane devices; the release is by diffusion and is driven by the concentration gradient. It can also be driven by osmotic pressure or matrix swelling. For matrices that are biodegradable or contain drug conjugates, the release is controlled by the hydrolytic or enzymatic cleavage of the relevant chemical bonds, although diffusion of the reactants and the free drug molecules may still be rate-limiting. Only a qualitative discussion is pursued here for understanding the release patterns ensuing from the more common delivery systems [53-56].
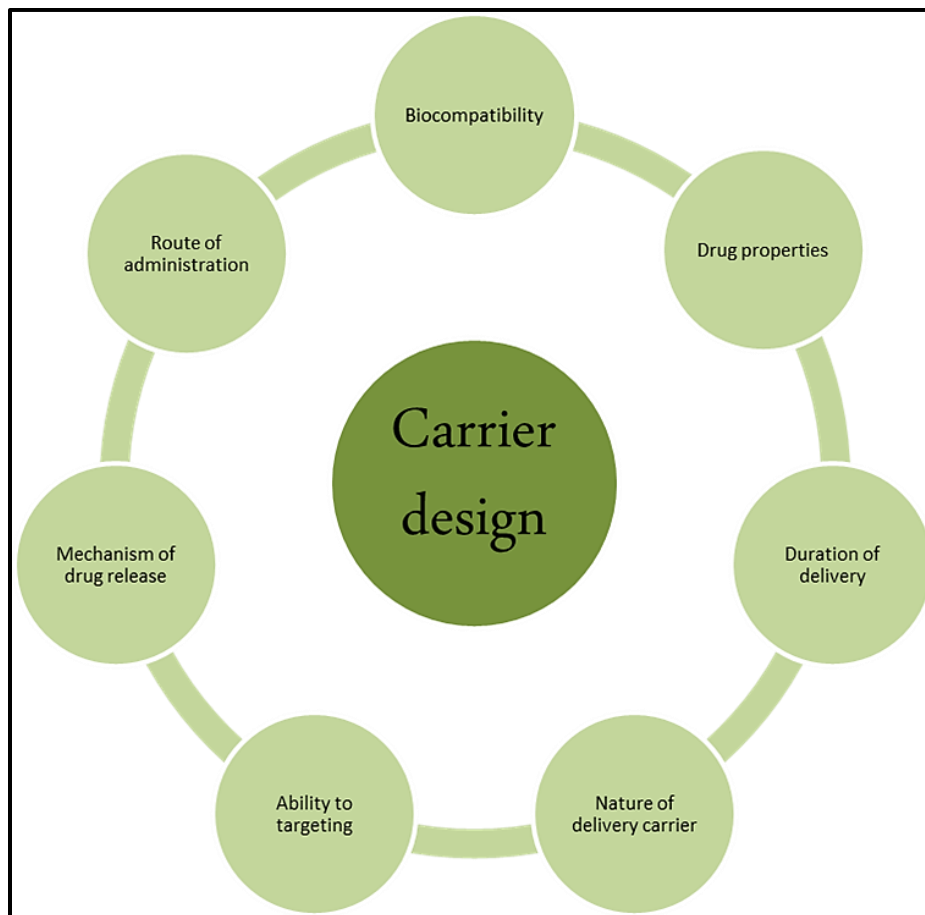

Figure 8 Design of polymeric carrier regarding the necessary background-requirements

2.2.1 Mechanism of controlled drug release from polymeric carries

Drug release systems can be classified into two main classes: *1. sustained release* and *2. controlled release*. Sustained-release systems are generally a mix of agents that affect the net rate of dissolution of the drug molecule. *Controlled-release* systems are established from a drug molecule (i.e., active agent) and a biocompatible carrier such as a polymer. This system also involves an operation that can be free or connected to the polymer chain, which allows for handling the release kinetics of the system. Controlled drug delivery systems can be applied to a person through oral, ocular, parenteral, and sublingual sites.

2.2.1.1 Diffusion-Controlled Systems

The process of the drug release in an aqueous environment has several main benefits in terms of the planning of the control and response of the system. The rate at which water can swell the matrix of a polymeric system can be significantly rapid. The term "*diffusion*" is related to the actions of the drug molecules upon exposure to stimuli affecting its external environment. The rate-limiting step of diffusion drug release systems is the diffusion through typically a water-insoluble barrier. The diffusion DDS are typically either **matrix-based** or **reservoir** diffusion systems [57-58]. In the matrix-based systems, the drug is combined with a polymer to shape a composite matrix where water permeation makes for either swelling or osmotically controlled systems. Since the matrix is composed of both polymeric carrier and drug molecules, the swelling influence is observed as a steady volume expansion of the bulk polymeric material, causing the opening of pores throughout the matrix structure [59-60]. To happen an effective diffusion of drug

molecules, the pore size of the swelled matrix has to exceed the size of the hydrophilic drug molecule or hydrophobic medicine particle significantly. In reservoir systems, the drug solution or dispersion is encapsulated within or into a polymer, creating a leaky barrier between the drug solution environment and the surrounding environment. Since the reservoir is composed of a polymer barrier coating, the swelling effect is observed as non-uniform volume expansion, that the barrier coating allows for water permeability and swells, while the internal ingredients can diffuse out of the system. This is not unlike a dialysis bag, which allows free diffusion of water and size-selective permeability of its internal constituents.

2.2.1.2 Degradation-Controlled drug delivery Systems

The main modes of erosion-based drug delivery systems are through the release of the drug molecule, characteristically from a bulk phase that includes a drug composite. Thus, the rate-limiting step of degradation-controlled release systems is dissolution [61-63].

Table 1 Common erosion effects encountered by biomedical materials

Erosion effects	Remarks
Adhesion	Physical interaction with another surface.
Erosion	Failure of material due to hard materials that are pressed against the surface.
Cavitation	Physical interaction with another physical state.
Fatigue (exhaustion)	Fatigue happens when a material is subjected to repeated loading and unloading.
Corrosion	The gradual destruction of materials by chemical and electrochemical reaction with their environment.

The composite can involve a polymer of a tailored degradation or deformation rate. The degradation or dissolution effects are evaluated as the erosion of the material over time in response to its immediate physiological environment. The erosion can happen through a variety of mechanisms related to either the surface or the bulk of the material. Erosion on the surface generates displacement of surface features or regularity due to several common effects (Table 1).

The degradation or deformation rate is evaluated from a matrix because of the adsorption or circulation of physiological, typically aqueous liquid around the body. In these matrices

or monoliths, systems, the drug is homogeneously dispersed throughout a matrix. The changes to the bulk state can be divided into two main categories: ***bulk erosion*** and ***surface erosion.***

In the case of the bulk erosion, the material degrades or deforms regularly throughout the bulk of the material. As the deformation continues, the volume of the material remains constant while the mass of the material decreases, resulting in a decrease in the density of the degrading material. In the case of surface erosion, the material degrades (or deforms) from the outer surface inside only at the interface between the bulk of the matrix and the external environment. As the deformation occurs, the volume of the material decreases linearly with mass, which results in the density of the material remaining constant [64-65].
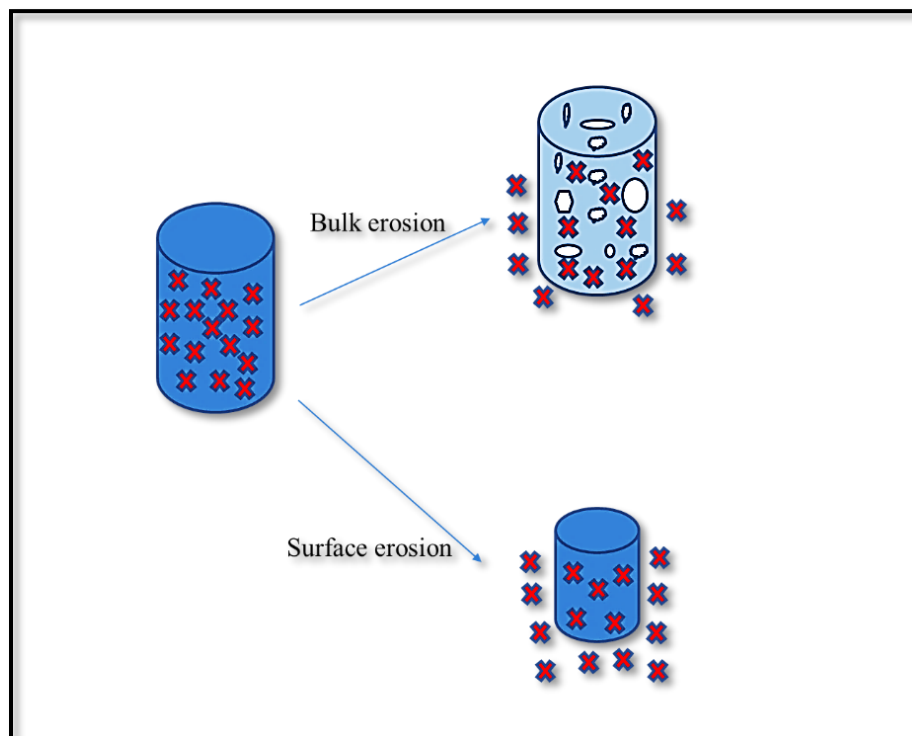

Figure 9 Degradation-Controlled Systems based on bulb and surface erosion

This is a critical differentiation between the two attempts that distinguish their responses to physical stress and dictates their application. Materials that keep volume but reduce density become porous and fragile over time, with weaker mechanical integrity. This effect can happen with swelling or dissolution, covalent bond break, and secondary bond dissociation within the system. Materials with fragile and porous structures are like weak ceramics that can crumble or crack in response to shear, compression, or tensile stress. If materials density is constant, they will have more calculable behavior to external physical stresses. If the volume is decreased, however, the function of the material may be compromised.

2.3 Factors affecting the drug release

The controlled release systems are primarily fabricated as matrix systems or reservoir types, which are more straightforward to design yet useful and programmable to release the drug at the desirable rate (kinetics). These systems create high and dynamic concentration flows across tissues and are hard to identify, characterize, and control [66-67]. The release kinetics for DDS are influenced by all constituents of which the DDS are formulated and the parameters of the process under which it is covered. The principal parameters on which release is dependent are depicted in Figure 10 and can govern the drug release rate individually and mutually. Many other biological parameters should also be considered simultaneously while investigating drug release kinetics for a given system. The delivery of the drug via diffusion-convection, biological properties of tissue and arterial ultrastructure, hydrodynamic conditions at the implantation site, and stent design

significantly modulate the release rate and the final biological response to drug-eluting
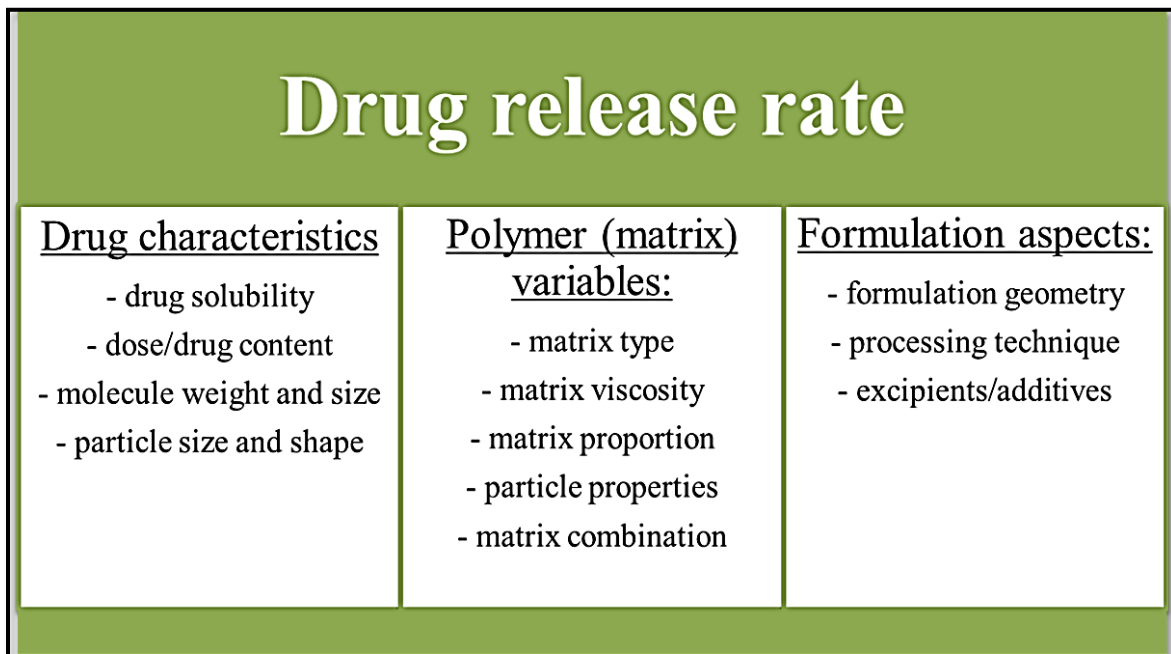
DDS [68-70].

Figure 10 general schematic overview of the summarized parameters affecting the rate of the drug
release

Table 2 Factors affecting the rate of drug release in details

Parameters	Possible effects on
Basic properties of the applied drug	
Drug hydrophobicity/hydrophilicity	aqueous solubility and local drug concentrations
Diffusion/dissolution characteristics	release kinetics
Solubility/mixability in a polymeric matrix	release kinetics
Solubility in release media	with higher degrees of solubility, higher drug release rates
Properties of the rate-controlling polymer	
Thermal properties (T_m, T_g)	affects degradation, hydrophobicity, drug release and drug solubility in the case of biodegradable polymers
Degree of crystallinity	affects water penetration and drug solubility in the case of non-erodible polymers Influences degradation and drug release for biodegradable polymers
For biodegradable polymers- initial molecular weight, copolymer ratio, absorption rate and period, the pH of dissolution medium	affects degradation behavior and time
Processing parameters	
Selection of coating process	coating film property and drug elution
Properties of solvent (BP, thermal history), Solvent evaporation rate and Phase diagram of the ternary system (drug-polymer-solvent)	residual solvent effects, merging of coating layers, thus influencing release kinetics
Drug to polymer ratio	effect on the drug-carrying capacity of polymer and drug elution rate
Drug (initial solid phase) concentration and distribution inside the matrix	Describes initial burst effect and dissolution mechanism
Coating design	
Coating layer composition and thickness	affects the diffusion of drug through the carrier
The microstructure of coating (spatial variation in physical and chemical composition)	exhibits process conditions and eventual effect on drug delivery kinetics
Mechanical properties of the coated drug-loaded carrier	the improper coating may induce adverse and interrelated effects such as local inflammation and thrombosis and hinder homogeneous drug uptake

2.4 Administration of drug-loaded polymeric carriers

Although recent studies have developed and summarized several novel aspects for micro- and nanomaterials that are applied as smart drug carriers, few of them have been finally translated into clinics for real-world applications [71-73]. There are different essential components that should be considered to ensure the clinical potential for real future applications. On the one hand, the construction of nanomaterials as drug carriers should contain the following critical issues:

1. satisfactory behaviors according to biocompatibility and biodegradability; 2. good stability in physiological environments; and 3. high capacity of drug loading and low toxicity nature.

Additionally, apart from the primary requirement for safety and therapeutic efficacy, industrialization for DDS is also a requirement for this type of novel nanomaterials in clinical applications. For the design of the, in reality, applicable DDS should be concentrated on some of the important scientific backgrounds (Fig. 11).
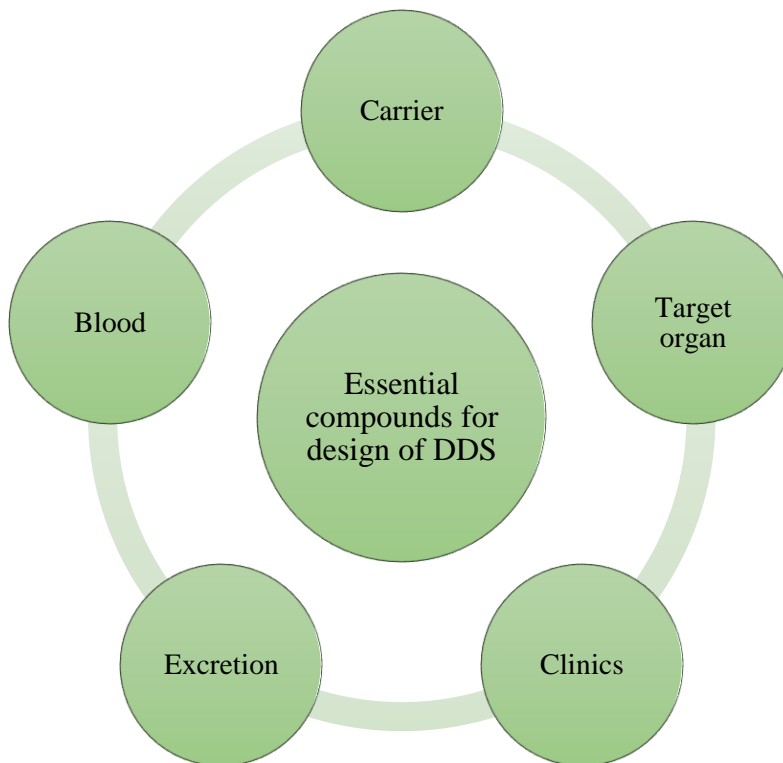
Figure 11 Essential compounds for the engineering of the DDS

Considering such physical, chemical, and biologicals elements can help effectively to manage the useful DDS, and unpleasant end-results can be avoided (Fig. 11 and Table 3).

Table 3 Necessary prerequisites to be considered for applicable DDS

Essential compounds for the design of polymeric DDS				
carrier	**blood**	**Target organ**	**excretion**	**clinics**
Non-toxic	Hemocompatible	Tissue-specific targeting	Low molecular weight	Safe and easy application
Drug stabilization	Controlled drug release	Uptake into the organ	Non-toxic degradation products	Good cost
Drug solubility	No aggregation	Biodegradable & biocompatible	No accumulation in organ	upscaling
Suitable physical, chemical, and biological stability	Prolonged circulation time	No cytotoxicity	Excretion by liver	Easy to use and store
biocompatible	No cause of embolism	Penetration via biological barriers	Excretion by kidneys	Easy to sterilize

A variety of smart DDS have been developed over the last years. Until now, some nanocarriers have been in reality approved in clinical applications, including liposomes, nano-suspension, polymer nanoparticles, microparticles, nanocapsule, micelles, *etc.* For example, the typical nanomedicines which are approved for clinical administrations are Doxil (Liposomal), Lipusu (Liposomal), and Abraxane (Nanoparticulate), to name a few [74-78]. Visudyne, a nanomedicine, was until now the only nanomedicine with nanoplatform concept licensed by the Food and Drug Administration (FDA) [79]. However, other DDS are yet at clinical stages.

These approved formulations have been sufficiently evaluated and deeply optimized over the years by different attempts. One significant property of these promising nanocarriers relies on the simple formulations. Inconsistently, due to achieving smart properties, most of the developed smart DDS were designed with refined structures and formulations, which is complicated to scale up for industrial production. Therefore, design simplicity is still one of the critical points for successful drug carrier translation in these smart carriers. Besides, a considerable number of optimizations and improvements experiments are required for the realization of each stimulus from preclinical, experimental models to real clinical practice. Clinically appropriate formulations have to possess the properties of reproducibility, scale up or industrialize possibility, and verifiability. Accordingly, more attempts should be focused on the development of advanced attempts that can precisely control the preparation process, to generate nanocarriers with essential features, high batch-to-batch reproducibility, and industrialization practicality. The standard production methods and dosage control may finally expedite the translation of smart drugs from the bench to the industry.

2.5 Malaria, a fatal disease for human beings

Malaria is caused by protozoan parasites of the genus Plasmodium [80-81]. Four of the >100 Plasmodium species infect humans and cause distinct disease patterns: P. falciparum (malaria tropica), P. vivax, P. ovale (both malaria tertiana), and P. malariae (malaria quartan). P. falciparum and P. vivax account for 95% of all malaria infections. Nearly all severe and fatal cases are caused by P. falciparum [82]. About 40% of the world's population lives in malaria-endangered areas. Malaria is found in tropical regions throughout sub-Saharan Africa, Southeast Asia, the Pacific Islands, India, and Central and South America [83-84]. P. falciparum is found throughout tropical Africa, Asia, and Latin America. It is the predominant species in most areas. P. vivax is more common in India and South America but is also found worldwide in tropical and some temperate zones. P. ovale is mainly confined to tropical West Africa, while the occurrence of P. malariae is worldwide, although its distribution is patchy. Malaria is the most important infectious disease.
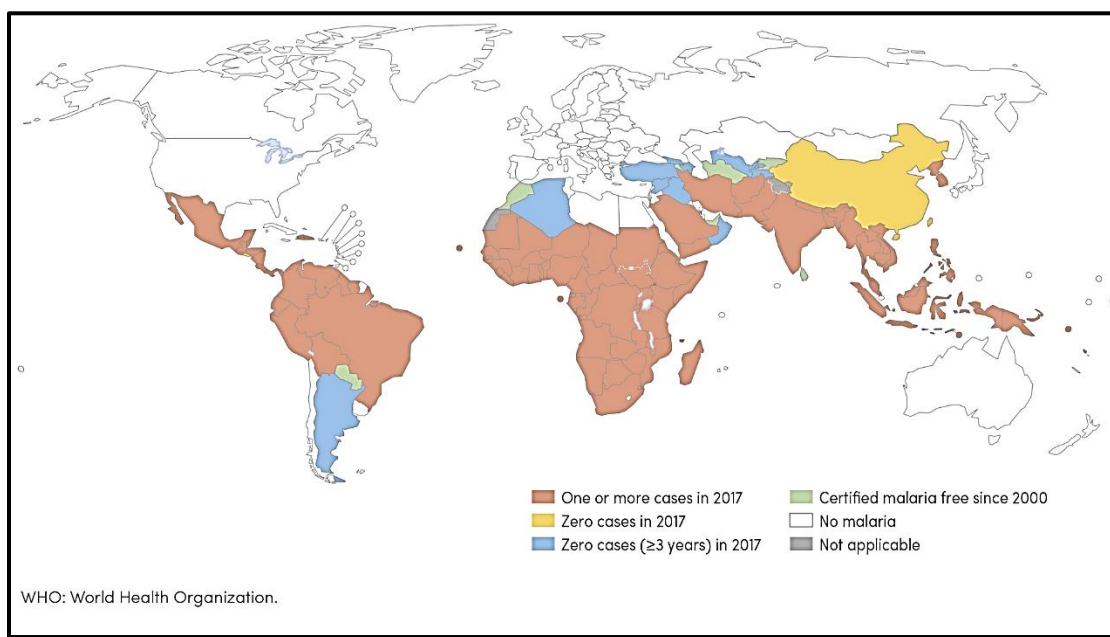

Figure 12 Geographical distribution of malaria cases around the world (WHO, 2017)

Malaria murders between 1 and 3 million people annually, most of whom are children under the age of 5 and pregnant women. It is estimated that every forty seconds a child dies from malaria. P. falciparum malaria (also known as malaria tropica) can progress within a few days from uncomplicated to severe malaria with a lethal end-result in 10–40% of all cases of severe malaria, depending on the time between the outbreak of the symptoms and curative treatment, as well as on the medical facilities for the management of complications [85-86]. Observed complications can include coma (cerebral malaria), respiratory distress, renal failure, hypoglycemia, circulatory collapse, acidosis, and coagulation failure [87-88].

Figure 13 Microscopic image of Anopheles mosquito body. [89]; *[Permission: this is an open article distributed under the terms of the creative commons CC BY license, which permits unrestricted use, distribution, and reproduction in any medium, provided the original work is properly cited.]*

2.5.1 Antimalarial agents

Today, malaria is still the essential transferable infectious disease worldwide. Considerable success in achieving control over this mortal threat was achieved in the 1950s and 60s through landscaping measures, vector control with DDT, and the widespread administration of chloroquine, the most crucial antimalarial agent ever.

In the late 1960s, the final triumph over malaria was believed to be within reach. However, the parasites could not be destroyed because they developed resistance against the most widely used and affordable drugs of that time. Today, the number of malaria cases are on the rise and have gained record numbers. Powdered bark from the cinchona tree containing the plasmodicidal quinoline alkaloids quinine and quinidine was the first medicine to be used against malaria (Fig. 14). In 1856, chemist William Henry Perkins set out to synthesize quinine. His efforts resulted not in quinine (the first total synthesis was accomplished later in 1944), but rather in the first synthetic textile dye called "mauve" [90-91].
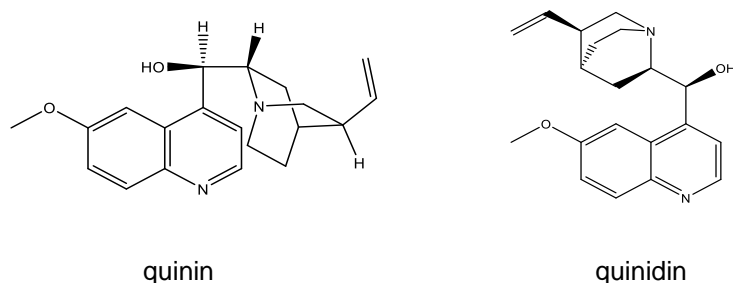

quinin   quinidin

Figure 14 Chemical structure of antimalarials quinine and quinidine

Chloroquine has been the most successful single drug for the treatment and prophylaxis of malaria [92-93]. Chloroquine is a safe and reasonably priced medication, and it was useful before resistant strains started to arise in the 1960s. It was one of the first curative choices recommended by the World Health Organization (WHO) Global Eradication Program.
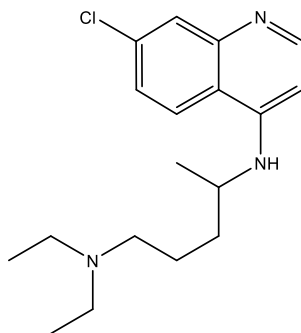

Figure 15 Chemical structure of antimalarial chloroquine

Due to the massive use of chloroquine, resistant malaria strains have developed independently in four different regions and have successively spread over almost the entire malaria-endangered area. Today, more than 80% of wild isolates are resistant to chloroquine [94-96].

2.5.2 Artemisinins and synthetic peroxides

Extracts of the herbage known as sweet wormwood have been widely used in China for the treatment of fever for as long as a thousand years. In 1971 the active substance, the sesquiterpene lactone artemisinin (ACT), was isolated, which is used in China for the treatment of malaria since the 1970s. Artemisinin is a highly active antimalarial agent [97-99].
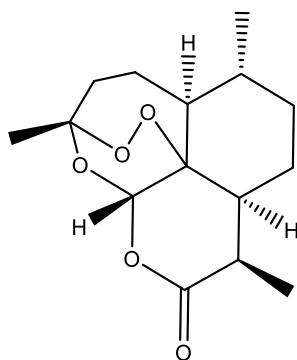
Figure 16 Chemical structure of artemisinin

A key structural characteristic of all artemisinins is the 1,2,4-trioxane substructure or, better explained, the endoperoxide, which is mandatory as a curative point for antimalarial activity. Despite the growing importance of artemisinins and serval kind of uses, their exact mechanism of action is till now unresolved and remains a matter of intense debate. It has been proposed that iron (II)-mediated cleavage of the endoperoxide bridge leads to the arrangement of different C-centered radicals, which may be primary or secondary (Fig. 16). Which, if not possibly both, of these radicals is the active species is unclear [100-102].
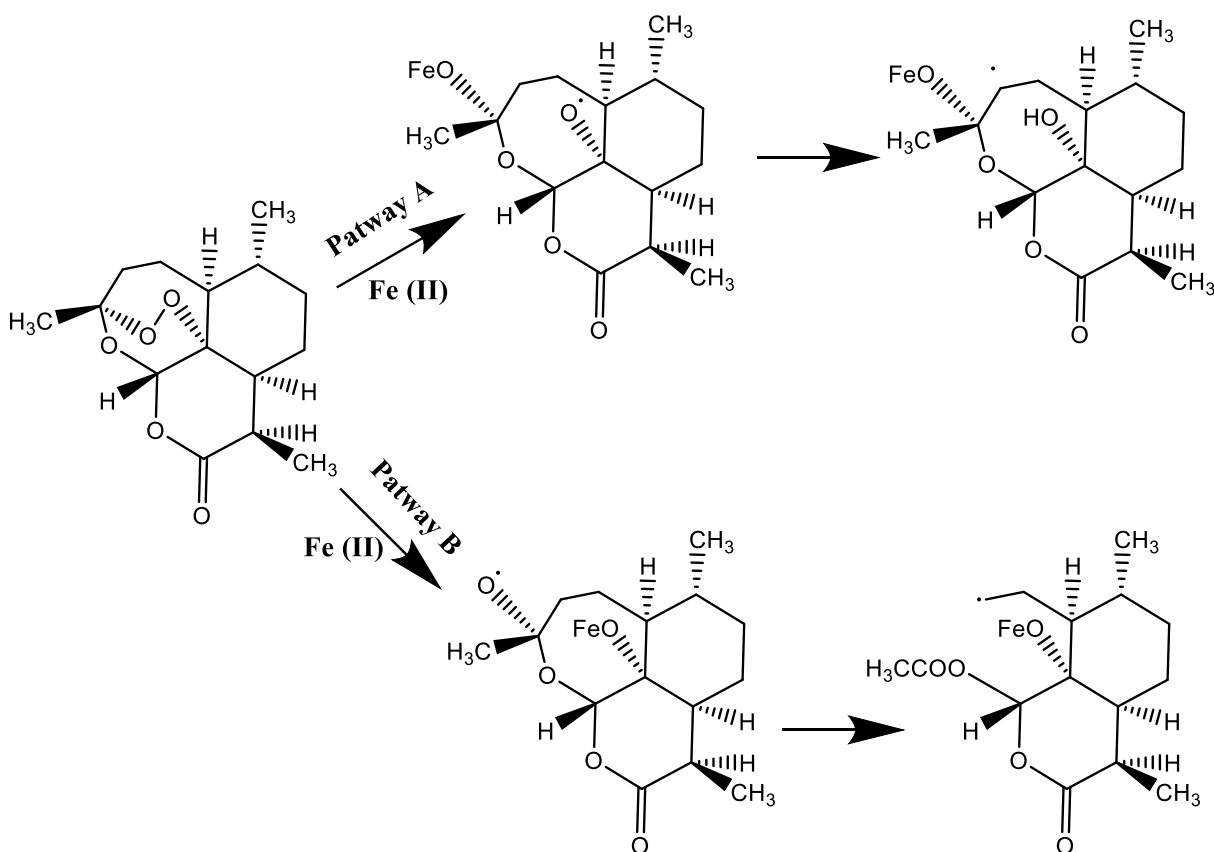
Figure 17 Mechanism of treatment of malaria by artemisinin in the presence of iron (II) ion

Semisynthetic derivatives of artemisinin have been developed because artemisinin is only poorly soluble in water and oil. The Derivatives of artemisinins have been until now classified mainly in two groups: 1. First-generation, and 2. Second generation [103-105]. Semisynthetic artemisinins of the first and second generations all rely on a sufficient supply of artemisinin isolated from plants. Maximum extracted yields of artemisinin are commonly about 0.6 %. Until now, the herb Artemisia annua is cultivated in China and Vietnam. Due to the growing need resulting from the increased adaptation of artemisinins by more and more countries, the raw material is already in short supply. Despite current efforts to cultivate Artemisia in Africa as well, it remains a question as to whether increasing future needs will be met [106-109].
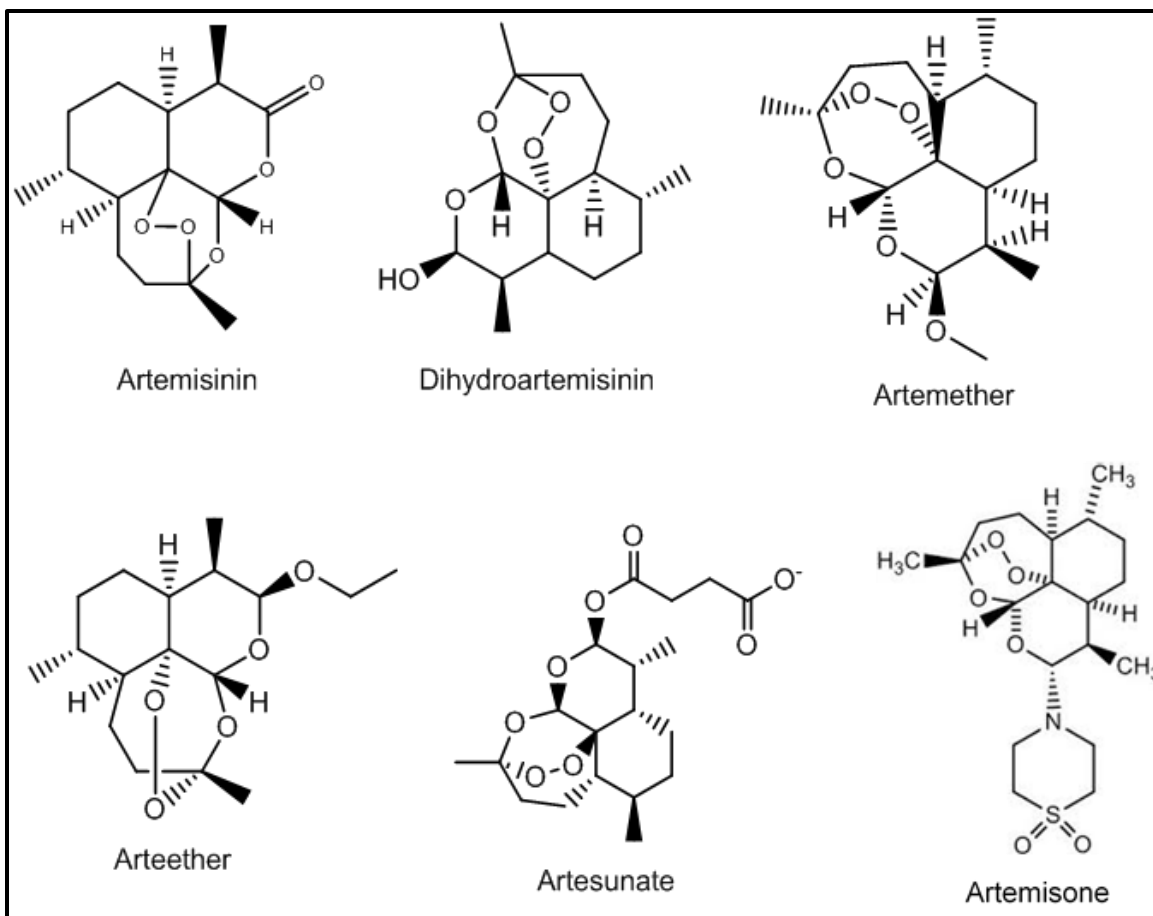
Figure 18 Chemical structures of artemisinin and some of its derivatives

A common problem of the so-called first-generation semisynthetic artemisinins is their rapid biotransformation that results in a short half-life and the formation of the neurotoxic dihydroartemisinin. Much work has been invested in the development of second-generation artemisinins. Methyl and ethyl residues of the first-generation semisynthetic artemisinins artemether and arteether have been replaced by numerous other residues, some of them carrying polar groups, as is the case with artelinate, to decrease the lipophilicity and enhance water solubility.

2.6 Artemisone, a more effective member of ACTs family

Artemisone (ART) is a semi-synthetic 10-alpha-amino derivative of artemisinin (see 2015 Nobel Prize in Physiology or Medicine). Artemisone was selected as a therapeutic product candidate based on properties that distinguish it from other artemisinin derivatives, including greater potency, lower predicted neurotoxicity, the total cost of treatment, better stability, half-life, and pH solubility. Notably, Artemisone relies on a non-DHA metabolic pathway which distinguishes it from currently used artemisinins. This feature may provide significant clinical advantages in terms of fighting resistance, blocking disease transmission, or treating severe and cerebral malaria [110-111]. Efficacies of ART against the malaria parasite are substantially higher than those of the current artemisinin or artesunate. Also, as opposed to most current artemisinins, it demonstrates low lipophilicity and negligible neuro- and cytotoxicity in in-vitro and in-vivo assays. Thus, the drug offers appeal for application in artemisinin-based combination therapy. In comparative studies in- vitro against a panel of multidrug-resistant isolates of P. falciparum, ART is greatly more active than artesunate, chloroquine, and pyrimethamine irrespective of the resistance profile. Ex vivo bioassay displays an effective method for assessing both the comparative bioavailability and efficacy of an orally administered drug [112-113].

Chapter 3

Results and discussions

3 Results and discussions

3.1 PCL-b-MPEG as an effective biocompatible and biodegradable carrier

The biodegradable diblock copolyester PCL_{16500}-b-$MPEG_{5000}$ (the subscript describes the M_n of the polycaprolactone (PCL) block and MPEG according to NMR analysis) (PCL-MPEG) was synthesized according to Fig. 19, following standard protocols [114-115] with some essential modifications, by ring-opening of ε-caprolactone catalyzed by stannous octoate in the presence of α-methoxy-ω-hydroxy-poly (ethylene glycol) (MPEG) as a macroinitiator. The reaction terms are demonstrated in Table 4.
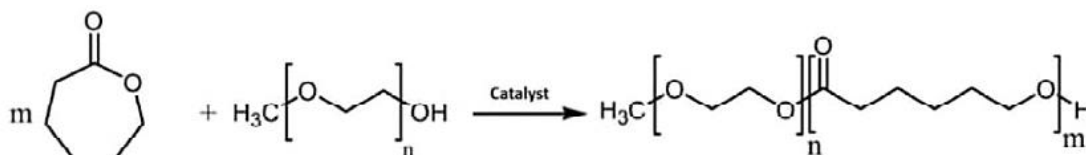

Figure 19 Formation of block copolymers of polycaprolactone (PCL) and methoxy terminated polyethylene glycol (MPEG)

Table 4 Parameters for the synthesis of PCL-MPEG

Caprolactone (g)	MPEG (g)	Catalyst (µL)	Time (h)	Temperature (°C)
13.95	4.65	30	3	130

For purification of the polymer, after precipitation in n-pentane, the polymer was extracted with water to remove the water-soluble parts of the product, like the oligo PCL-b-MPEG and unreacted MPEG. The purified polymer showed a monomodal GPC curve (Fig. 20). The x-axis represents molar mass and y-axis intensity.
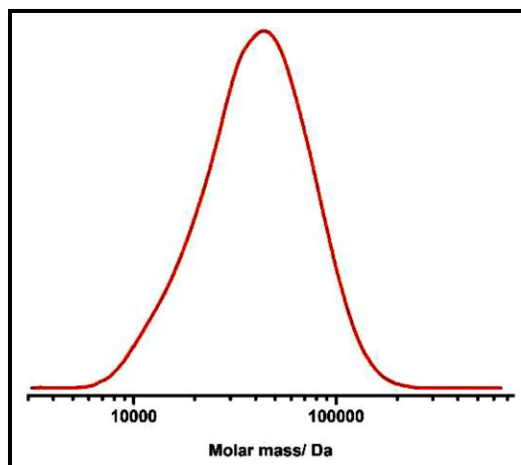

Figure 20 GPC chromatogram of synthesized PCL_{16500}-b-$MPEG_{5000}$

The isolated yields were in the order of 90–92% for the different synthesis attempts. The conventional chemical structure of PCL-MPEG was confirmed by observation of characteristic peaks of both MPEG and PCL in the ^{1}HNMR spectrum. $-OCH_2$-(protons of MPEG, 6/6') and PCL (1) were observed at 3.61(s) and 4.03 (t) ppm, respectively. The other protons of PCL were obtained at 2.27 (t) ppm [CH_2CH_2C (O) O-, 5], 1.56−1.67 (t) ppm [$-OCH_2CH_2CH_2CH_2$-, 2; -C (O) $CH_2CH_2CH_2$-, 4], and 1.29−1.40 (m) ppm [C (O)$CH_2CH_2CH_2CH_2CH_2O$-,3] (Fig. 21).
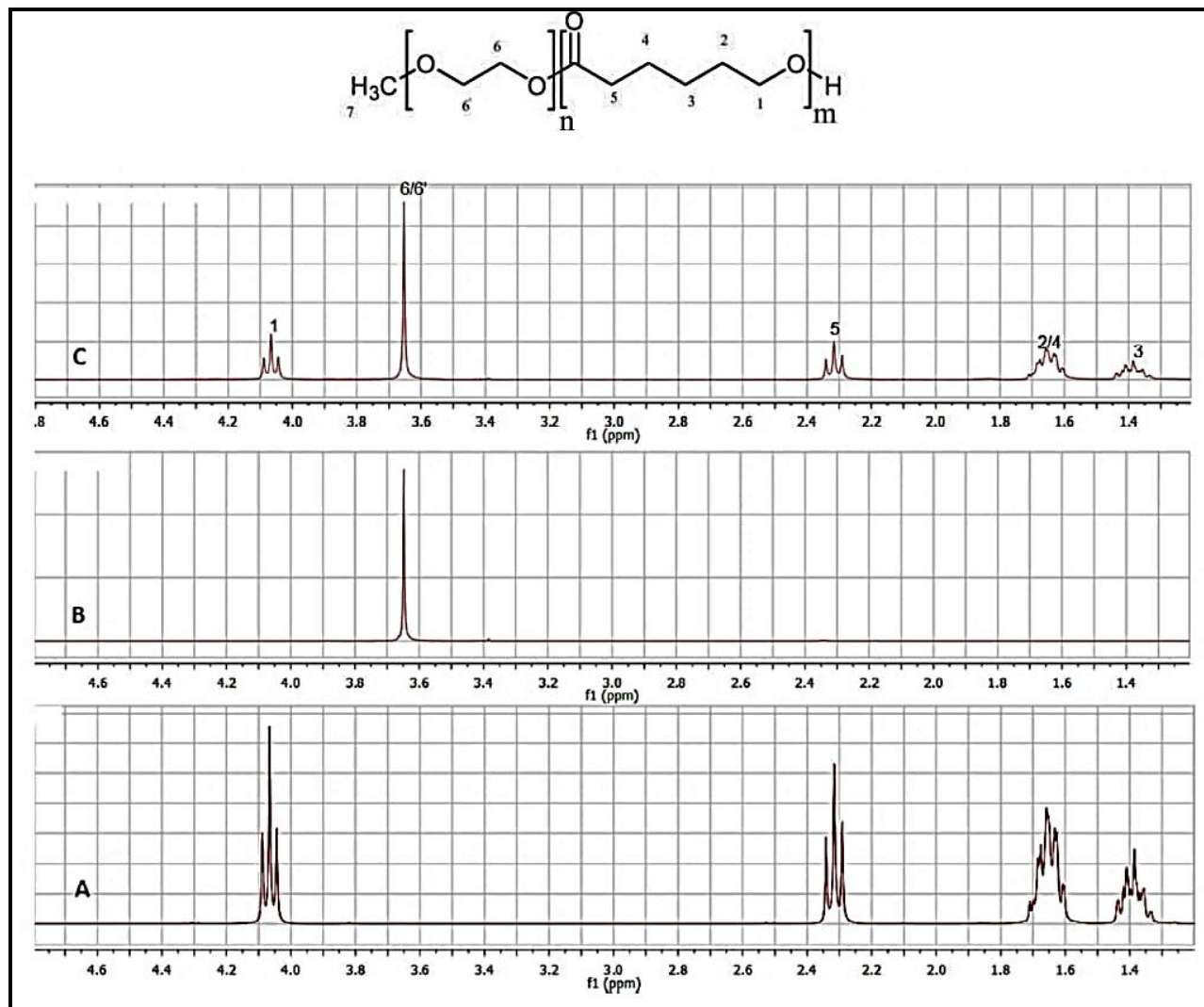
Figure 21 ^{1}HNMR spectra of A. PCL, B. MPEG, and C. PCL$_{16500}$-b-MPEG$_{5000}$

3.2 Loading of ART in DDS based on electrospun structures as the carrier

First, we studied the loading of nanofiber nonwovens (NFN) with ART and its release properties without and with additional coatings due to tailor the ART release profiles. The polymer applied for the preparation of ART-loaded NFN by electrospinning was the very well-known block copolymer polycaprolactone $(PCL)_{16500}$-b-α-hydroxy-ω-methoxy-poly (ethylene glycol) $(MPEG)_{5000}$ (PCL-MPEG). The polymer applied for the additional coating was poly(xylylene) (PPX), which provides established biocompatible coatings [116]. PCL-MPEG was prepared by ring-opening polymerization, as demonstrated previously in detail. ART-loaded NFN were obtained by solution electrospinning of mixtures of PCL-MPEG and ART in different compositions (0–20 wt.% ART).

NFN with smooth fiber surfaces and an average fiber diameter of 220 ± 65 nm (for samples with contents of 12.5 wt% ART) were obtained (Fig. 22). The content of ART in NFN was quantified by ^{1}H-NMR and high-pressure liquid chromatography (HPLC). While NFN with 12.5 wt.% of ART was homogenous (Fig. 22a), NFN with a more considerable amount of ART (20 wt%) showed the formation of ART crystals (Fig. 22b). The distribution of ART in NFN with 12.5 wt% ART was analyzed by energy dispersive X-ray analysis (EDX) by tracing sulfur of ART. The EDX showed the homogeneous incorporation of ART on the surface and cross-section of NFN (Fig. 22c, d). Consequently, the NFN samples loaded with 12.5 wt.% ART were further studied in order to advance their practical application.
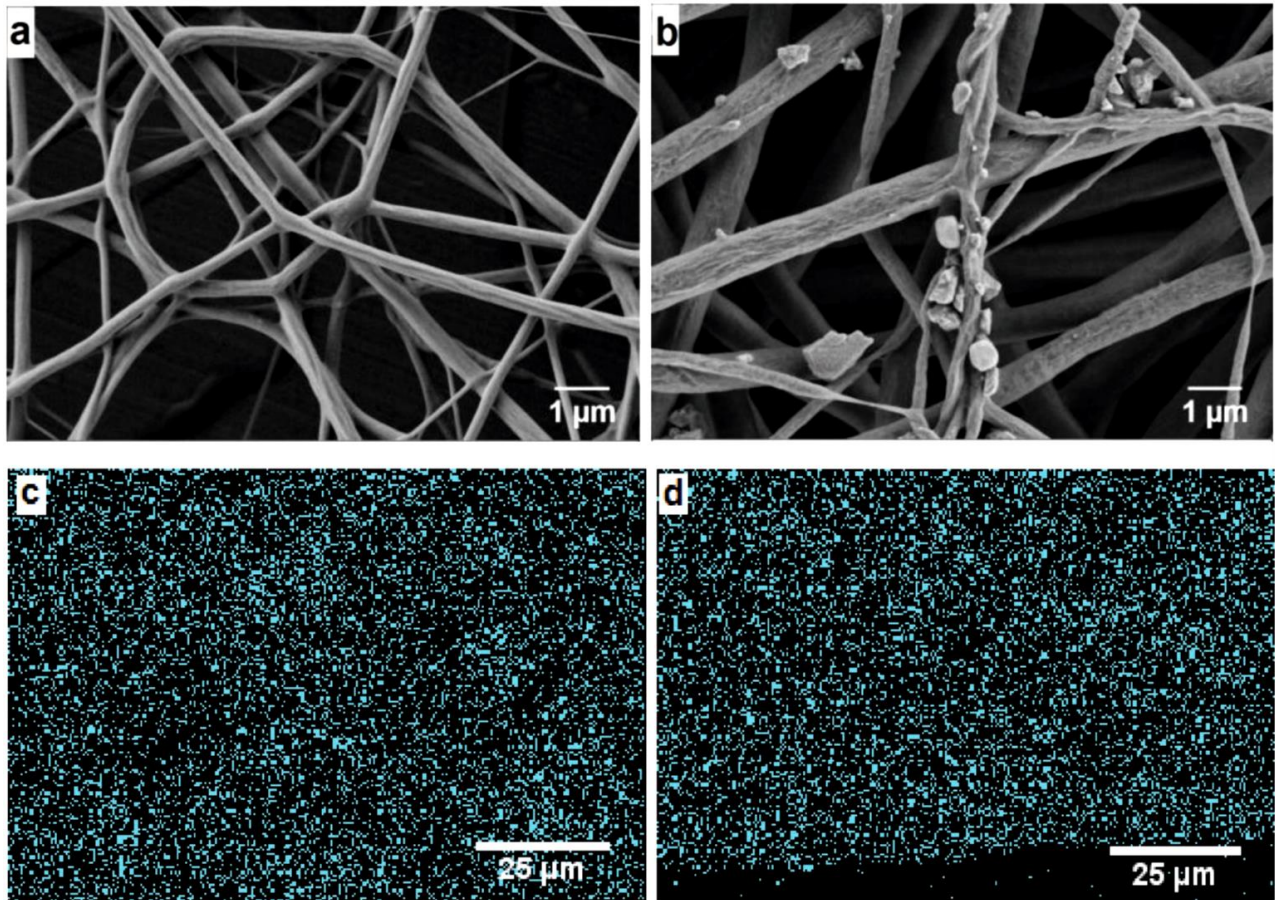
Figure 22. SEM and EDX images of ART loaded electrospun NFN. a) 12.5 and b) 20 wt% ART-loaded NFN. c) The surface and d) cross-section of ART-NFN with the content of 12.5 wt% ART

Furthermore, the crystallinity of ART powder, polymer powder, and final product ART loaded NFN with the content of 12.5 wt.% ART was investigated by X-ray (Fig. 23). This study approved the crystallinity nature of ART and semi- crystallinity of the carrier (PCL-MPEG). Furthermore, in the final product (ART loaded NFN with 12.5 % ART content), ART could be integrated mainly in the amorphous phase of the polymer. The final product showed only some reduced peaks (2θ: 7-12°)
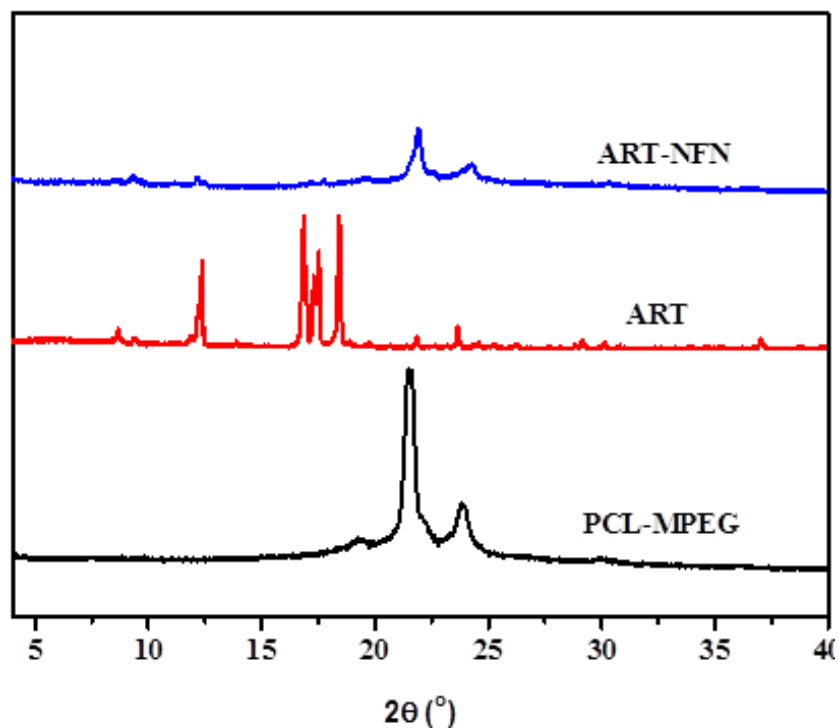
Figure 23 X-ray studies on ART-NFN, ART powder and PCL-MPEG powder

3.3 Determination of drug content in nanofibrous DDS

Two analytical methods could be applied during this project for identification as well as for quantification of drug content which was encapsulated or incorporated in polymeric DDS:

1. Nuclear magnetic resonance spectroscopy (NMR) and 2. High-performance liquid chromatography (HPLC). In this project, HPLC was used mainly as the key device to quantify the drug contents in NFN, and all other polymeric carriers applied during this thesis. NMR was applied randomly to support the obtained results from HPLC. HPLC method could be validated during this project, and furthermore, NMR results could also confirm the validity of the HPLC method.

3.3.1 Determination of drug content in electrospun DDS by NMR

NMR spectroscopy was applied to identify and quantify the ART content in drug-loaded samples as a supportive method (Fig.25 and Fig.26). This technique could recognize different hydrogen atoms in the chemical structure of ART, but two main peaks, first one at δ: 5.3 ppm (1H, s, H-1) and the second one at 4.2 ppm (1H, d, H-2) were employed as the most characteristic peaks to follow the presence of ART. A single signal at δ: 5.3 is used in this work as the unique peak for the quantification of ART content (Table 5). For the determination of ART content, each sample has been quantified by examining at least three NFN mats, and assay values were reported as the mean value ± standard deviation.
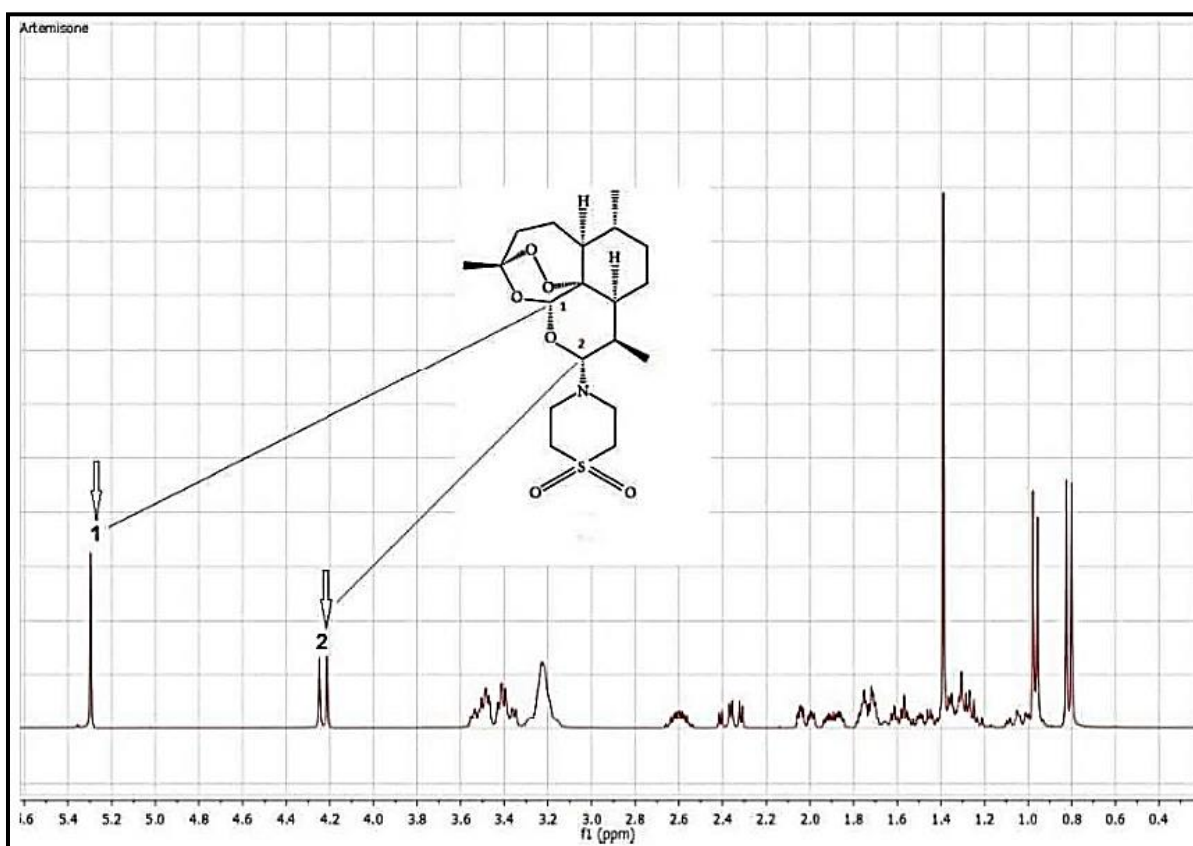

Figure 24 1HNMR spectrum of pure ART in CDCl3.

Table 5 Determination of ART content by NMR spectroscopy (solvent: CDCl3)

ART loaded sample	Theo. ART content (% wt.)	Integral$_{ART}$/Integral$_{PCL-b-MPEG}$	Exp. ART content (% wt.)	Assay (%) ± SD
NFN-formulation 1	14.3	4.15	14.26	99.70 ± 0.5
NFN-formulation 2	12.5	3.61	12.41	99.28 ± 0.5

It should be noticed that for all assay determination studies, a previously calibration line (Fig. 26) obtained from the standard calibration line was used as the reference.
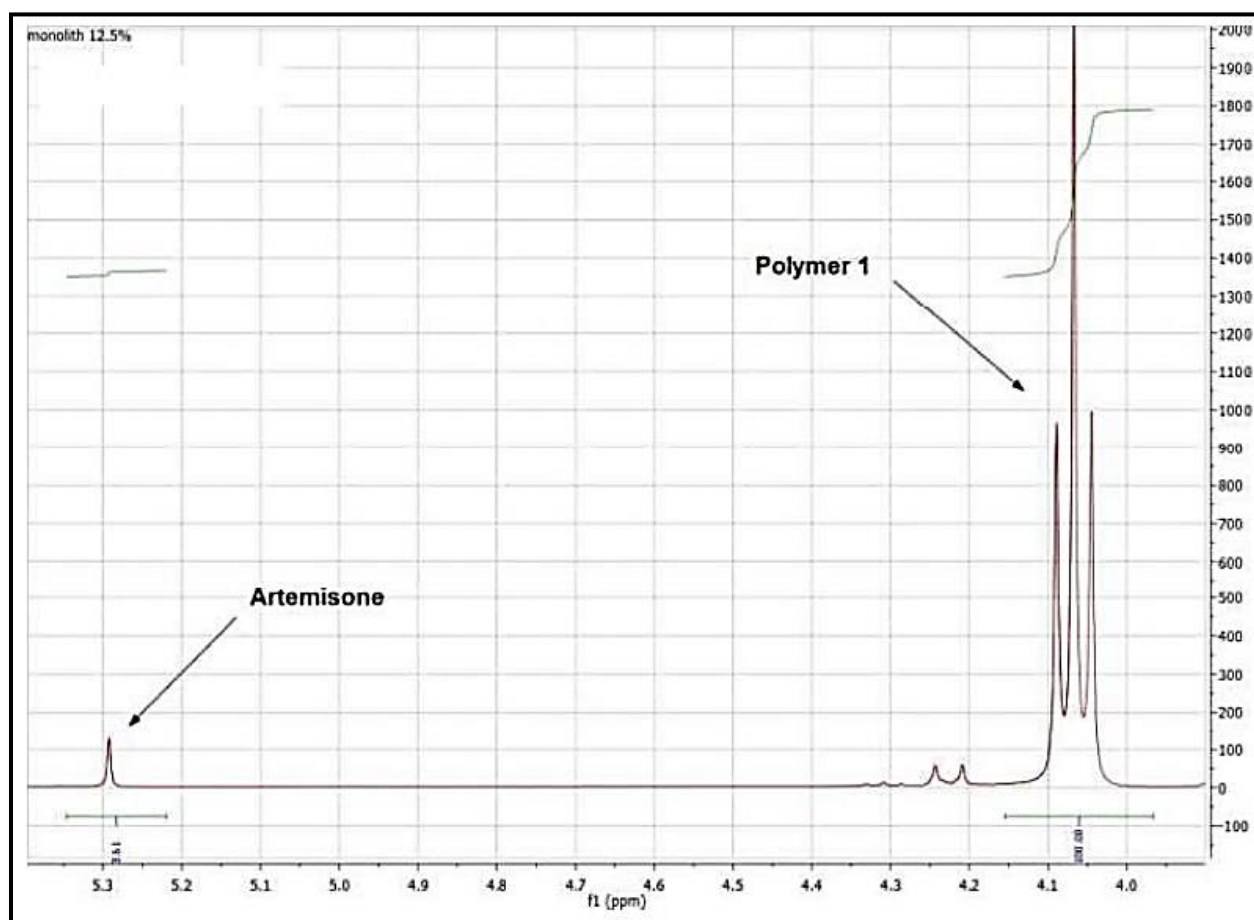

Figure 25 1HNMR spectrum of ART loaded NFN with the drug content of 12.5 wt. %
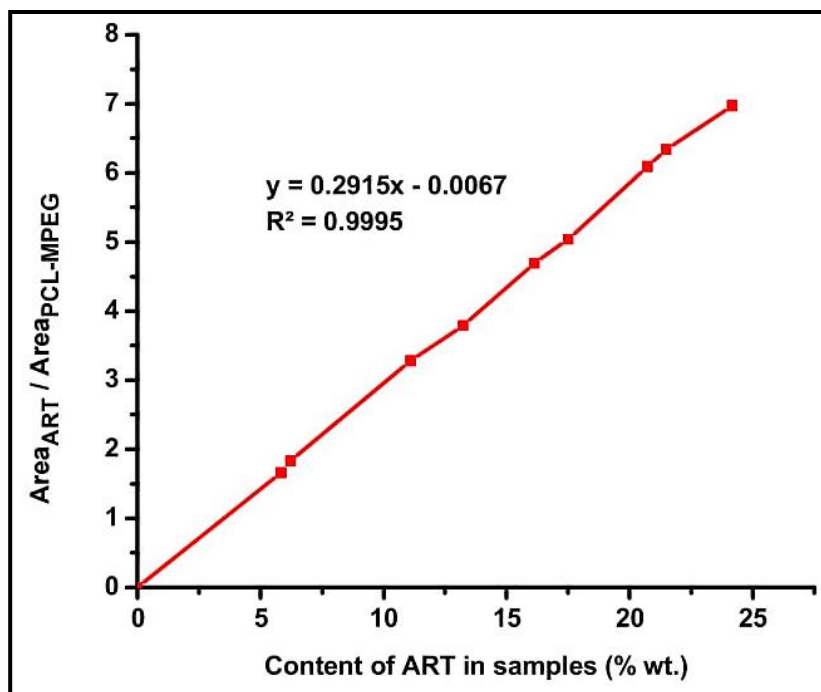
Figure 26 Calibration line of standard solutions of ART and polymer in CDCl$_3$, relative standard deviation (RSD) values were for all experiments below 2%

3.3.2 Determination of drug content in electrospun DDS by HPLC

HPLC instrument was equipped with an Eclipse XDB-C18, 4.6 x 150 mm, 5 µm column. The acetonitrile (50 % v), H$_2$O (30 % v), and methanol (20 % v) was used as mobile phase with a UV detector at λ: 260 nm. The temperature of the column was set to 35°C, the flow rate of the mobile phase was 0.8 ml/min, and the injection volume was 20 µl**.** The different NFN were dissolved in the mobile phase, and encapsulated ART was readily dissolved in the solvent after stirring at room temperature for estimation by HPLC. For this purpose, at least three samples of ART loaded products were dissolved in the mobile phase and then analyzed at λ: 260 nm by HPLC (Fig. 27). The assay values were achieved by comparison between data obtained from ART loaded samples and the standard data which were gained from standard solutions (Fig. 28). These results were compared with

results from quantitative NMR. This comparison confirmed that all assay data are reproducible and repeatable in both methods.

Table 6 Determination of ART contents by HPLC

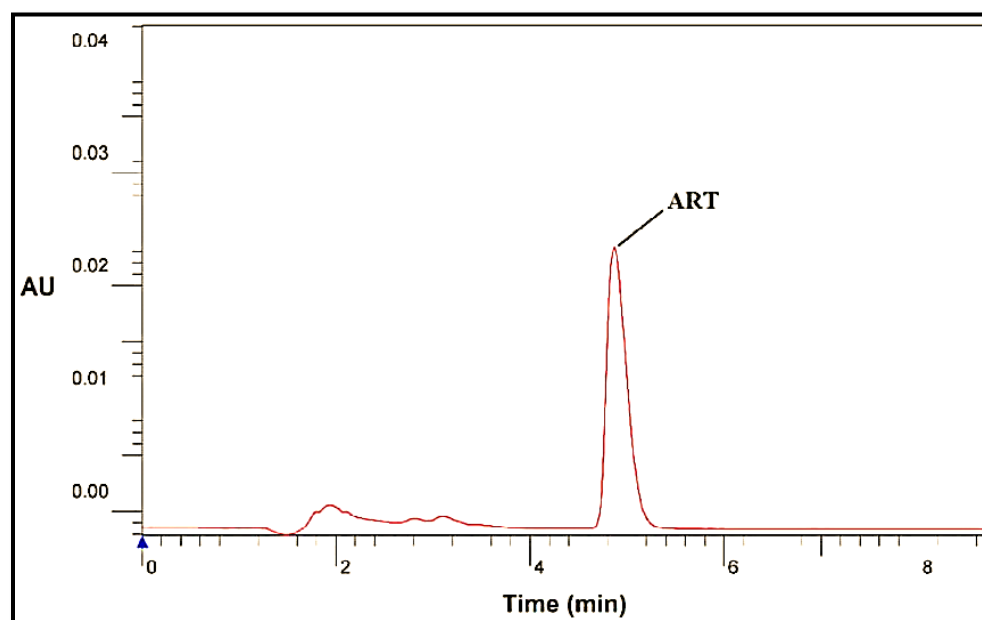| ART loaded sample	Theo. ART content (% wt.)	Exp. ART content (% wt.)	Assay (%) ± SD
NFN-formulation 1	14.3	14.26	99.70 ± 0.5
NFN-formulation 2	12.5	12.41	99.28 ± 0.5

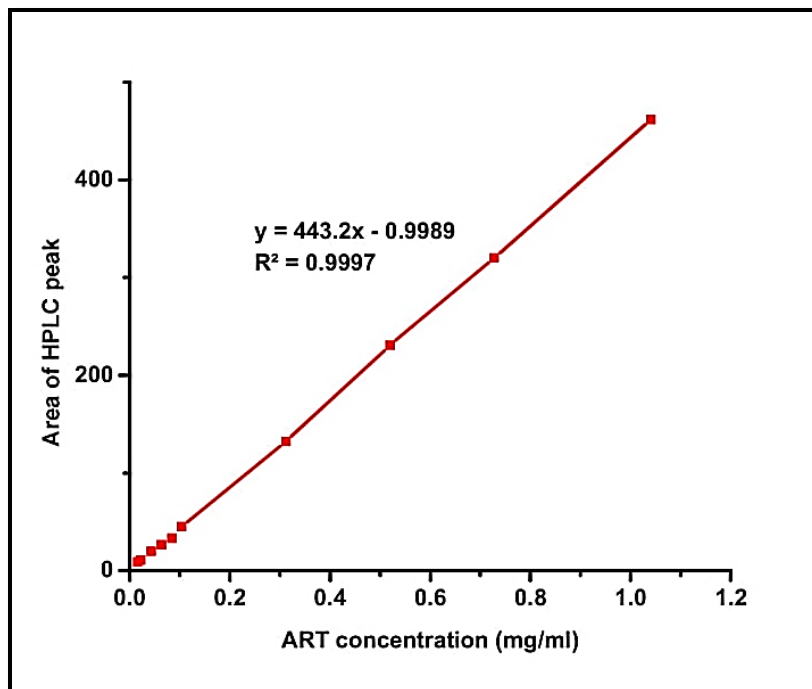**Figure 27** HPLC chromatogram of eluted ART from NFN in the mobile phase

Figure 28 Validation of HPLC method based on repeatability for different solutions. RSD values were for all experiments below 2%.

3.4 Studies on drug release behaviors of ART from NFN

HPLC studied the in vitro ART release characteristics from NFN with PBS (phosphate-buffered saline) of pH 7.4 as release test medium (Fig. 29). The complete release of ART within 5 hours in PBS solution was only about 13.23 ± 0.036 wt.%. The explanation for this relatively low and slow release of ART from NFN is its limited solubility in PBS: the maximum solubility of ART in PBS as determined by HPLC analysis was only 0.074 ± 0.002 mg mL^{-1}. Even with an extended-release time of several days (not shown here) a 100 wt.% Cumulative ART release was never observed. The solubility and release of ART were enhanced significantly to 1.79 ± 0.01 mg mL^{-1} with 1% w/v of sodium lauryl sulfate (SLS) in water as release medium (pH ~ 7.4, adjusted with sodium bicarbonate). SLS acts naturally as a surfactant for ART, as it is known to enhance solubility for other

hydrophobic drugs [117-119]. Consequently, fast and 100 wt.% the release of ART from NFN could be achieved by using the SLS medium in less than 1 h, with more than 70% drug released in about 30 min (Fig.30).
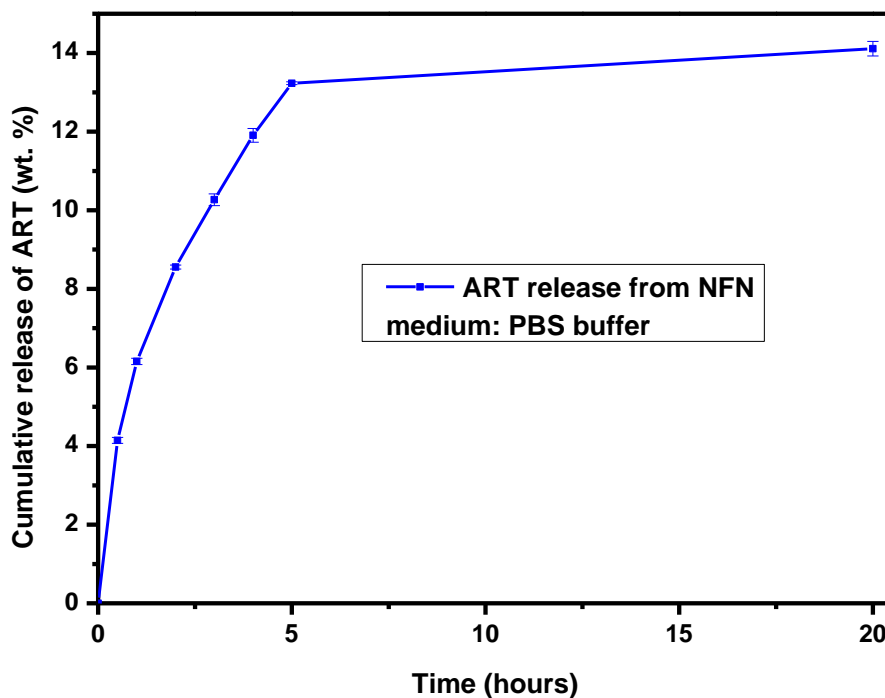

Figure 29 In vitro cumulative release of ART from uncoated NFN, in an aqueous solution containing PBS buffer, ART content for all samples: 12.5 wt% and mean quantities of ART in all samples: 5.55 ± 0.34 mg.
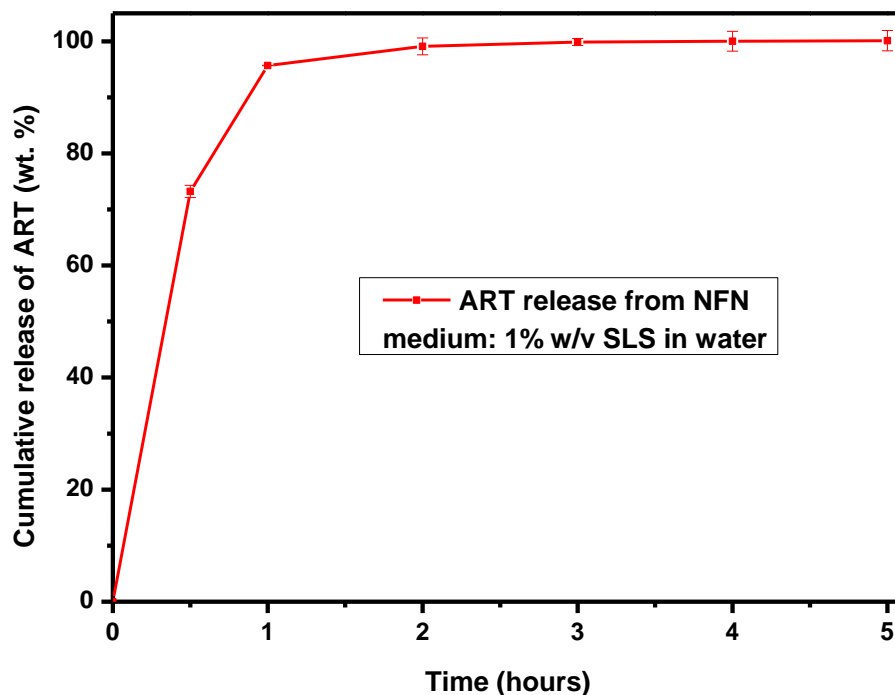
Figure 30 In vitro cumulative release of ART from NFN in an aqueous solution containing 1 w/v % SLS, ART content for all samples: 12.5 wt% and mean quantities of ART in all samples: 5.55 ± 0.34 mg.

3.5 Degradation of ART in an aqueous environment

We also carried out stability studies of ART powder to have the basis for comparison. In our studies, at 37 ± 0.5 °C, almost 10 wt.% of the ART powder was degraded in 1% w/v SLS at pH 7.4 ± 0.1 in the first 5 h. Whereas, ≈86 wt.% of ART was decomposed in contact with SLS medium after 19 d (Fig. 31). The appearance of new signals in HPLC, in combination with the decline of the signal for ART, became evident by comparison of the HPLC traces of a fresh ART solution, with a solution after storage for 308 h. The dissolved drug was analyzed by HPLC for checking the stability (Fig. 32). The instability of ART in aqueous media is one of the known problems giving degradation products of unknown toxicity and wastage of the valuable drug.
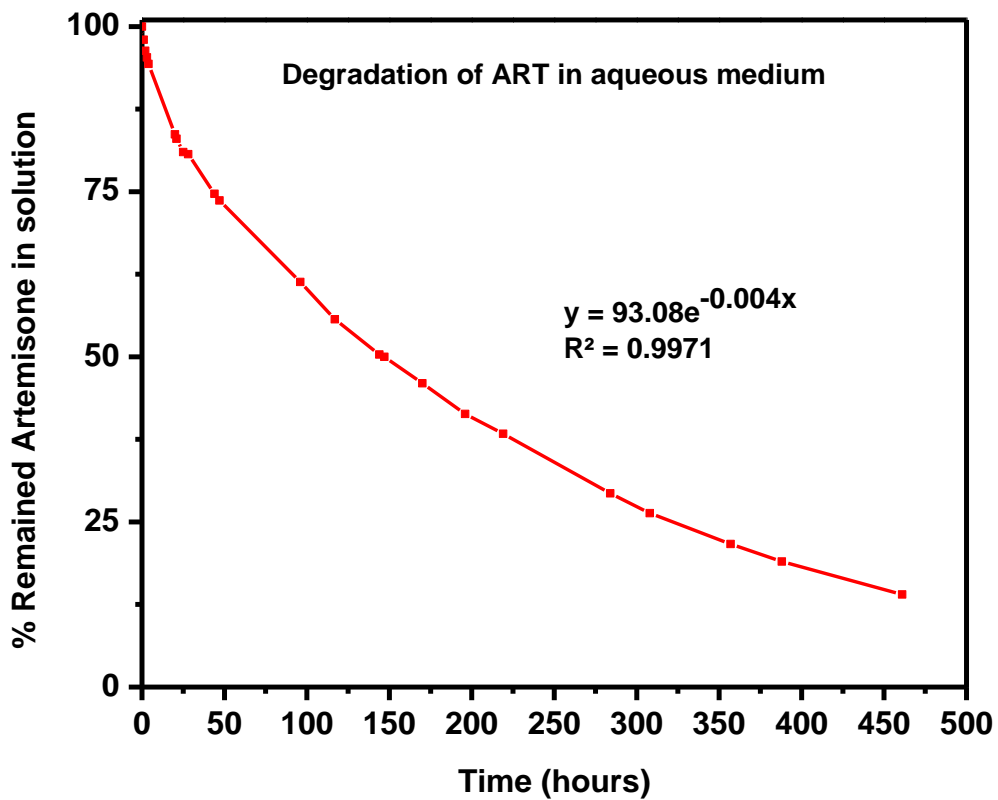
Figure 31 Decomposition of ART in aqueous medium composed of 1 % w/v SLS, pH of medium: 7.4 ± 0.1 and temperature: 37 ± 0.5 °C. Concentration of ART: 1.03 ± 0.02 mg/ml. All tests were repeated three times. RSD *values for all experiments were below 2 %.*
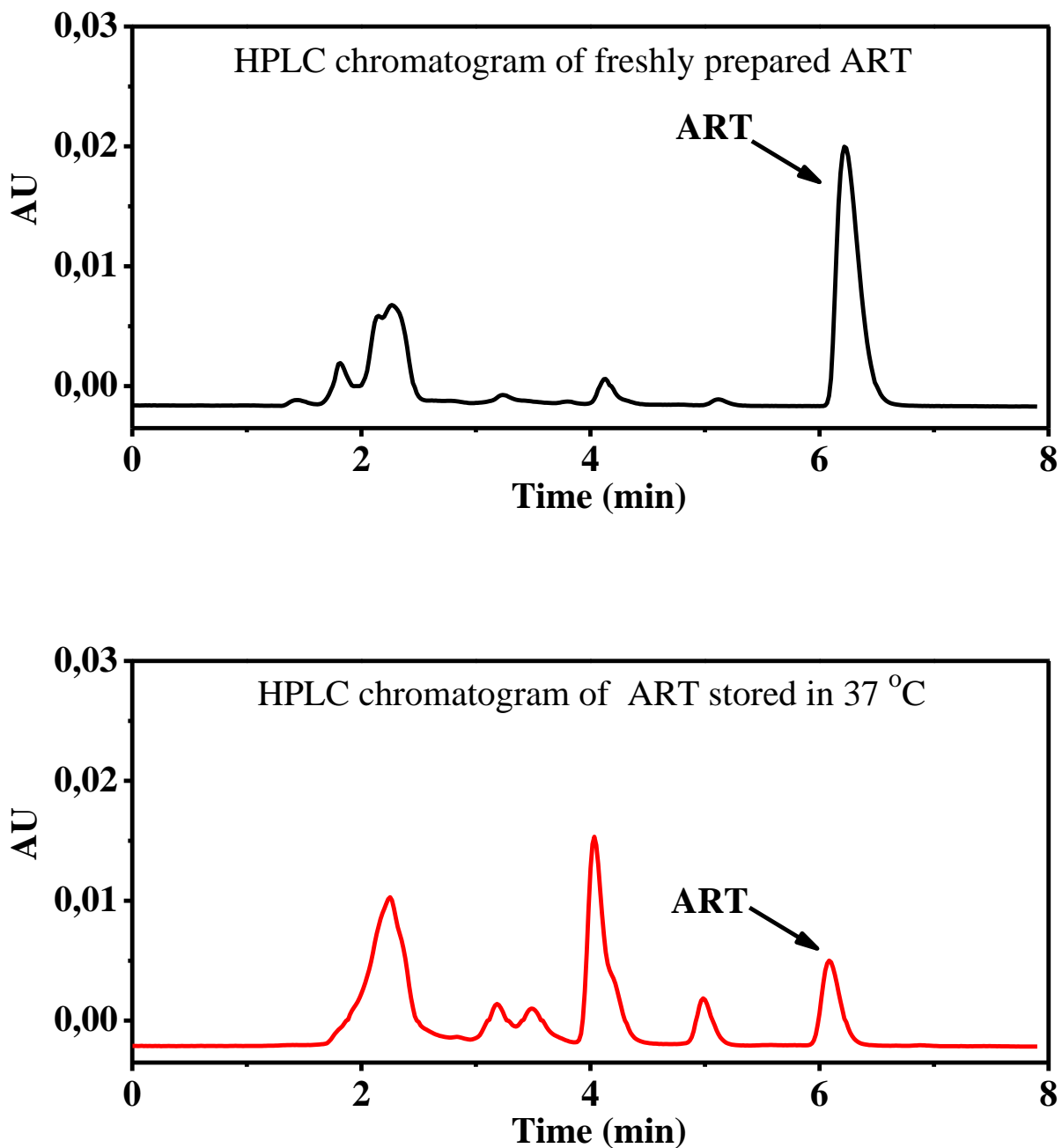
Figure 32 HPLC chromatograms of fresh ART solution before and after 20 days of storage

3.6 Managing of the rate of ART release from NFN by coating

HPLC studied the in vitro ART release characteristics from NFN with PBS (phosphate-buffered saline) of pH 7.4 as the release test medium. The complete release of ART within 5 h in PBS solution was only about 13.23 ± 0.036 wt.%. The explanation for this relatively low and slow release of ART from NFN is its limited solubility in PBS; the maximum solubility of ART in PBS as determined by HPLC analysis was only 0.074 ± 0.002 mg mL^{-1}. Even with an extended-release time of several days (not shown here) a 100 wt.% Cumulative ART release was never observed. The solubility and release of ART were enhanced significantly to 1.79 ± 0.01 mg mL^{-1} with 1% w/v of sodium lauryl sulfate (SLS) in water as a release medium. SLS acts obviously as a surfactant for ART, as it is known to enhance solubility for other hydrophobic drugs. Consequently, fast and 100 wt.% the release of ART from NFN could be achieved by using the SLS medium in less than 1 h, with more than 70% drug released in about 30 min.

To overcome the burst release of ART and the problem of the instability of ART in contact with media, we applied the CVD coating of PPX of different thicknesses (68–870 nm) on the ART containing NFN.
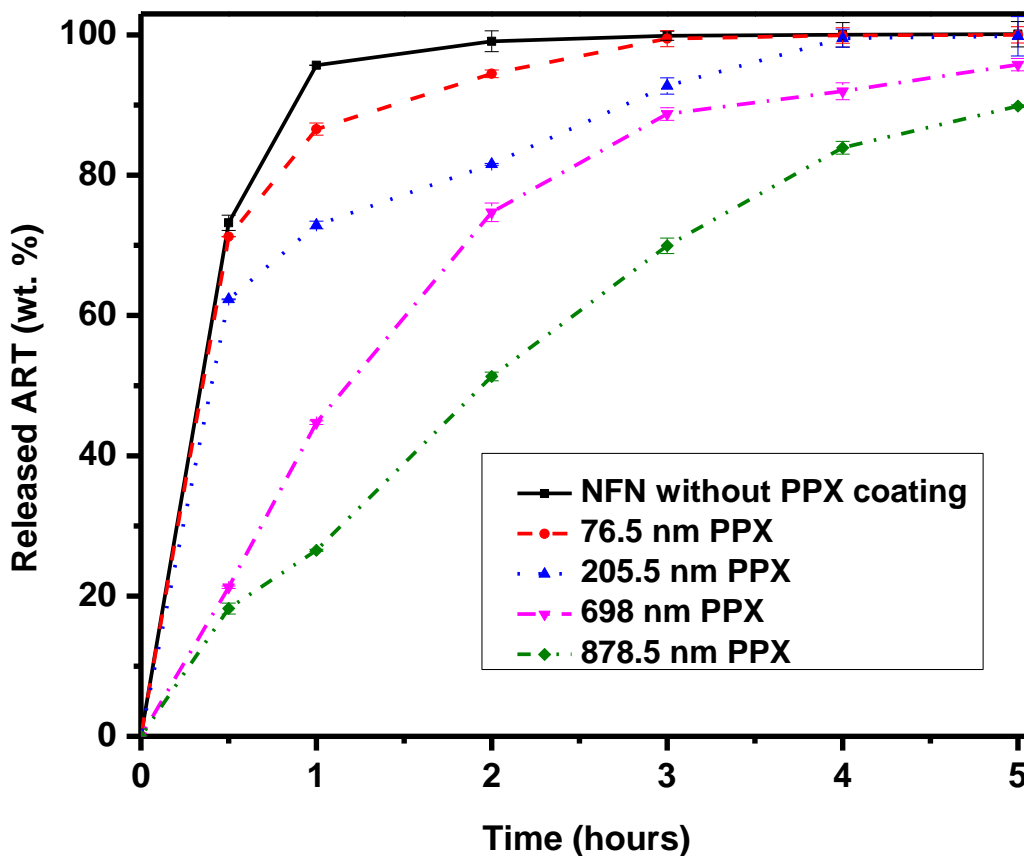
Figure 33 In vitro cumulative release of ART from uncoated and PPX coated NFN in an aqueous solution containing 1% SLS, ART content for all samples: 12.5 wt% and mean quantities of ART in all samples: 5.55 ± 0.34 mg.

Two other coating agents were also used for the fabrication of biocompatible nanofibrous structures: 1. Aqueous dispersions of PCL-MEPG and 2. In water dissolved Gelatin. Coated membranes were produced by the dip-coating technique. Both of the coatings could reduce the rate of drug release from nanofibrous mats. The more retarded release could be earned by PCL-MPEG coated fibers because of its dispersity but not solubility nature in water compared to the solubility of gelatin.

The kinetic of the drug release from coated mats are presented below (Fig. 34). All these attempts could confirm this reality that the coatings are an excellent device to overcome the burst release kinetics from nanofibrous mats and to control the rate of the drug release. The dispersion coatings showed more retarded release compared to gelatin coatings due to its more hydrophobic tendency.
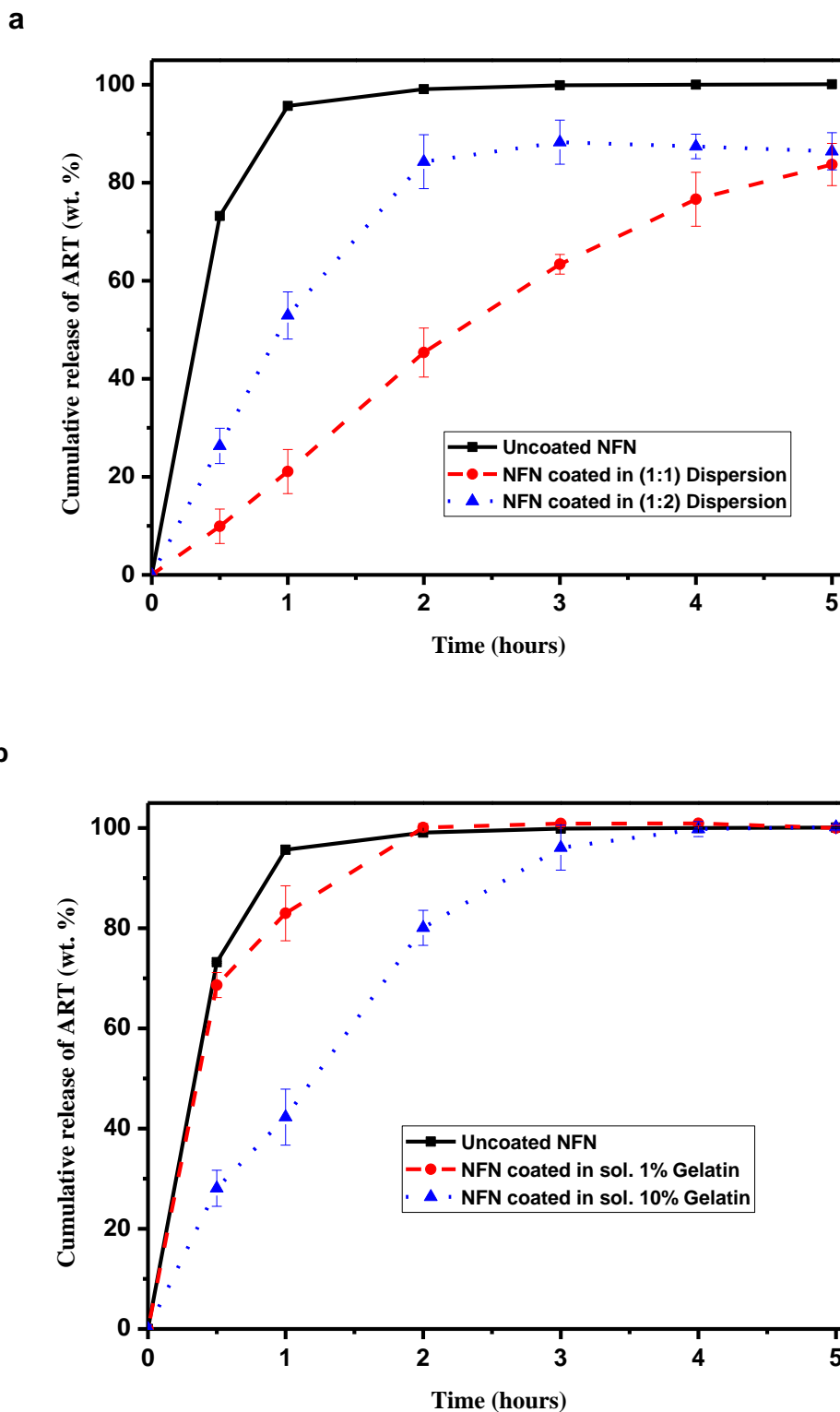
a

b

Figure 34 In vitro cumulative release of ART from uncoated and coated NFN in an aqueous solution containing 1% SLS, ART content for all samples: 12.5 wt.% and mean quantities of ART in all samples: 5.0 ± 0.5 mg.

3.6.1 Coating with PPX

PPX is a biocompatible polymer, which has been used successfully as a coating on films for the retardation of the release of dexamethasone and NFN for the retardation of enzyme release [116]. The particular advantages of the CVD coating by PPX are very mild conditions (no solvent, no catalyst, room-temperature processing) and the formation of conformal, pin-hole free coatings. As expected, the PPX coating retarded the ART release, and we observed a change from burst release (for uncoated fibers) to a linear ART release profile depicting a delay that depends on the PPX coating thickness (Figure 35).
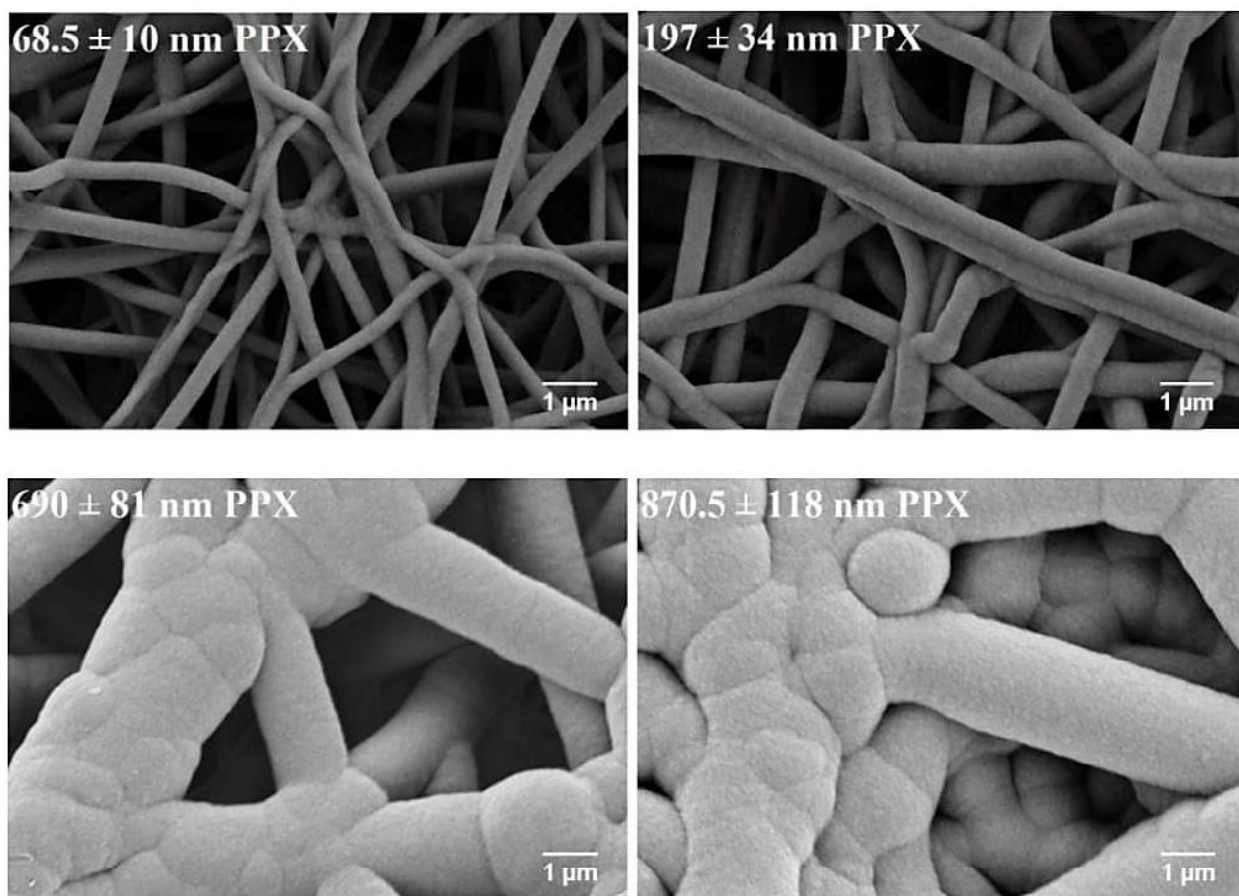

Figure 35 SEM images of PPX coated NFN with thicknesses from 68.5 to 870.5 nm used for in vitro release studies

3.6.2 Coating of NFN by dip-coating in the aqueous solution of gelatin and the aqueous dispersion of PCL-b-MPEG

Dip coating is the precision-controlled immersion and withdrawal of any substrate into a reservoir of liquid for the settlement of a layer of material. Many chemical and pharmaceutical research projects in academia and industry make use of the dip-coating technique.

In theory, dip coating is straightforward. The sample is perpendicularly dipped into a solution or dispersion. The sample is let to stay immersed in the solution to allow some time. After this, the sample is withdrawn out from the solution and let to dry.

The SEM images of ART loaded fibrous structures are demonstrated in (Fig. 36 a-e). It can be observed that by the addition of coating agents on the surface of membranes, the thickness of the resulting fibers has been increased. As showed, there were no detectable drug aggregates on the surface of NFN. A tendency to form the films from fibrous structures could be observed by increasing the concentration of coating agents and by fabrication of the structures wither thicker diameters (Fig. 36 c, d).

The EDX measurements confirmed the homogeneous distribution of ART in membranes (Fig. 36, f-e). The sulfur atom of medication was used as an indicator to follow the locations of encapsulated ART in nanofibrous structures. It should be noticed that EDX was applied here as a supporting method to investigate the homogenous distribution of ART in the carrier. Generally, the homogenous distribution of ART was investigated during the determination of the drug content by HPLC.
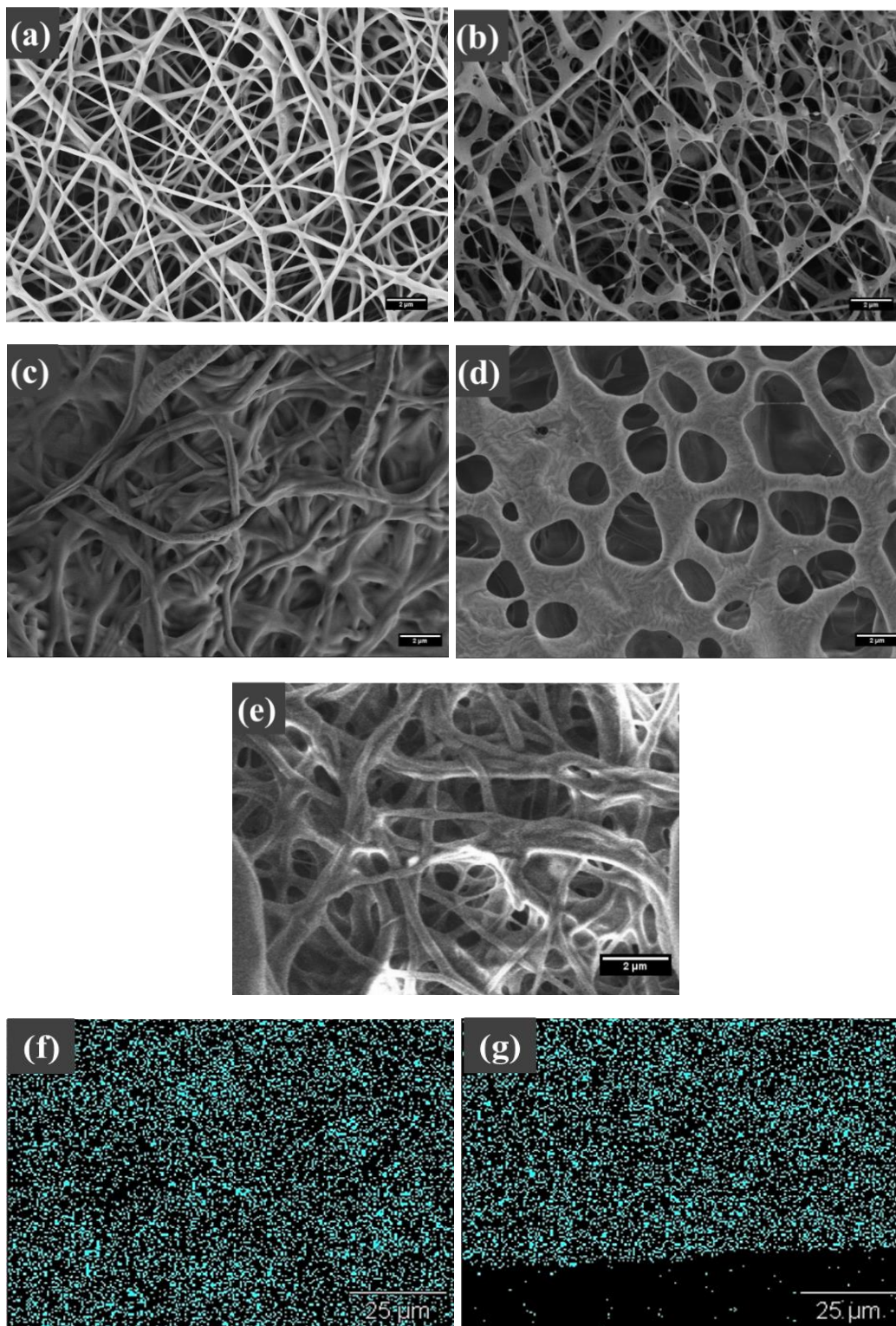
Figure 36 Morphological studies: a) original NFN, 193.82 ± 72.27 nm. b) NFN coated with 1% gelatin, 302.84 ± 73.49. c) NFN coated with 10% gelatin, 493.17 ± 89.88. d) NFN coated with dispersion 1, 1136.46 ± 336.04. e) NFN coated with dispersion 2, 461.74 ± 134.57. EDX-mapping of ART: f) surface of original ART loaded NFN and g) its cross-section.

3.7 Studies on drug release behaviors of ART from drug-loaded films

By entrapment of ART in pressed films, the rate of the drug release could be significantly reduced. Furthermore, the burst release, which typically can be observed during the drug release from the drug-loaded nanofibrous structure, could be reduced by the fabrication of such ART loaded films. While 100% release could be achieved from nanofibrous membranes during 3 hours, approx. 40% drug could be released from the film (thickness of 500 ± 20 µm) during 5 hours (Fig. 37). Additionally, as to be observed, the thickness of the carriers plays an essential role in controlling the rate of the drug release. More retarded drug release could be achieved by thicker films.
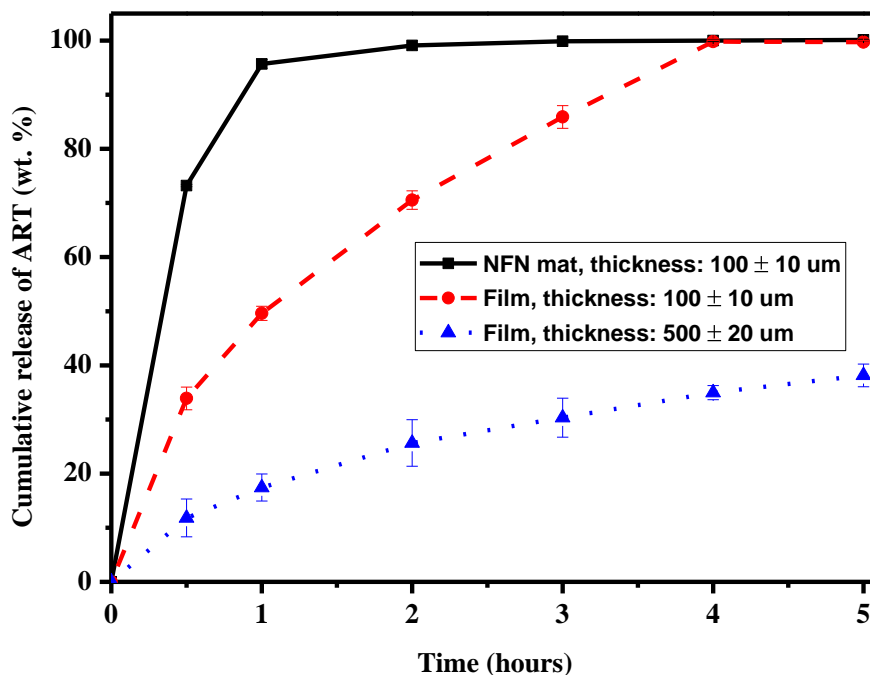

Figure 37 ART release from films and fibrous structures in an aqueous solution containing 1% SLS, ART content for all samples: 12.5 wt.% and mean quantities of ART in all samples: 5.0 ± 0.5 mg.

Morphological studies of the drug-loaded films showed the non-smooth surfaces because of the presence of crystalline ART pressed in films (Fig. 38a). Anyhow, the EDX measurements confirmed the homogenous distribution of ART in polymeric films not only in surface but also in the inside of films (Fig. 38 b,c).
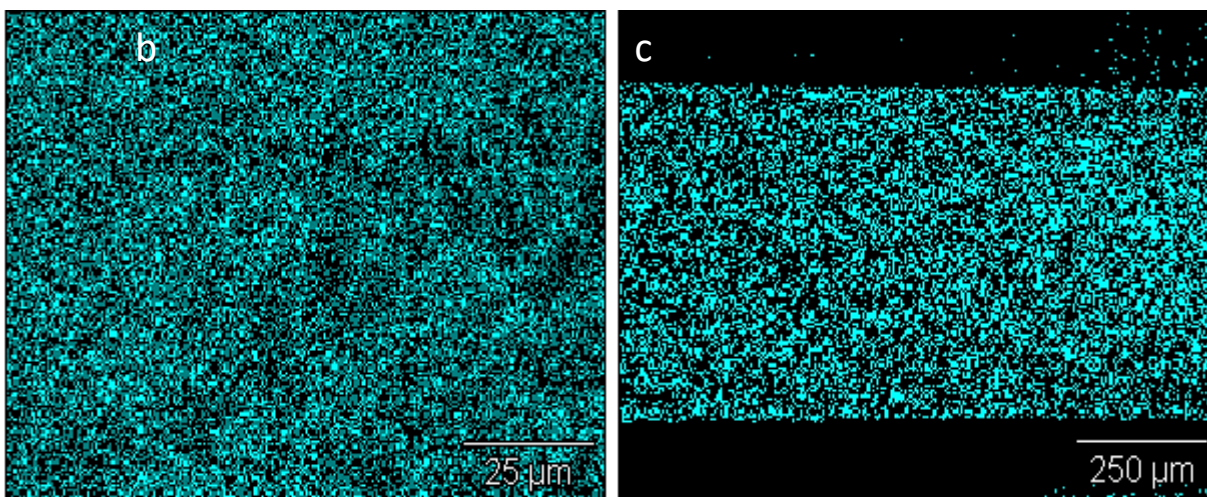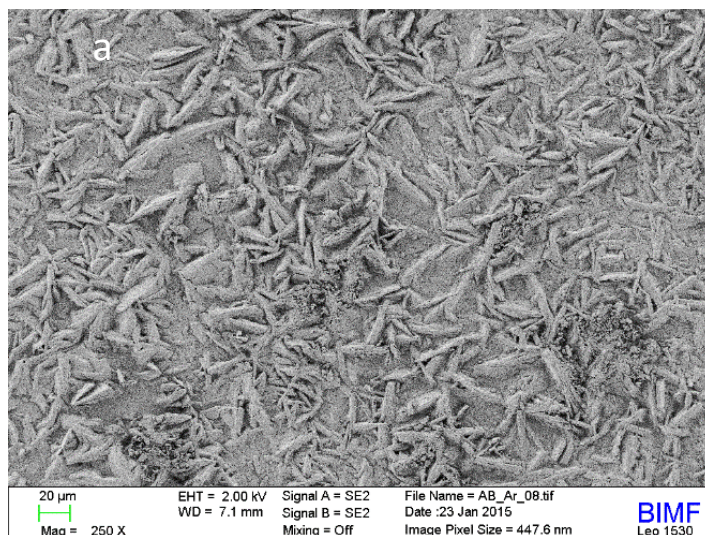

Figure 38 Morphological studies of ART loaded films (thickness: 500 ± 20 µm), ART content for all samples: 12.5 wt.%

X-ray tests were performed to determine the physical status of ART in films. As showed in Fig. 39, PCL-MPEG as a semi-crystalline polymer, demonstrated detectable peaks at 2θ: 21.6° and 23.8°. ART also showed a crystalline structure so that the clear signals at 12.30°, 16.80°, 17.50° and 18.40° could be detected (Fig. 39). Interestingly in WAXS patterns of ART loaded NFN, no main characteristic signals of ART could be observed. It means ART was no longer present as a crystalline material and had been converted mainly into an amorphous state. The pressed films, unlike the electrospun nonwoven, showed visible signals composed of standard characteristic signals of both ART and polymer. The films could keep their crystalline structures because, during the film pressing, they have enough time to be recrystallized, unlike the electrospinning process.
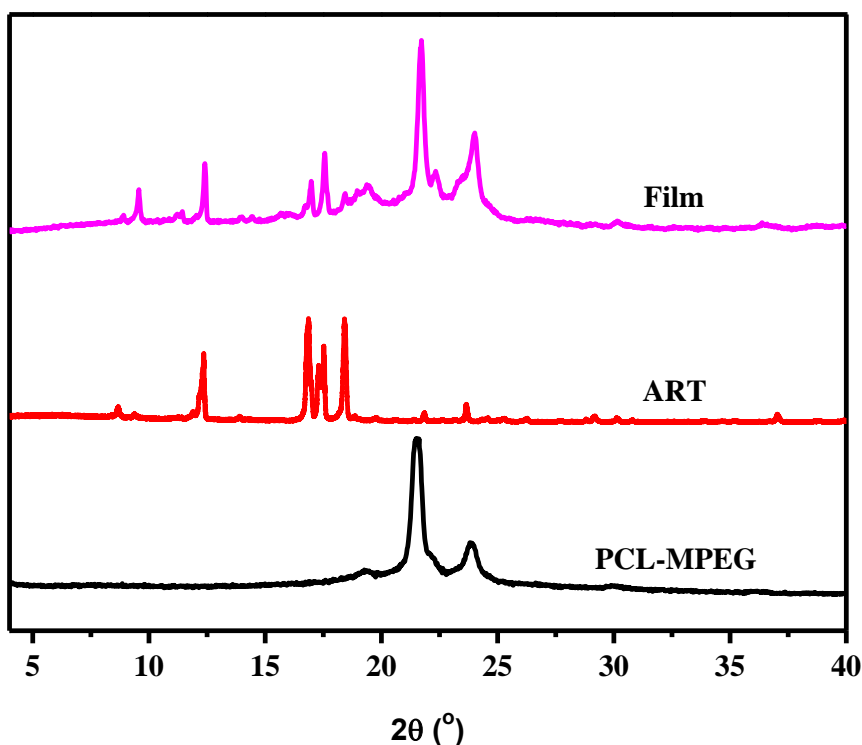

Figure 39 Morphological studies of ART loaded films (thickness: 500 ± 20 μm), ART content for all samples: 12.5 wt.%

3.8 Degradation studies on NFN and films fabricated from PCL-MPEG

The enzymatic degradation experiments of polymeric carriers showed interesting behaviors (Fig. 40). The films showed higher stability in the enzymatic environment (Esterase EL-01) compared to nanofibrous structures. By increasing the thickness of films, they could be more resistant. Mainly, the films were till 3 hours, relatively stable against degradation but after 3 hours, degradation was accelerated after the first bulk degradation and incorporation of water in films. Unlike this mechanism, NFN mats showed a linear degradation behavior. It can be interpreted because of porous structures of NFN and higher water uptake capacity. More retarded degradation nature of films supports more retarded drug release behavior of these carriers additionally.
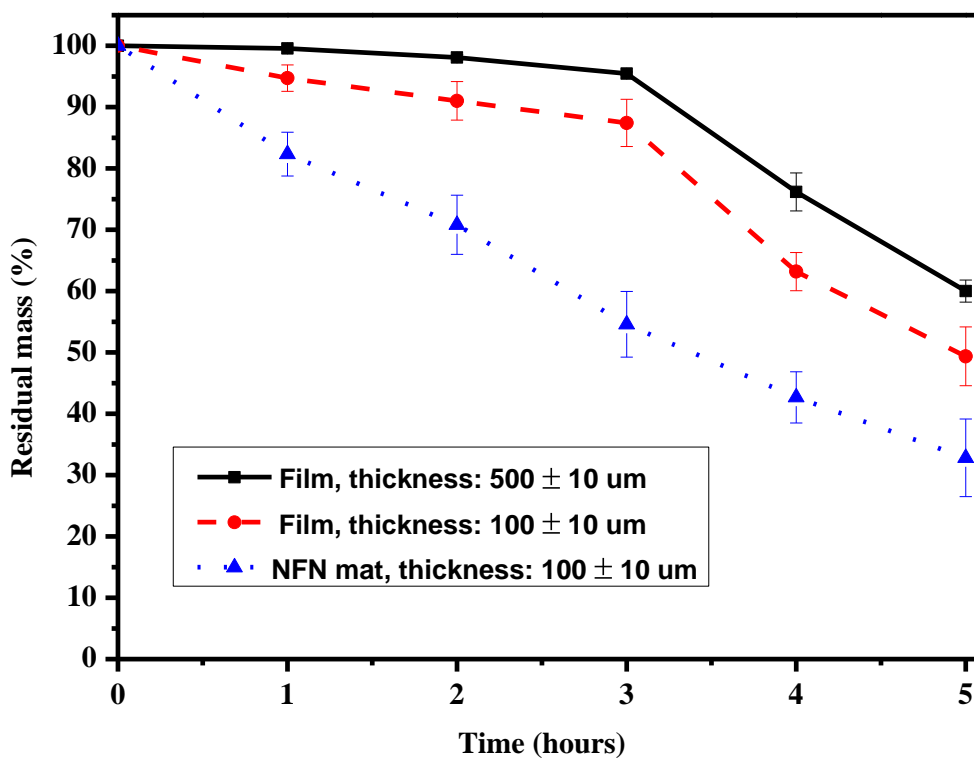
Figure 40 Enzymatic degradation of the polymeric carrier (matrix)

3.9 Water uptake by NFN and films fabricated from PCL-MPEG

The determination of swelling ratios of matrix structures (NFN and films without drug) can be observed in Fig. 41. The water uptake ability by NFN higher compared to the films. This could be interpreted probably because of a large amount of water retained in the fibrous pores and also due to the higher surface area of NFN. Interestingly, by increasing in the thickness of the films, the swelling ratio values were decreased. All these findings support the more retarded drug release from films, particularly thick films. The swelling results were calculated according to the following equation for each sample:

$$\text{Swelling ratio (\%)}: \frac{m_2 - m_1}{m_1} \times 100$$

m_2 represents the weight of the scaffold in wet condition and m_1 the weight of the same dried scaffold.

Figure 41 Comparison between swelling ratios of matrix

3.10 Studies on drug release behaviors of ART from drug-loaded 3D structures
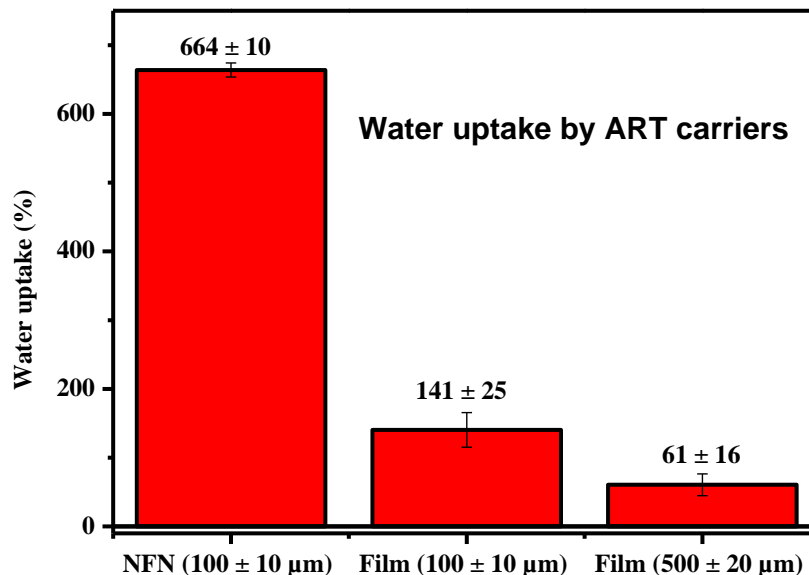
In this study, the ultralight sponge fabricated by an acrylate copolymer [poly(methyl acrylate(MA)-co-methylmethacrylate(MMA)-co-4-methacryloyloxybenzophenone (MABP) was used as 3D carrier. Two different densities, 3.5 and 6 mg/cm^3 of this sponge were explicitly considered for drug loading and also studies on the drug release. The applied sponges are shown here as d3.5 and d6 (d3.5= sponge with density of 3.5 mg/cm^3 and d6= sponge with density of 6 mg/cm^3).The sponges included pores with a size of about 100 µm and pores of a few micrometers, between the fiber interconnections (Fig. 42 A, B). High ART loading was accomplished with sponge d6, which is shown in Fig. 42 C, D. Generally, the mechanical properties of sponge d3.5 due to its very low density was too low for the applied loading procedure. Regarding to the much better mechanical stability of d6, most of the following experiments were focused on the d6.
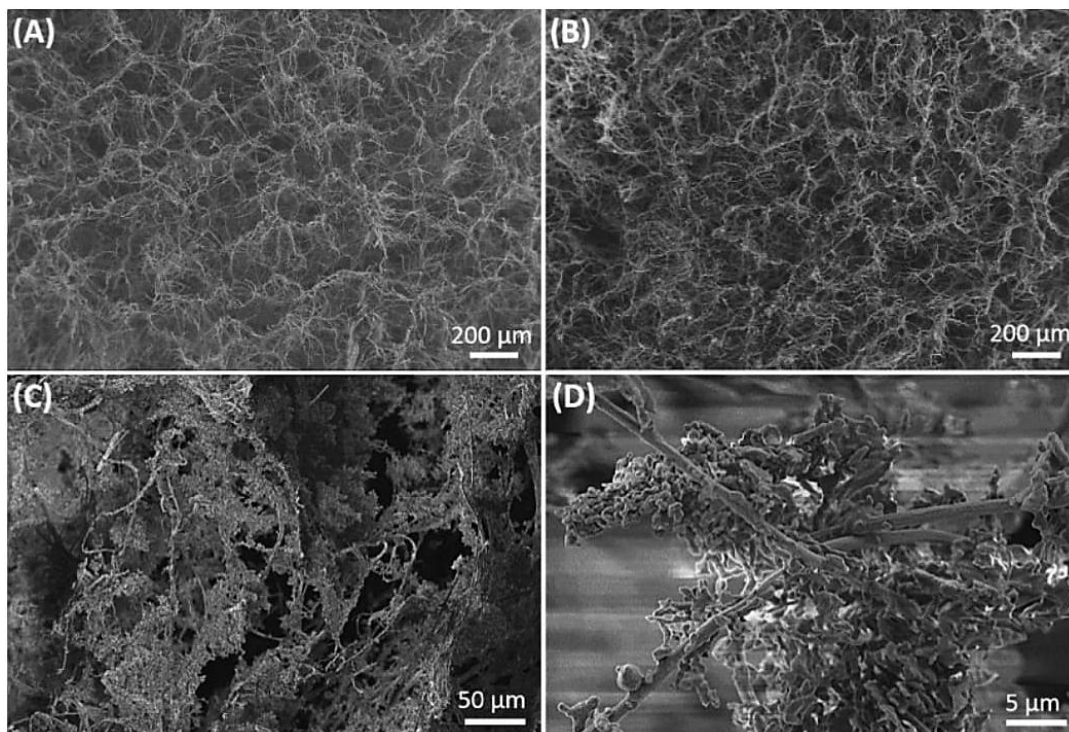

Figure 42 Cross-sectional SEM images of as-prepared sponges d3.5 (A) and d6 (B), and d6 after loading with ART (C, D).

In parallel with the increased concentration of the ART solution from 14 to 25 mg/mL, the ART loading amount of d6 (2.51 mg) was changed from approx. 4. 7 to 6.6 mg, meaning that the loading capacity was increased from 1870 to 2640 mg/g (ART loading ratio increasing from 1.87 to 2.64) (Table 7).

Table 7 Change of ART Loading Capacity of d6 by Using tert-Butanol Solutions of ART with Concentrations of 14 and 25 mg/mL

Concentration of ART in t-butanol (mg/ml)	mass d6 (mg)	mass d6+drug (mg)	mass ART (mg)	ART loading ratio (mass ART/mass sponge)
14	2.47	6.78	4.31	1.75
	2.56	7.32	4.76	1.90
	2.51	7.45	4.94	1.97
	Mean: 2.51 ± 0.05	Mean: 7.18 ± 0.36	Mean: 4.67 ± 0.32	Mean: 1.87 ± 0.11
25	2.38	8.71	6.34	2.66
	2.62	9.31	6.70	2.56
	2.54	9.39	6.85	2.70
	Mean: 2.51 ± 0.12	Mean: 9.14 ± 0.37	Mean: 6.63 ± 0.26	Mean: 2.64 ± 0.07

Overall, the macroporous sponge had very high ART loading capacity. However, ART was loosely placed on the surface of the fibrous network of the sponges or just settled in the pores, which would lead to losses induced by mechanical stress and to burst release of ART during the initial release process.

The small crystals of ART could be dissolved in the first stages of the release process. This behavior caused a burst release, seen in the initial 20 min. After that, the bigger particles of ART crystals gradually dissolve, initiating the retarded release. By loading the drug in the fibrous sponge with small density (3.5 mg/cm^3, d3.5), 100% of the drug was released within the first hour. The ART loaded sponges were treated by freeze-drying that could cause ART recrystallization into small crystals with a size of several micrometers, which led to the fast dissolution in the liquid medium and the fast burst release.

In comparison, when the sponge with higher density (6 mg/cm^3, d6) was used, a more retarded release could be achieved: about 50 and 87 wt. % of ART was released in 2 and 5 h, respectively. The different drug release profiles from the sponges (d3.5 and d6) could be related to the much higher specific pore volume (SPV) of d3.5 compared to d6, which facilitated the mass transfer of ART to the liquid medium.
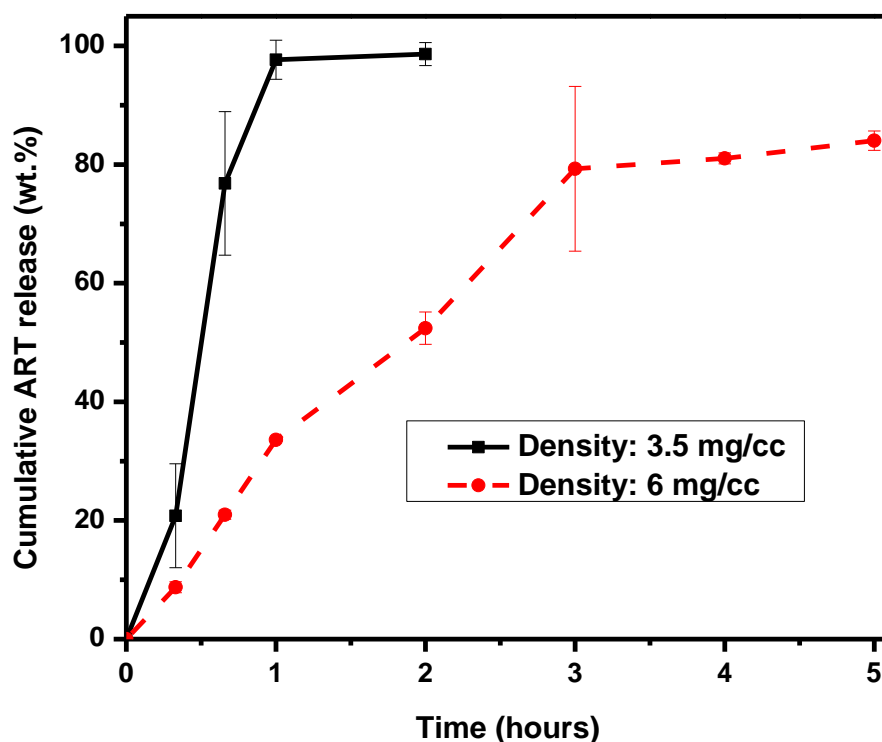

Figure 43 In vitro ART release from the ART loaded sponges with different densities (3.5 and 6 mg/cm^3)

3.11 Studies on drug release behaviors of ART from drug-loaded microparticles

In the last parts of this project, several kinds of carriers were used to deliver the antimalarial ART. As demonstrated previously, several kinds of kinetics from burst release to retarded release behavior could be achieved. Investigation of the release behavior of a hydrophobic drug like ART is essential to manage the drug release. Microparticles, as another kind of carrier, can also play an essential role in controlling the drug release.

In this part of this project, we focused on gelatin as the biocompatible and soluble biopolymer to fabricate ART loaded microparticles. A spray drying technique could produce gelatin microparticles. This technique is especially well known and applicable to solubilize the hydrophobic drugs because, by this technique, the size of drug molecules can be managed in a wide range from few nanometers to micrometers. Furthermore, the re-crystallization of the drug molecules is de facto so fast that the crystallinity behavior of substance can be changed and generally moderated. Therefore, the hydrophobicity of the drug molecule can also be moderated, and a shift in the solubility nature of the drug can be observed. Finally, the drug molecule will be more soluble in the aqueous environment after spray-drying.

This behavior could be easily observed by ART loaded gelatin particles in this project. In this work, particles with 2-4 μm could be fabricated from aqueous solutions, and during approximately 40 minutes, the 100 %-drug release could be earned (Fig. 44). This release behavior can be fascinating, especially for nasal administrations.
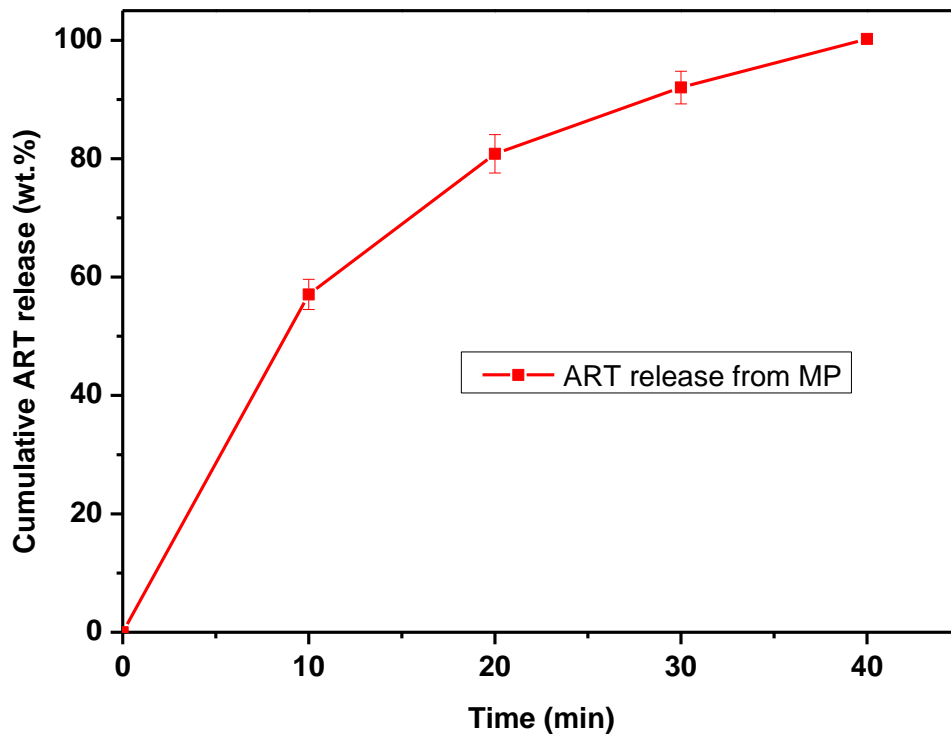
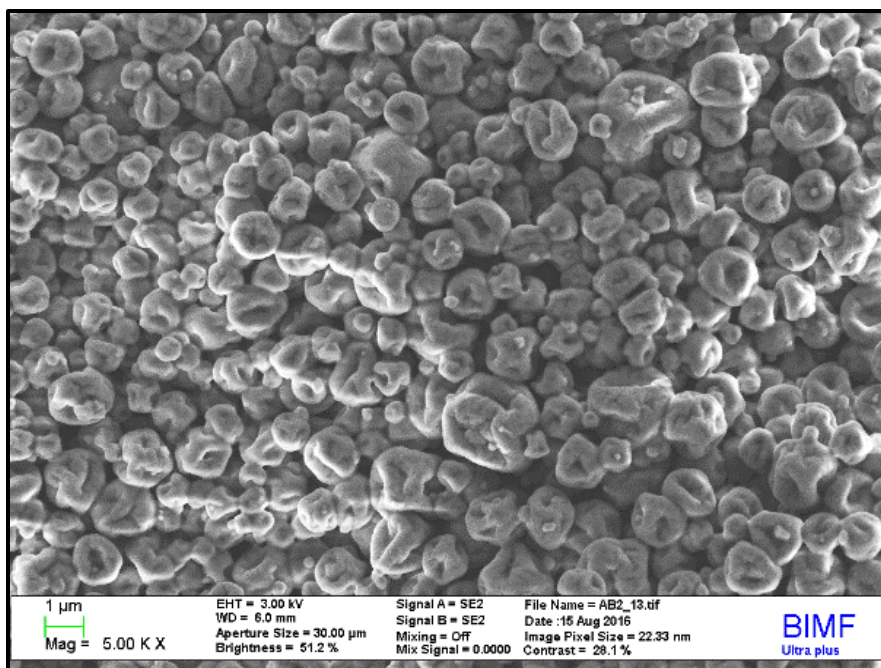**Figure 44** In vitro ART release from the ART loaded microparticles

Figure 45 SEM images of ART loaded gelation microparticles

3.12 Administration of ART loaded macromolecular carriers

ART loaded macromolecular scaffolds were administrated in mice models in biological labor to study the curative effects of these structures in frame of the in vivo studies. These studies were performed by Prof. Jacob Golenser's research group at Hebrew University of Jerusalem. The results obtained from these in vivo studies are reported in this thesis after discussion with Prof. Golenser and presented here as supporting information.

3.12.1 Administration by implantation

Mice were injected intraperitoneally with *Plasmodium berghey* ANKA. Inserts (including films and NFN) containing artemisone or blank inserts were introduced subcutaneously on different days post or before infection, as indicated (n= number of mice in the group. D= dead.) Death of mice with parasitemia below ~20% parasitemia accompanied by a typical disease is considered as the death of cerebral malaria (CM). All control mice died of CM. Each line represents a single mouse.

3.12.2 In vivo studies of ART loaded films

ART loaded films were applied to insert into the infected mice after 1- and 6-days infection. The results have been demonstrated in Fig. 46. As shown, all infected mice were cured, even those who had 6-days infection. These results confirmed that a dose of 2 mg ART is a curing dose for the treatment of infected mice under defined in vivo conditions. As expected, films with approx. 500 µm thickness support the retarded release and furthermore, the loaded ART can be stabilized longer and, therefore, longer effective against infection if it is entrapped in thick films.
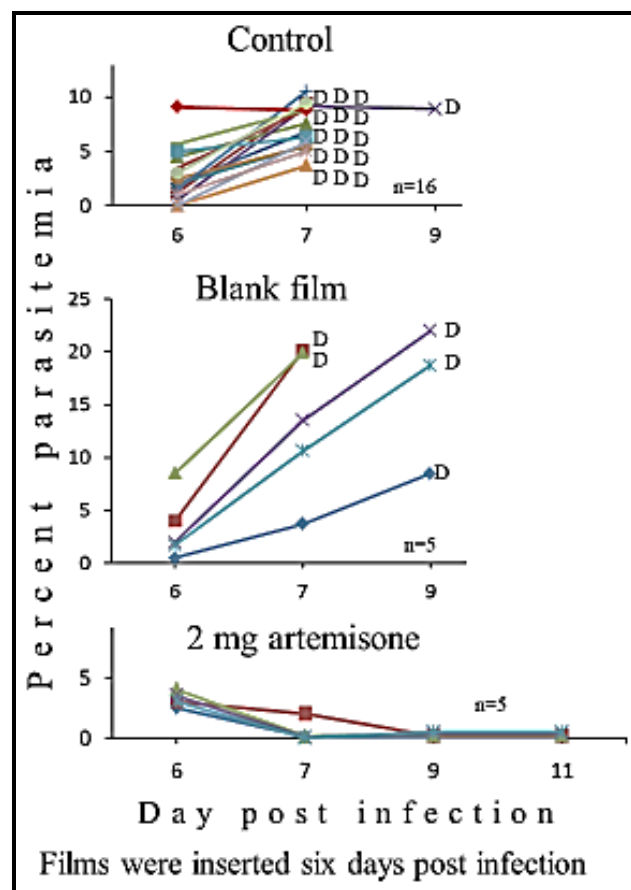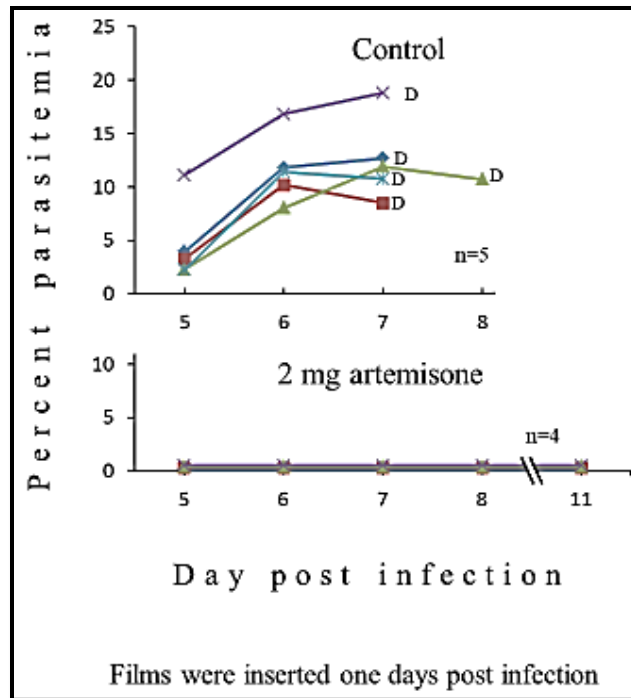
Figure 46 Insertion of ART loaded films after 1- and 6-days post-infection, the dose of ART: 2 mg

3.12.3 In vivo studies of ART loaded NFN

ART loaded NFN were applied to insert into the infected mice after 2- and 7-days infection. The results have been demonstrated in Fig. 47. As shown, all infected mice were cured after 2 days of infection. However, the infected mice which had 7-days infection could not be cured anymore. These results confirmed that loaded 2 mg ART were not enough to rescue the infected mice.
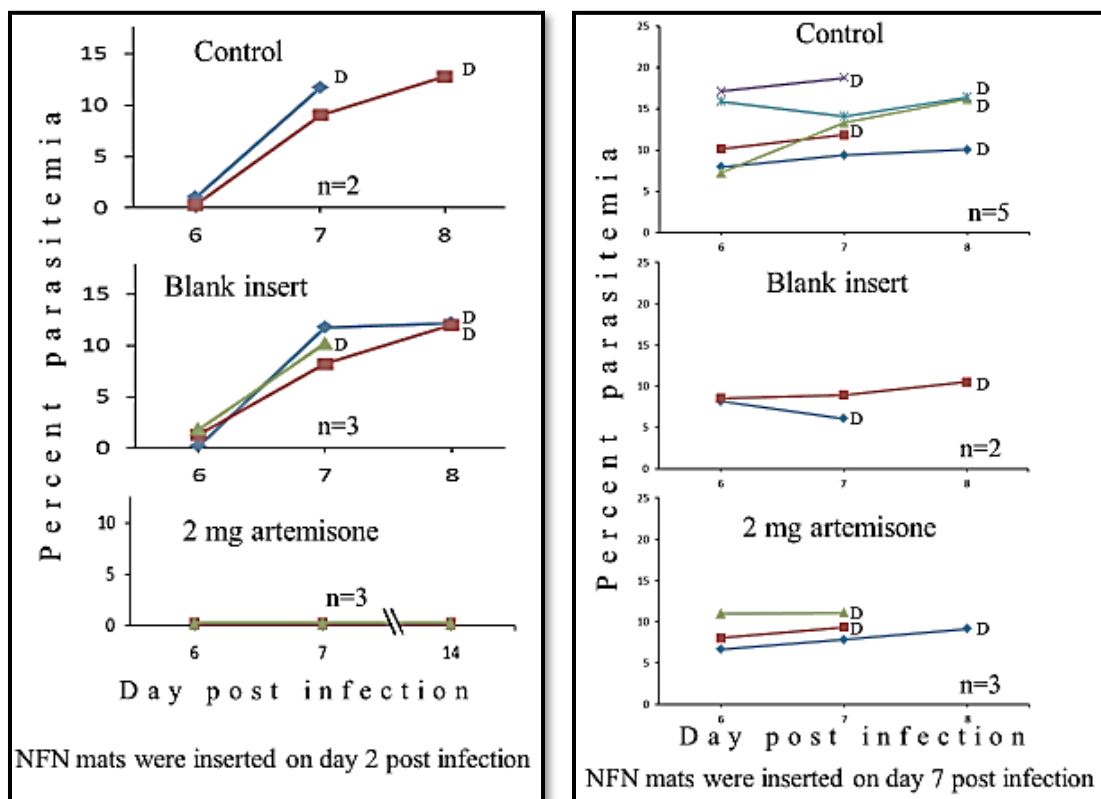
Figure 47 Insertion of ART loaded NFN after 2- and 7-days post-infection, the dose of ART: 2 mg

Experiments were repeated for ART loaded films with 2 mg ART on mice with 7dayspost-infection (Fig. 48). Interestingly, after the insertion of ART loaded films, the mice could be partially cured, and infection could be decreased meaningfully. The life of the infected mice could be prolonged, and even 2 mice from 5 mice could be cured. Therefore, these studies confirmed that 2 mg ART could be an effective dose against infection. These studies confirmed that the more retarded release obtained from thick films supports the curing process during a prolonged release period since ART loaded NFN, which produce faster release are the better choice for the treatment of infected mice, which are freshly (after 1- or 2-days post-infection) infected.

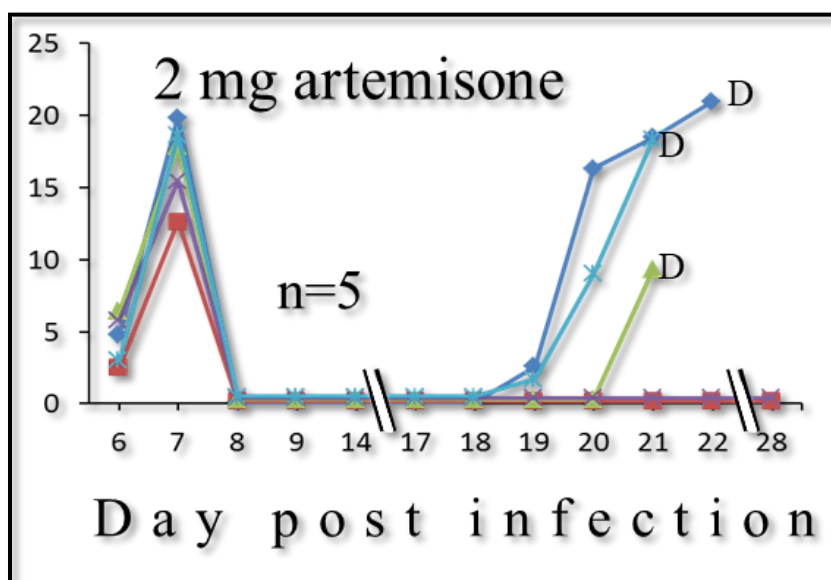**Figure 48** Insertion of ART loaded film after 7-days post-infection, the dose of ART: 2 mg

3.13.1 Administration by infusion therapy

The main issues with artemisinins are low bioavailability, short half-life, low solubility, and stability in an aqueous medium. The decomposition of artemisinins in the aqueous medium is critical as the physiological effect of the decomposition products is uncertain. ART is rather expensive and cannot be stored in the form of liquid formulations for delivery purposes, ruling out simple infusion formulations as one of the ways of controlled drug delivery. Although there are some efforts in the literature to provide controlled release of artemisinins in vitro from nanovesicles and solid lipid particles, due to the complexity of the situation, the systems are far away from any practical utility. Due to the complexity of the problem and restrictions imposed by the nature of the drug, no simple solution is applicable. This is the general problem in the field of drug delivery wherein Vitro studies using various drug delivery carriers, including nanofiber nonwoven (NFN) made by electrospinning, are indicative of applicability but not transferable to actual in vivo applications.

To solve this problem, we decouple the programmed drug release from the physiological environment. In this work, we suggest that the combination of the advantage of precise and reproducible programmed release from NFN in vitro with the drug delivery infusion system is very beneficial (Fig. 49).
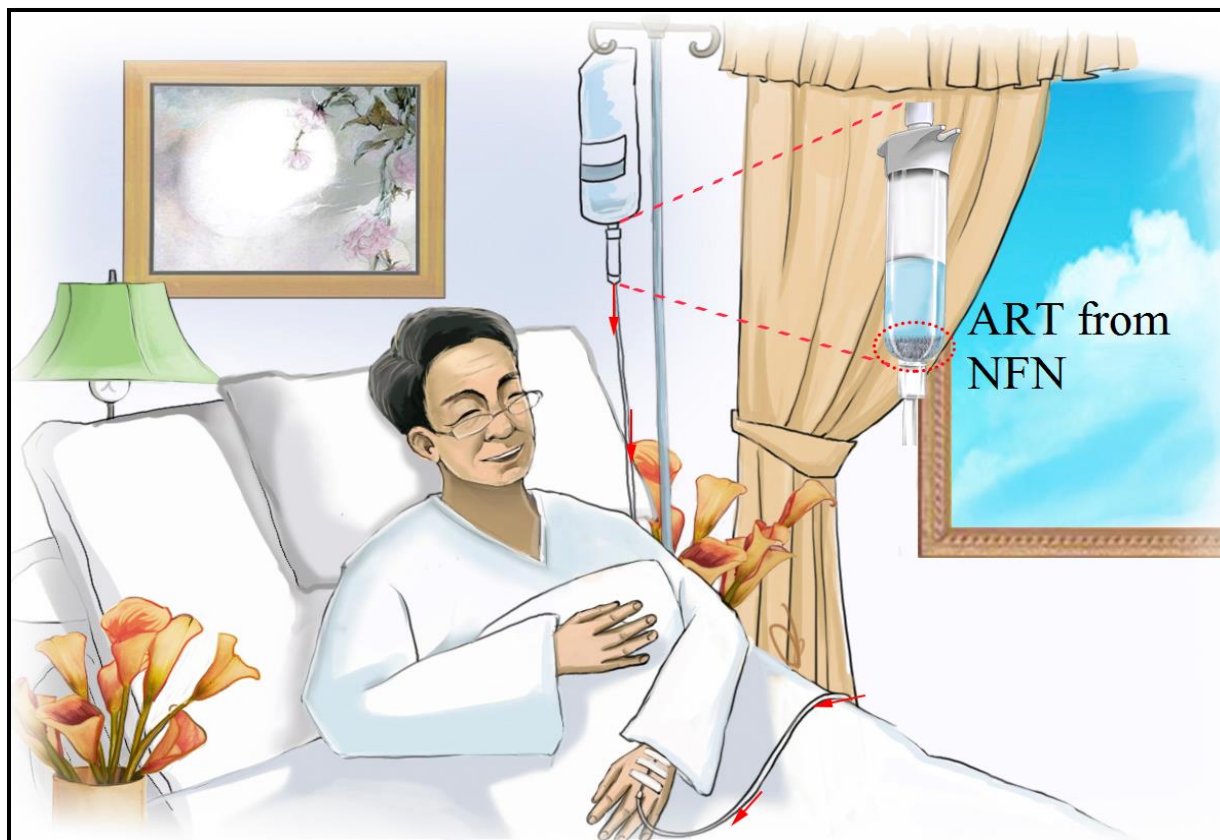
Figure 49 The depiction of the concept of programmed drug release from drug-loaded polymeric nanofiber nonwoven carrier placed in the drip chamber of an infusion system [120]; [*Creative Commons Attribution License; Permission is not required for academic or commercial reuse.*]

In our system, the control over drug release is achieved outside the physiological environment by placing ART-loaded NFN in the drip chamber of an infusion system, which can release ART in an adjustable manner. The ART-loaded NFN were additionally coated with the biocompatible polymer poly(*p*-xylylene) (PPX) by chemical vapor deposition (CVD) to control the release profile and stability of the drug in infusion medium by confinement. Our drug-delivery concept also takes care of the low solubility of ART in aqueous media by using an infusion medium with appropriate surfactant (Tween 80) helping the release of the hydrophobic drug. The maximum solubility of ART could be

increased linearly by increasing the quantity of the surfactant (Tween 80), as shown in additional experiments (Fig. 50).
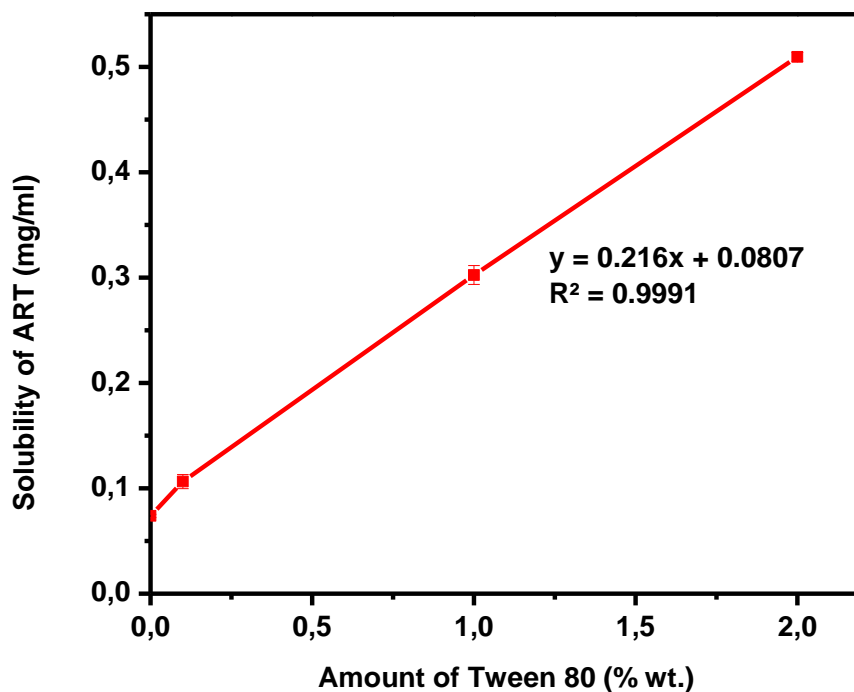
Figure 50 Increasing the solubility of ART in the aqueous media by addition of Tween 80 as a biocompatible solubilizer.

Our concept and setup are rather simple and could be manufactured under sterile conditions by the placement of the ART loaded NFN in the drip chamber of the infusion set. Programming of ART release and the dose was accomplished by the management of the flow rate, the formulation of the infusion medium, and the amount of ART in NFN placed in the drip chamber.

First of all, the amount of drug released and release profile could be controlled by changing the flow rate of the infusion medium (0.9% w/v saline solution with 1 wt.% biocompatible surfactant (Tween 80)) from the ART-loaded NFN. The lower flow rate (0.083 mL min^{-1}) avoided burst release, and the release of the drug was completed in ≈5.5 h. Whereas, the higher flow rate (0.23 mL min^{-1}) led to the release of more than 20 wt.% a drug already in the first 30 min and the drug release was completed in ≈3 h (Fig. 51a).

Further, at a constant flow rate of the infusion medium, the drug release profile could be changed by using different concentrations of surfactant in the medium (Fig. 51b). The amount of Tween 80 affects the solubility of the drug and hence the release profile. Therefore, the maximum dose of ART eluting out could be well controlled by the amount of Tween 80 in the infusion medium, which is critical as overdoses of ART would be harmful. The released drug could be sustained at a constant amount for more than 5 h on using the low concentrations of Tween 80 (0.5 wt.%) at a flow rate of 0.083 mL min^{-1} besides avoiding the burst release. In this case, a relatively linear increase in the cumulative release curve from 1 to 6 h could be observed (Fig. 51c). The sustained release of ART could be further extended from ≈7 to 14 h by increasing the mass of drug-loaded NFN in the drip chamber (Fig. 51c).

The release profile could also be changed by an additional PPX coating on the NFN without a change of the amount of ART in the NFN (Fig. 51d). Under similar conditions (infusion medium: 0.5 wt.% Tween 80; flow rate: 0.083 mL min^{-1}), the drug release experiment using ART powder in the drip chamber of an infusion system led to not the controllable release of ≈30 wt.% drug in 15 h. The release curve showed a fast release

regime in which about 20 wt.% of the drug was released in about 7 h, followed by a prolonged release. The faster release, in the beginning, might be due to the dissolution of small ART crystals. The dissolution of hydrophobic drugs is dependent on the crystal size; smaller crystals dissolve faster than more significant.
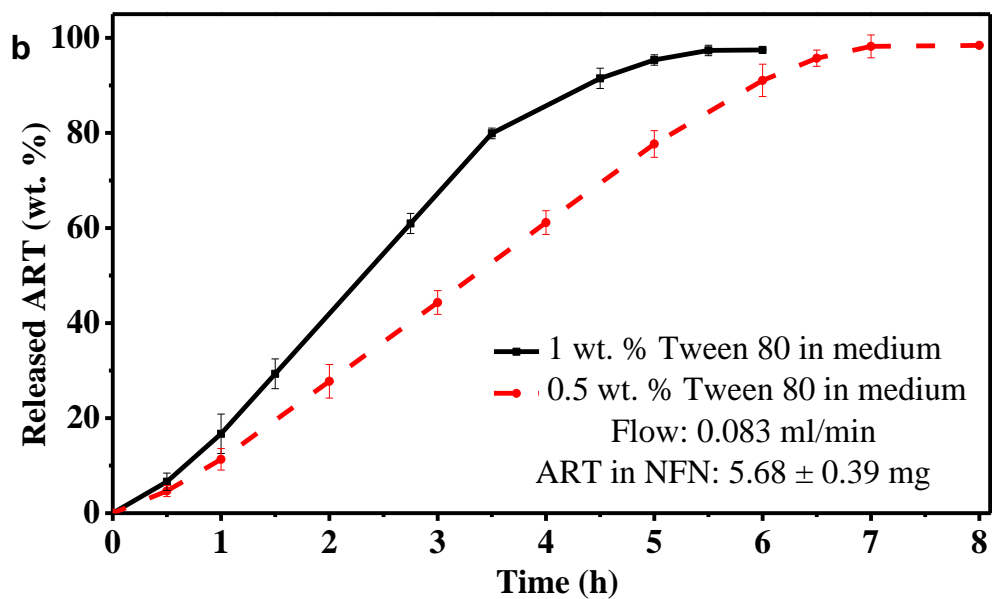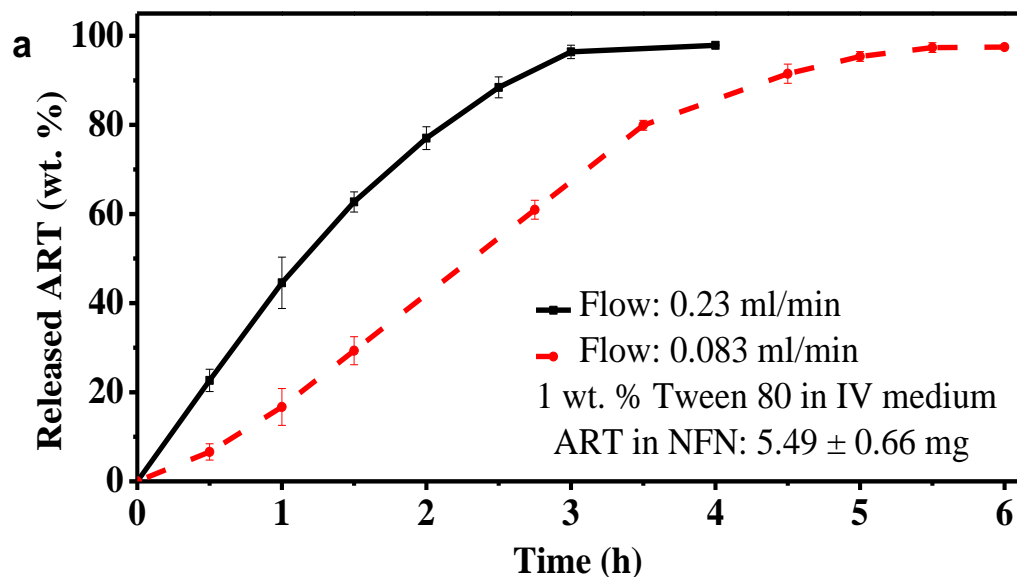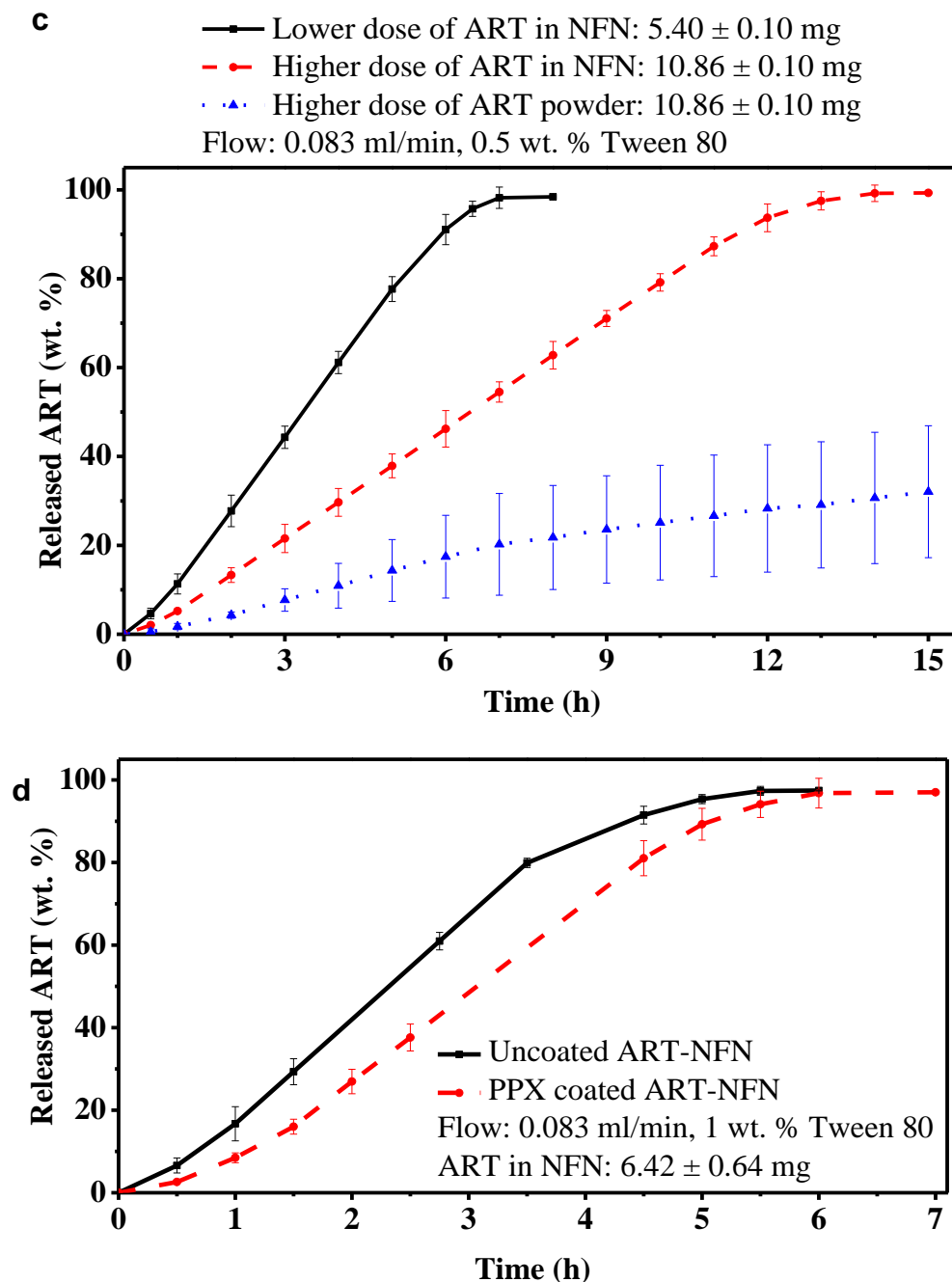
Figure 51 The programmed release of ART from NFN by infusion system, ART content for all formulation: 12.5 wt.%. a) The effect of flow rates on ART release from NFN at two different flow rates of 0.083 and 0.23 mL min−1, the medium contains 1 wt% Tween 80. Mean amounts of ART in NFN: 5.49 ± 0.66 mg. b) The effect of the amount of Tween 80 on ART release from NFN at the adjusted flow rate of 0.083 mL min−1, but intravenous (IV) media include 0.5% and 1% Tween 80. Mean amounts of ART in NFN: 5.68 ± 0.39 mg. c) The effect of doses of the drug on release behavior of ART from NFN, lower doses: 5.40 ± 0.10 mg drug and higher doses: 10.86 ± 0.10 mg, the comparison was also done by putting 10.86 mg of ART powder in the drip chamber (blue curve) and d) the effect of PPX coated layer with a thickness of 68.5 ± 10 nm on ART release from NFN, mean amounts of ART in NFN: 6.42 ± 0.64 mg.

Chapter 4

Experimental part

4. Experimental part

4.1 Materials

ε- Caprolactone (CL) was purchased from Alfa Aesar and was dried over calcium hydride (Merck Co.) for 24 hours and purified by vacuum distillation. α-Hydroxy-ω-methoxy-poly(ethylene glycol) (MPEG, Mw: 5000) from Aldrich Co. was dried out in a vacuum oven at 40 °C for 2 hours. The poly(ethylene oxide) (PEO, Mw: 900,000) was purchased from Acros Co., and it was used in dried form after drying in a vacuum oven at 40 °C for 2 hours. Stannous octoate [$Sn(Oct)_2$] and sodium dodecyl sulfate (SLS), Tween 80, pyridine, THF, methylene chloride from Sigma-Aldrich and formic acid from Fluka were used as received. Parylene N was used as received (Specialty Coating Systems, SCS). ART was donated by CIPLA and used without further purification.

4.2 Synthesis of PCL₁₆₅₀₀-b-MPEG₅₀₀₀

The biodegradable diblock copolyester PCL16500-b-MPEG5000 (the subscript describes the Mn of the polycaprolactone (PCL) block and MPEG according to NMR analysis) (PCL-MPEG) was synthesized according by ring-opening of ε-caprolactone catalyzed by stannous octoate in the presence of α-methoxy-ω-hydroxy-poly (ethylene glycol) (MPEG) as a macroinitiator. The reaction was started with 13.95 gr caprolactone and 4.65 gr MPEG. The mixture was heated up to 130 °C, and then 30 μL catalyst had to be added to the mixture. Finally, the mixture started to form a high viscose product, which was cooled down to room temperature after 3 hours as the reaction time. For purification of the polymer, after precipitation in n-pentane, the polymer was extracted with water to remove the water-soluble parts of the product, like the oligo PCL-b-MPEG and unreacted MPEG.
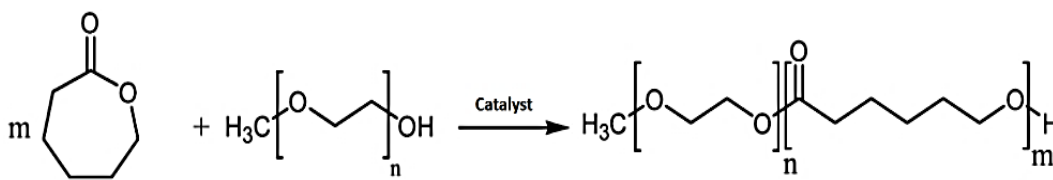
4.3 Degradation studies of ART in an aqueous environment

The degradation studies were carried out by putting a definite amount of ART powder in 1% w/v SLS at 37 ± 0.5 °C. The amounts of ART were quantified before incubation, and then all solutions were stored in a thermostatic incubator at a temperature of 37 ± 0.5 °C and shaken at 50 rpm. 1 ml of each solution was taken out and, finally, the dissolved amounts of ART were quantified by the HPLC method, which was described previously. All experiments have been repeated three times, and mean data have been reported in this work. Relative standard deviation (RSD) for all experiments was below 2%, and they were repeatable. Our long-term studies demonstrated only 14 % ART remained after 19 days.

Storage at rel. humidity approx. 60% and temperature of 37 ± 0.5 °C

Clearance: from white to yellow
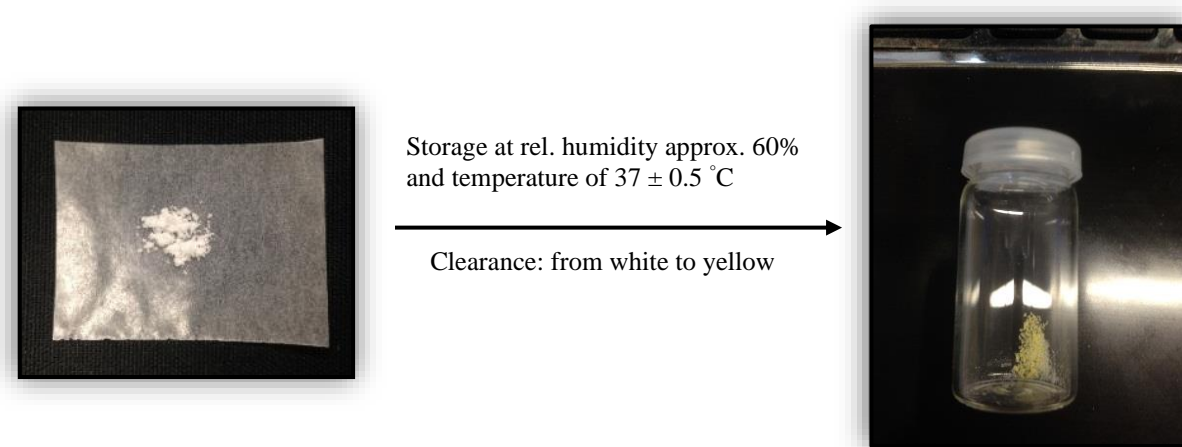
Figure 52 Change in the appearance of ART powder after two weeks of stress under a relative humidity of approx. 60% and a temperature of 37 ± 0.5 °C

4.4 Fabrication of ART loaded NFN

Drug loaded polymeric solutions composed of 15 wt. % PCL-MPEG, 2.5 wt. % pyridinium format (PF) and different amounts of ART in methylene chloride (MC) were prepared. ART quantities could be variable due to the fabrication of different drug-loaded samples with different contents of the drug. PF has been produced by mixing of 1:1 (mol: mol) pyridine and formic acid. The mixtures were protected from light and stirred at least for 5 hours at room temperature to form homogenous solutions. The solutions were electrospun with a voltage of 30 kV at a distance of 15 cm and a flow rate of 1.33 ml. hr^{-1} on aluminum foil collecting electrode. An air humidifier controlled the humidity at 18–25%, and the temperature was adjusted to 20-22 °C. PF was added to the electrospinning solution for control of the electric conductivity of the formulation. During electrospinning, PF evaporates as pyridine and formic acid and cannot be traced anymore in the deposited ART containing NFN. The increase in electrical conductivity by the addition of PF caused a significant reduction of bead formation. The integrity of ART after electrospinning was verified by solution NMR.
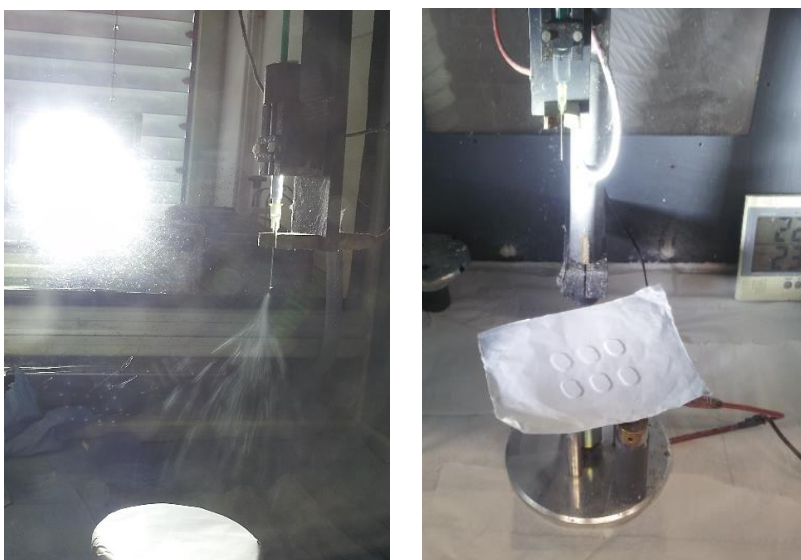
Figure 53 Fabrication of ART loaded NFN by electrospinning

4.4.1 Coating of ART loaded NFN by PPX

PPX coating was done by lab coater 2010 (SCS) using [2.2] paracyclophane (Parylene N) as a precursor, according to Gorham's method. ART loaded nanofibrous mats with the different thicknesses could be fabricated based on this method and also an internal calibration method.

Figure 54 PPX coater machine and a PPX-coated NFN mat

4.4.2 Coating of ART loaded NFN by dip-coating

One day before the coating, all weighed NFN samples were dried out in freeze-dryer and put in a desiccator. For the preparation of gelatin-coated NFN, each scaffold was dipped in the solution of gelatin (1 % and 10 % w/v in distilled water) for 20 seconds. After that, the excess coating solution droplets were wiped off from the surface of fibrous mats by glass slides. The same method was also applied for the production of dispersion coated NFN by the exception of some differences. In this case, instead of 20 seconds, the samples were dipped in dispersion for 10 seconds. Instead of a gelatin solution, the dispersions of PCL-MPEG in water by two different ratios were used. The initial dispersion involved 15 wt.% PCL-MPEG, 2.5 wt. % PEO (900,000 g/mol) in water. This dispersion was produced in this work according to previously reported work [114]. For the preparation of two dip-coating emulsions, the dispersion was added by two different ratios to water, 1:1 (dispersion 1) and 1:2 (dispersion 2) (w/w, dispersion: water). The mixtures were stirred over the night.

Figure 55 Preparation of a dip-coating solution containing an aqueous dispersion of PCL-MPEG

4.5 Fabrication of ART loaded Films

Block polymer PCL-MPEG was synthesized according to a previously described procedure. Block copolymers of PCL-MPEG were fabricated by different ratios of PCL: MPEG. To create a homogeneous mixture of PCL-b-MPEG and artemisone, different ratios of both compounds were dissolved in small amounts of tetrahydrofuran (THF; p.a. ≥ 99.9%). After all, particles were dissolved, the solvent was completely evaporated. Using a heat press at 65 °C the mixture was pressed into a polytetrafluoroethylene matrix (internal size about 0.5 ×10 × 20 mm^3) and then cooled down to room temperature under a second press at about 20 °C. After 2 min pressing, the templates were taken out and cooled down to 20 °C. The obtained films had a thickness of 500 ± 20 μm. This protocol was also used for the production of other films with 100 μm thickness by using other shaping templates (internal size: 0.1 x 10 x 20 mm). The films produced by these templates had average dimensions of 100 ± 10 μm.
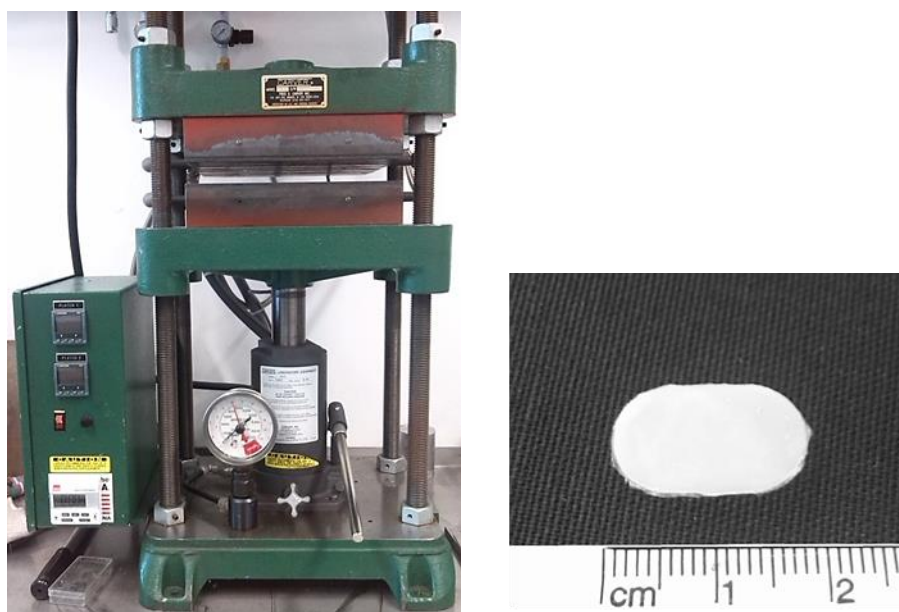
Figure 56 Heat-presser machine for fabrication of drug-loaded films

4.6 Enzymatic degradation of NFN and films fabricated from PCL-MPEG

The enzymatic degradation was made by cutting the films, and NFN mats into the small pieces with the same dimension, and the weight of each piece was recorded (m_1). All samples were dried out before recording the initial weight values. Then, each sample was placed in the vial, which was filled by a medium made of 4 ml PBS-buffer and 0.35 ml (containing 9 mg enzyme) of enzyme solution (Esterase EL-01). All vials were transferred into a shaking incubator so that the incubation took place for the specified time at 37 ± 0.5 °C and 50 rpm shaking speed. The time started with the input of the enzyme and ended with the removal of the media. After removing the media, the samples were washed several times with distilled water and freeze-dried over the night. After drying, all samples were weighed again (m_2) to get their mass-loss, according to bellow's equation:

$$\text{remained residual mass (\%)}: \frac{m_2}{m_1} \times 100$$

4.7 Water uptake by NFN and films composed of PCL-MPEG

To investigate the swelling behaviors of the carriers, the ART loaded NFN and films with known weights (m_1) were put in vials containing 10 ml distilled water (pH: neutral) and incubated for 24 hours at 37 ± 0.5 $^{\circ}$C. Finally, the water droplets on the surfaces of samples were removed with the pieces of paper, and finally, the weight of the wet samples was recorded (m_2). The swelling results were calculated according to the following equation for each sample:

$$\text{Swelling ratio (\%)}: \frac{m_2 - m_1}{m_1} \times 100$$

4.8 Loading of ART in ultralight sponges as 3D structures

The ultralight sponges were chemically prepared from poly (methylacrylate-co-methyl methacrylate-4-methacryloyloxybenzophenone).

For the loading of drug in 3D scaffolds, ART (CIPLA, India) was dissolved in tert-butanol in concentrations of 14 and 25 mg/mL. Then, 1 mL of drug solution was filled in a syringe and slowly dropped onto the precut d3.5 and d6 (10 × 10 × 5 mm) at room temperature (22 ± 1 °C) until the whole sponge was wetted by the solution. Drug-wetted sponges were put in liquid nitrogen for freezing and drying in vacuum for 24 h by a freeze-dryer. The amount of ART in the sponge was determined by a high precision analytical balance with the readability of 0.01 mg.

Figure 57 Appearance of ART loaded sponges

4.9 Fabrication of ART loaded microparticles by spray-drying

1.93-3.96 g gelatin was dissolved in 100 ml distilled water. The solution was stirred for several hours so that a homogenous solution could be gained.

Parallel, a saturated solution of ART in an aqueous medium including 1 wt. % tween 80 in distilled water has been produced. The mixture was stirred for some hours at room temperature, and then it was centrifuged and filtered. The filtered solution had a concentration of approximately 0.302 mg/ml after all experiments and all attempts. 30 ml of this solution (9.06 mg ART) was added to a gelatin solution, and the mixture was stirred for some hours. The spray drying of this mixture was done by mini spray dryer B-290 (Fig. 58).
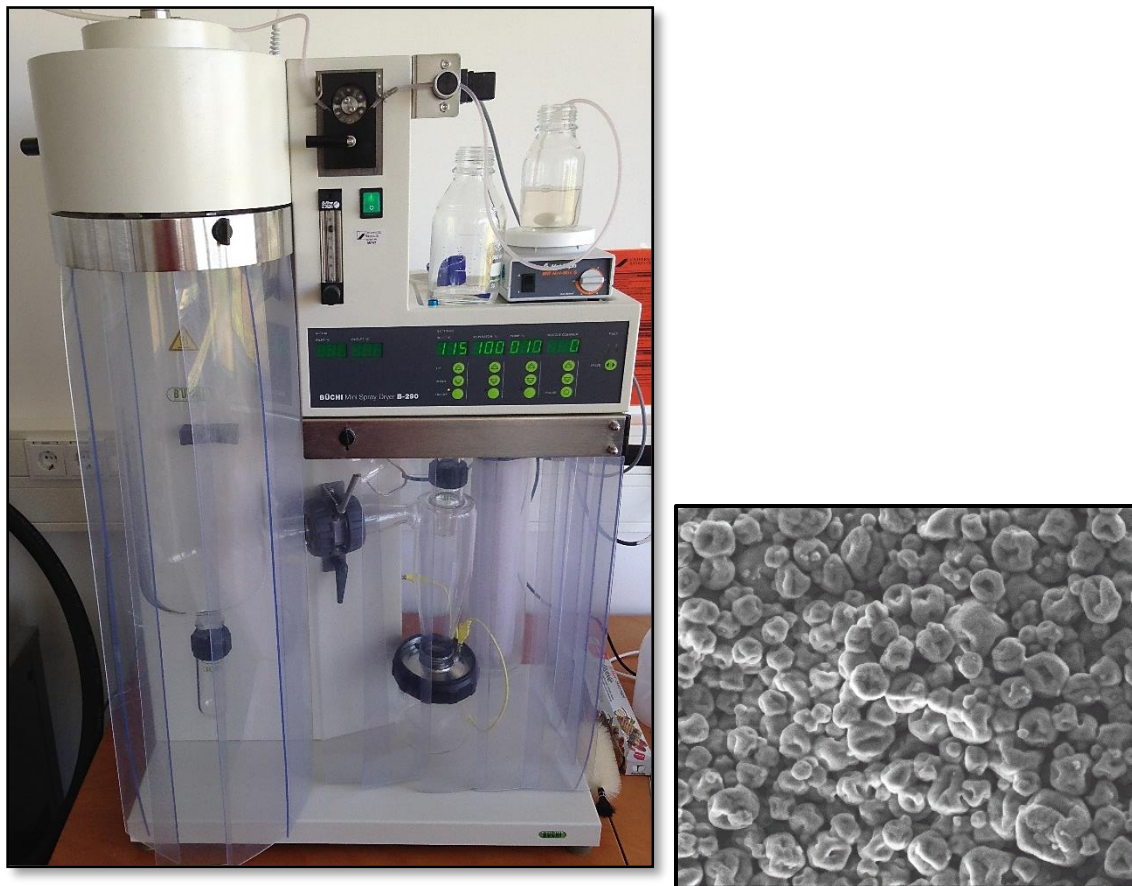
Figure 58 spray-dryer B-290

The adjusted parameters for the spray-drying of the solutions can be observed below in

Table 8.

Table 8 Adjusted instrumental parameters

Inlet temperature (º C)	115
Outlet temperature (º C)	75
Aspirator (%)	100
Pump (%)	10
Gas flow (mm)	50

Figure 59 Appearance of ART loaded gelatin microparticles

4.10 In vivo controlled release of ART

Mice were injected intraperitoneally with Plasmodium berghey ANKA. Inserts containing ART or blank inserts were introduced subcutaneously on different days post or before infection, as indicated. N represents a number of mice in the group, and D means dead. Death of mice with parasitemia below ~20% parasitemia accompanied by a typical disease is considered as the death of cerebral malaria (CM). All control mice died of CM. Each line represents a single mouse. All these experiments have been performed in the Hebrew University of Jerusalem under the supervision of Prof. Jacob Golenser.

4.11 Set-up for infusion experiments

An infusion pump from B. Braun Melsungen was used together with a standard infusion system, as shown in Fig. 60. The drip chamber was opened, equipped with the ART-loaded NFN, and closed again before the infusion experiment.

Figure 60 The infusion set-up used for the infusion experiments with ART-loaded NFN.

Chapter 5

Summary

5 Summary

Cerebral malaria (CM) is a significant reason for malarial death, and its treatment is complicated because of the role of the parasite and the baneful immunopathological response. In the face of the etiology of CM, both anti-plasmodial and anti-inflammatory treatments are essential, in addition to adjunctive therapy.

Currently, artemisinin derivatives are administrated as a first-line anti-malarial treatment. Artemisone (ART), being antiplasmodial and anti-inflammatory, was selected for the current studies. It is a lately produced artemisinin derivative with longer in vivo half-life relative to other derivatives and has a superior antiplasmodial activity. However, in mice models, repeated injections, twice a day for at least three days, are necessary for a significant anti-plasmodial effect. Artemisinin derivatives are poisonous at high concentrations that cannot be accurately controlled by the usual route of injections. Oral treatment may reduce toxicity. However, due to the very low absorption, much higher doses have to be used (limiting the use of the drugs for economic reasons). Although ART has improved pharmacokinetics compared to other artemisinins, low patient compliance may limit its use. As an alternative approach, we fabricated macromolecular carriers and incorporated the drug into such effective carriers, to enable the controlled release.

In this work, different classifications of materials based on electrospun nanofibers, polymeric films, 3D structures, and particles could be successfully applied to carry the ART. Drug molecules could be efficiently immobilized in these materials, and the drug release from these carriers could be adequately studied. Effectively, the kinetics of the ART release from macromolecular carriers could be adjusted by modification of the

carrier. Polymeric structures that contained ART were inserted subcutaneously and released the drug during at least a week in non-toxic quantities that were sufficient to prevent or delay CM in a mouse model, even when applied at a very late stage of the disease. We demonstrate as a proof-of-concept this controlled-sustained release system for safe and effective treatment of malaria, underlining the benefits of treatment of CM where a conventional mode of treatment is complicated. Similar methods could be applied for other parasites that are sensitive to artemisinins.

Until now, implantation is almost the unique suggested administration route for the delivery of drug-loaded scaffolds. Although implantation is seen as an efficient administration route, practical in vivo application possesses different complications that do not satisfy the need for programmable and straightforward drug administration. Our introduced concept presented in this work and its setup in frame of an infusion system is rather simple and could be manufactured even under sterile conditions by the placement of the ART-loaded polymeric carriers in the drip chamber of an infusion set. Overall, we could decouple the programmed release of drugs from the influence of the physiological environment and provided a precise and reproducible drug release with different release profiles for a drug with problems of low bioavailability, low solubility, and instability in an aqueous medium.

Each type of the carriers offers different horizons for application. For example, in our studies, we could also successfully apply the ultra-light polymeric sponges as another classification of the macromolecular carriers for the delivery of ART. Polymeric fibrous sponges have been successfully used as a carrier system for the programmed release of the antimalarial drug ART. The extremely high pore volume of the sponges enables a

very high loading capacity of ART. In contrast and oppositely, the polymeric films as other classification of the carrier cannot offer such porosity characteristics but the rate of the drug release can be efficiently retarded. Furthermore, microparticles as another kind of carries could be investigated for delivery of ART. ART loaded gelatin microparticles could be successfully produced by spray-drying technique, and an accelerated rate of drug release could be achieved.

Concretely in this Ph.D. work, a wide range of drug release behaviors not only in form of retarded release kinetics but also in increased (or even burst) form of release kinetics could be explicitly investigated and followed. The controlling handles responsible for a particular release profile are precisely under control (or better called managable) through the smart design and controlling of the macromolecular carries for delivery of the drug molecules.

The ART-loaded polymeric structures provide an optimal platform for precise programmed drug release, which could also be applied in the future particularly for other hydrophobic drugs. For programmable release profiles, the smart design of the carries and furthermore optimization (such as coating) are essential and versatile enough as they provide excellent control of preparation, handling, and mass transfer. This work presents not only fundamental studies based on using the macromolecular carriers for the treatment of Malaria but also tries to offer a new paradigm for the programmed drug release from macromolecular structures.

Chapter 6

Zusammenfassung

6 Zusammenfassung

Zerebrale Malaria (CM) ist ein wesentlicher Grund für den Malaria-Todesfälle, und ihre Behandlung ist aufgrund der Rolle des Parasiten und der verbannten immunopathologischen Reaktion kompliziert. Angesichts der Ätiologie von CM sind neben der Zusatztherapie sowohl anti-plasmodiale als auch entzündungshemmende Behandlungen unerlässlich.

Derzeit werden Artemisininderivate als Erstbehandlung gegen Malaria verabreicht. Artemison (ART), das antiplasmodial und entzündungshemmend ist, wurde für die aktuellen Studien ausgewählt. Es ist ein kürzlich hergestelltes Artemisinin-Derivat mit einer längeren in vivo-Halbwertszeit im Vergleich zu anderen Derivaten und weist eine überlegene antiplasmodiale Aktivität auf. In Mäusemodellen sind jedoch wiederholte Injektionen zweimal täglich für mindestens drei Tage erforderlich, um eine signifikante antiplasmodiale Wirkung zu erzielen. Artemisininderivate sind in hohen Konzentrationen giftig, die auf dem üblichen Injektionsweg nicht genau kontrolliert werden können. Die orale Administration kann die Toxizität verringern. Aufgrund der sehr geringen Absorption müssen jedoch viel höhere Dosen verwendet werden, was die Verwendung der Arzneimittel aus wirtschaftlichen Gründen einschränkt. Obwohl ART die Pharmakokinetik im Vergleich zu anderen Artemisininen verbessert hat, kann eine geringe Compliance des Patienten die Verwendung einschränken.

Als alternativen Ansatz stellten wir makromolekulare Träger her und bauten das Arzneimittel in solche wirksamen Träger ein, um die kontrollierte Freisetzung zu ermöglichen.

In dieser Arbeit konnten verschiedene Klassifikationen von Materialien auf der Basis von elektrogesponnenen Nanofasern, Polymerfilmen, 3D-Strukturen und Partikeln erfolgreich angewendet werden, um die ART zu tragen. Arzneimittelmoleküle können in diesen Materialien effizient immobilisiert werden, und die Arzneimittelfreisetzung aus diesen Trägern kann dann angemessen untersucht werden. Effektiv konnte die Kinetik der ART-Freisetzung von makromolekularen Trägern durch Modifikation des Trägers eingestellt werden.

Polymerstrukturen, die ART enthielten, wurden subkutan inseriert und setzten das Arzneimittel während mindestens einer Woche in nichttoxischen Mengen frei, die ausreichten, um CM in einem Mausmodell zu verhindern oder zu verzögern, selbst wenn es in einem sehr späten Stadium der Krankheit angewendet wurde. Als Proof-of-Concept demonstrieren wir dieses System mit kontrollierter verzögerter Freisetzung zur sicheren und wirksamen Behandlung von Malaria und unterstreichen die Vorteile der Behandlung von CM, wenn eine herkömmliche Behandlungsmethode kompliziert ist. Ähnliche Methoden könnten für andere Parasiten angewendet werden, die gegenüber Artemisininen empfindlich sind.

Bis jetzt ist die Implantation fast der einzigartige empfohlene Verabreichungsweg für die Lieferung von arzneimittelbeladenen Gerüsten. Obwohl die Implantation als effizienter Verabreichungsweg angesehen wird, weist die praktische In-vivo-Anwendung verschiedene Komplikationen auf, die die Notwendigkeit einer programmierbaren und unkomplizierten Arzneimittelverabreichung nicht befriedigen. Unser in dieser Arbeit vorgestelltes Konzept und sein Aufbau im Rahmen eines Infusionssystems ist recht einfach und könnte auch unter sterilen Bedingungen hergestellt werden, indem die ART-

beladenen Polymerträger in die Tropfkammer eines Infusionssets eingebracht werden. Insgesamt konnten wir die programmierte Freisetzung von Arzneimitteln vom Einfluss der physiologischen Umgebung entkoppeln und eine präzise und reproduzierbare Arzneimittelfreisetzung mit unterschiedlichen Freisetzungsprofilen für ein Arzneimittel mit Problemen von geringer Bioverfügbarkeit, geringer Löslichkeit und Instabilität in einem wässrigen Medium bereitstellen.

Jeder Trägertyp bietet unterschiedliche Anwendungshorizonte. Zum Beispiel konnten wir in unseren Studien auch die ultraleichten Polymerschwämme erfolgreich als eine weitere Klassifizierung der makromolekularen Träger für die Abgabe von ART anwenden. Polymere faserige Schwämme wurden erfolgreich als Trägersystem für die programmierte Freisetzung des Malariamedikaments ART verwendet. Das extrem hohe Porenvolumen der Schwämme ermöglicht eine sehr hohe Belastbarkeit von ART. Im Gegensatz dazu und im Gegensatz dazu können die Polymerfilme als andere Klassifizierung des Trägers solche Porositätseigenschaften nicht bieten, aber die Geschwindigkeit der Arzneimittelfreisetzung kann effizient verzögert werden. Darüber hinaus könnten Mikropartikel als eine andere Art von Trägern für die Abgabe von ART untersucht werden. Mit ART beladene Gelatine-Mikropartikel konnten erfolgreich durch Sprühtrocknungstechnik hergestellt werden, und eine beschleunigte Geschwindigkeit der Arzneimittelfreisetzung konnte erreicht werden.

Konkret in dieser Ph.D. Dissertation konnte ein breites Spektrum von Wirkstofffreisetzungsverhalten nicht nur in Form einer Kinetik der verzögerten Freisetzung, sondern auch in Form einer erhöhten (oder sogar platzenden) Form der Freisetzungskinetik explizit untersucht und verfolgt werden. Die Kontrollgriffe, die für ein

bestimmtes Freisetzungsprofil verantwortlich sind, werden durch das intelligente Design und die Kontrolle der makromolekularen Träger für die Abgabe der Arzneimittelmoleküle genau kontrolliert (oder besser als handhabbar bezeichnet).

Die ART-beladenen Polymerstrukturen bieten eine optimale Plattform für eine präzise programmierte Arzneimittelfreisetzung, die auch in Zukunft insbesondere für andere hydrophobe Arzneimittel angewendet werden könnte. Für programmierbare Freigabeprofile sind das intelligente Design der Träger und darüber hinaus die Optimierung (z. B. Beschichtung) wesentlich und vielseitig genug, da sie eine hervorragende Kontrolle über Vorbereitung, Handhabung und Stoffaustausch bieten. Diese Arbeit präsentiert nicht nur grundlegende Studien, die auf der Verwendung der makromolekularen Träger zur Behandlung von Malaria basieren, sondern versucht auch, ein neues Paradigma für die programmierte Arzneimittelfreisetzung aus makromolekularen Strukturen anzubieten.

Chapter 7

Outlook

7 Outlook

The introduction of nanotechnology has changed all scientific fields, including medical, pharmaceutical, and drug delivery systems radically. Nanotechnology has provided an excellent device to pharmaceutical scientists which is supportive in developing novel formulations of existing problematic drugs. The majority of the drugs administrated for treatment of dreaded diseases such as cancer, Malaria, and Leishmaniasis have poor selectivity and severe toxicity towards normal body cells. The toxicity of such drugs can be fundamentally decreased by incorporation inside nano- and microsized carrier systems.

The presented studies in this thesis set a milestone to realize the strength and weakness points of different types of polymeric carriers for the delivery of a hydrophobic drug. Nowadays, there are many classes of the drug with the same characteristics as Artemisone.

There are some interesting scientific aspects which can be observed as potential future works:

- Application of dual or triple-drug release system by incorporation of other drug molecules such as antibiotics or anti-inflammatory agents in polymeric carriers: The incorporated drug molecules can consist of different natures in case of hydrophilicity or hydrophobicity.

- Smart drug delivery system by incorporation of drugs in thermoresponsive particles and incorporation of particles in polymeric carriers. The system can be worked smartly on time in case of requirements like urgent, vital situations such as high grades of fever.

- Drug-loaded 3D-structures offer many advantages as the polymeric carriers because of their high loading capacities. Furthermore, the shapes and forms of 3D-structures play a vital role in controlling the kinetics of the drug release. In this field, complementary studies are needed.

- Finally, as presented in this work, the introduced infusion system equipped with nanofibrous structures can be a useful device for the administration of drug-loaded nanofibers for real medical purposes. In this field, different kinds of in vivo studies are needed.

Chapter 8

Acknowledgments

8 Acknowledgments

The practical work forming the fundamentals of this Ph.D. thesis was mainly performed at the Department of Macromolecular Chemistry (MCII) of the University of Bayreuth under the guidance of Professor Dr. Andreas Greiner from September 2013, to September 2017. I thank Professor Dr. Andreas Greiner for the brilliant guidance, the fascinating subject, and the freedom while completing this thesis as well as in choosing a cooperation network.

Special thanks to Prof. Dr. Jacob Golenser for his fruitful cooperation, scientific discussions, and supporting this work with providing the in vivo and biological studies on fabricated macromolecular structures.

Many thanks to Prof. Dr. Seema Agarwal for her supporting actions to me in many stages of my Ph.D. work.

I want to acknowledge Prof. Dr. Thomas Scheibel and Prof. Dr. Rainer Schobert for taking the time and being my BayNat mentors and for supporting me during my Ph.D. time.

I would like to thank Dr. Viola Buchholz for the introduction and for helping me to have a good start in the GIP project.

Also, I would like to say my thanks to the University of Bayreuth Graduate School for financial support for my conference participation.

Very thanks to my cooperation partners and collaborators Prof. Golenser's group (special thanks to Maysa Jbarien), Prof. Charles Greenblatt, Dr. Steffen Reich, Dr. Gaigai Duan.

Chapter 9

References

9 References

[1] G. Tiwari, et al., *International Journal of Pharmaceutical Investigation* **2012**, *2*, 1-11.

[2] J. F. Coelho, et al., *EPMA Journal* **2010**, *1*, 164-209.

[3] B. Hassan*, Pharmaceutica Analytica Acta* **2012**, *3*, 137-137.

[4] N. Martinho, *Journal of Biomaterials and Nanobiotechnology* **2011**, *2*, 510-526.

[5] N. Rajgor, et al., *Systematic Reviews in Pharmacy* **2011**, *2*, 91-95.

[6] J. Folkman, et al., *Science* **1966**, *154*, 148-149.

[7] S. Senapati, et al., *Signal Transduction and Targeted Therapy* **2018**, *3*, 7-26.

[8] R. Tiwari, et al., *World Journal of Pharmaceutical Research* **2016**, *5*, 1704-1720.

[9] S. Deepu, et al., *International Journal of Pharmaceutical and Chemical Sciences* **2014**, *3*, 636-641.

[10] G. Dikmen, et al., *Journal of Materials Science and Engineering* **2011**, *5*, 468-472.

[11] N. Gujrathi, S. Pawar, *International Journal of Pharmaceutical, Chemical and Biological Sciences* **2014**, *4*, 529-536.

[12] B. Jeong, et al., *Journal of Controlled Release* **1999**, *62*, 109-114.

[13] A. J. Gavasane, H. A. Pawar, *Clinical Pharmacology and Biopharmaceutics* **2014**, *3*, 121-127.

[14] S. Hyon, *Yonsei Medical Journal* **2000**, *41*, 720-734.

[15] H. E. Gültekin, Z. Degim, *FABAD Journal of Pharmaceutical Sciences* **2013**, *38*, 107-118.

[16] Y. Zhang, et al., *Advanced Drug Delivery Reviews* **2013**, *65*, 104-120.

[17] E. Biazar, *International Journal of Polymeric Materials and Polymeric Biomaterials* **2017**, *66*, 53-60.

[18] Y. Liu, et al., *Asian Journal of Pharmaceutical Sciences* **2019**, *14*, 130-143.

[19] A. M. Al-Enizi, et al., *Nanomaterials* **2018**, *8*, 259-280.

[20] S. Agarwal, et al., *Polymer* **2008**, *49*, 5603-5621.

[21] S. Ramakrishna, et al., *materialstoday* **2006**, *9*, 40-50.

[22] Kenry, C. T. Lim, *Progress in Polymer Science* **2017**, *70*, 1-17.

[23] Su. Kalluri, et al., *RSC Advances* **2013**, *3*, 25576-25602.

[24] M. Liu, et al., *Materials Science and Engineering: C* **2017**, 76, 1413-1423.

[25] A. Haidar, et al., *Arabian Journal of Chemistry* **2018**, *11*, 1165-1188.

[26] X. Wang, et al., *Materials Today* **2013**, *16*, 229-241.

[27] Q. P. Pham, et al., *Tissue Engineering* **2006**, *12*, 1197-1211.

[28] D. Yu, et al., *Health* **2009**, *1*, 67-75.

[29] Y. J. Son, et al., *Archives of Pharmaceutical Research* **2014**, *37*, 69-78.

[30] I. J. Barrientos, et al., *International Journal of Pharmaceutics* **2017**, *517*, 329-337.

[31] A. A. Almetwally, et al., *Journal of the Textile Association* **2017**, *78*, 5-14.

[32] S. Watanabe, et al., *Colloids and Surfaces A: Physicochemical and Engineering Aspects* **2012**, *399*, 83-91.

[33] A. Greiner, J. H. Wendorff, *Angewandte Chemie International Edition* **2007**, *46*, 5670-5703.

[34] Z. Huang, et al., *Composites Science and Technology* **2003**, *63*, 2223-2253.

[35] H. Homayoni, et al., *Carbohydrate Polymers* **2009**, *77*, 656-661.

[36] M. Lin, et al., *Journal of Biomedical Materials Research – Part B: Applied Biomaterials* **2009**, *90*, 939-944.

[37] M. Barde, et al., *Journal of Applied Polymer Science* **2018**, *135*, 46467-46477.

[38] J. Boateng, et al., *BioMed Research International* Article ID 198137

http://dx.doi.org/10.1155/2013/198137.

[39] U. Westedt, et al., *Journal of Controlled Release* **2006**, *111*, 235-246.

[40] S. E. Moulton, G. Wallace, *Journal of Controlled Release* **2014**, *193*, 27-34.

[41] C. Korte, J. Quodbach, *AAPS PharmSciTech* **2018**, *19*, 3333-3342.

[42] G. Duan, A. R. Bagheri, S. Jiang, J. Golenser, S. Agarwal, A. Greiner, *Biomacromolecules* **2017,** *18,* 3215.

[43] J. I. Hare, et al., *Advanced Drug Delivery Reviews* **2017**, *108*, 25-38.

[44] J. Chen, et al., *Chemical Engineering Science* **2015**, *125*, 20-24.

[45] S. R. Mudshinge, et al., *Saudi Pharmaceutical Journal* **2011**, *19*, 129-141.

[46] M. J. Abdekhodaie, et al., *Chemical Engineering Science* **2015**, *125*, 4-12.

[47] P. L. Soti, et al., *European Polymer Journal* **2015**, *68,* 671-679.

[48] S. Al-Qadi, C. Remunan-Lopez, *Polymer* **2014**, *55*, 4012-4021.

[49] T. Peng et al., *Scientific Reports* **2017**, *7,* 46517.

[50] A. S. Hoffman, *Journal of Controlled Release* **2008**, *132*, 153-163.

[51] K. J. Rambhia, P. X. Ma, *Journal of Controlled Release* **2015**, *219*, 119-128.

[52] T. Nakajima, et al., *Journal of Pharmaceutical Sciences* **2018**, *107*, 1896-1902.

[53] P. I. Lee, C. Kim, *Journal of Controlled Release* **1991**, *16*, 229-236.

[54] F. M. Carbinatto, et al., *Asian Journal of Pharmaceutical Sciences* **2014**, *9*, 27-34.

[55] P. Colombo, et al., *Journal of Controlled Release* **1996**, *39*, 231-237.

[56] C. Ding, Z. Li, *Materials Science and Engineering C* **2017**, *76*, 1440-1453.

[57] P. Lee, *Journal of Controlled Release* **1986**, *4*, 1-7.

[58] N. J. Chang, K. J. Himmelstein, *Journal of Controlled Release* **1990**, *12*, 201-212.

[59] A. Y. Polishchuk, et al., *Polymer Science U.S.S.R.* **1990**, *32*, 2117-2123.

[60] J. Siepmann, et al., *Journal of Controlled Release* **1999**, *60*, 379-389.

[61] Y. Aso, et al., *Journal of Controlled Release* **1994**, *31*, 33-39.

[62] L.K. Chiu, et al., *International Journal of Pharmaceutics* **1995**, *126*, 169-178.

[63] J. Heller, *Journal of Controlled Release* **1985**, *2*, 167-177.

[64] R. P. Batycky, *Journal of Pharmaceutical Sciences* **1997**, *86*, 1464-1477.

[65] S. S. Shah, et al., *Journal of Pharmaceutical Sciences* **1992**, *18*, 261-270.

[66] C.A. Gifligan, A. Li Wan Po, *International Journal of Pharmaceutics* **1991**, *73*, 51-68.

[67] C. G. Pitt, et al., *Journal of Pharmaceutical Sciences* **1979**, *68*, 1534-1538.

[68] H. Lapidus, N. G. Lordi, *Journal of Pharmaceutical Sciences* **1966**, *55*, 840-844.

[69] T. Hu, et al., *ACS Applied Material and Interfaces* **2015**, *7*, 11695-11712.

[70] J. H. Lee, Y. Yeo, *Chemical Engineering Science* **2015**, *125*, 75-84.

[71] C. Fornaguera, M. J. García-Celma, *Journal of Personalized Medicine* **2017**, *7*, 12-31.

[72] A. Anselmo, S. Mitragotri, *Bioengineering & Translational Medicine* **2016**, *3*, 10-29.

[73] B. Joob, V. Wiwanitkit, *Medical Journal of Dr. Patil University* **2017**, *10*, 401-405.

[74] F. Haghiralsadat, et al., *Chemical Biology & Drug Design* **2017**, *90*, 368-379.

[75] T. Daemen, et al., *International Journal of Cancer* **1995**, *61*, 716-721.

[76] U. Bulbake, et al., *Pharmaceutics* **2017**, *9*, 12-44.

[77] D. Yuan, et al., *Thoracic Cancer* **2012**, *3*, 341-347.

[78] B. Borresen, et al., *Veterinary and Comparative Oncology* **2018**, *16*, E1-E15.

[79] C. I. Frennesson, S. E. G. Nilsson, *Acta Ophthalmologica Scandinavica* **2004**, *82*, 645-650.

[80] D. E. Loy, et al., *International Journal for Parasitology* **2017**, *47*, 87-97.

[81] A. F. Cowman, et al., *Cell* **2016**, *167*, 610-624.

[82] R. M. Kaushik, et al., *International Journal of Infectious Diseases* **2009**, *13*, e292-294.

[83] I. Kleinschmidt, et al., *Tropical Medicine and International Health* **2001**, *6*, 779-786.

[84] Y. Ye, et al., *Tropical Medicine and International Health* **2013**, *18*, 219-221.

[85] H. Charles, J. Godfray, *Journal of Animal Ecology* **2013**, *82*, 15-25.

[86] R. Geldhill, et al., *Concurrency and Computation: Practice and Experience* **2008**, *20*, 225-238.

[87] A. Strang, et al., *British Journal of Obstetrics and Gynecology* **1984**, *91*, 399-403.

[88] C. J. F. Fontes, S. Munhoz, *Tropical Medicine and International Health* **1996**, *1*, 820-823.

[89] T. Mori, M. Hirai, T. Mita, *Scientific Reports* **2019**, *9*, 1768-1775.

[90] R. A. Jones, et al., *European Journal of Medicinal Chemistry* **2015**, *97*, 335-355.

[91] S. E. Haas, et al., *International Journal of Antimicrobial Agents* **2009**, *34*, 156-161.

[92] G. Watt, et al., *Transactions of the Royal Society of Tropical Medicine and Hygiene* **1988**, *82*, 205-208.

[93] E. Abolghasemi, et al., *Asian Pacific Journal of Tropical Biomedicine* **2012**, *2*, 311-314.

[94] K. C. Kain, *Wilderness and Environmental Medicine* **1995**, *6*, 307-324.

[95] R. A. Bayoumi, et al., *Acta Tropica* **1989**, *46*, 157-165.

[96] A. M. Thu, et al., *FEBS*, **2017** *284*, 2569-2578.

[97] Y. Tu, *Angewandte Chemie International Edition* **2016**, *55*, 2-19.

[98] R. J. Maude, *Drug Development Research* **2010**, *71*, 12-19.

[99] E. M. B. El Maggar, *Journal of Applied Pharmaceutical Science* **2012**, *2*, 77-91.

[100] Y. K. Wong, et al., *Medicinal Research Reviews* **2017**, *37*, 1492-1517.

[101] S. R. Meshnick, *International Journal for Parasitology* **2002**, *32*, 1655-1660.

[102] A. Shandilya, et al., *Scientific Reports* **2013**, *3*, 2513-2519.

[103] U. P. Okorji, O. A. Olajide, *Bioorganic & Medicinal Chemistry* **2014**, *22*, 4726–4734.

[104] A. Presser, et al., *Monatshefte für Chemie* **2017**, *148*, 63-68.

[105] Y. Liu, et al., *Archives of Pharmaceutical Research*, **2012**, *35*, 1525-1531.

[106] T. D. Nguyen, et al., *The Lancet Global Health* **2015**, *3*, e758-766.

[107] S. Triemer, et al., *Angewandte Chemie International Edition* **2018**, *57*, 5525-5528.

[108] D. Kopetzki, et al., *Chemistry – A European Journal* **2013**, *19*, 5450 – 5456.

[109] B. Kazaz, et al., *POMS* **2016**, *25*, 1576-1600.

[110] Y. Wu, et al., *ChemMedChem* **2016**, *11*, 1-13.

[111] R. K. Haynes, et al., *Angewandte Chemie* **2006**, *118*, 2136-2142.

[112] J. H. Waknine-Grinberg, *Malaria Journal* **2010**, *9*, 227-242.

[113] L. Vivas, et al., *Journal of Antimicrobial Chemotherapy* **2007**, *59*, 658-665.

[114] K. Bubel, et al., *Macromolecules* **2013**, *46*, 7034-7042.

[115] H. Danafar, *Cogent Medicine* **2016**, *3*, 1142411.

[116] P. Hanefeld, et al., *Macromolecular Chemistry and Physics* **2010**, *211*, 265-269.

[117] P. Knöös, et al., *Results in Pharma Sciences* **2013**, *3*, 7-14.

[118] S. Kalepu, V. Nekkanti, *Acta Pharmaceutica Sinica B* **2015**, *5*, 442-453.

[119] V. P. Shah, et al., *International Journal of Pharmaceutics* **1995**, *125*, 99-106.

[120] A. Bagheri, S. Agarwal, J. Golenser, A. Greiner, *Global Challenges* **2017**, *1*, 1600011.

(Eidesstattliche) Versicherungen und Erklärungen

(§ 9 Satz 2 Nr. 3 PromO BayNAT)

Hiermit versichere ich eidesstattlich, dassich die Arbeit selbstständig verfasst und keine anderen als die von mir angegebenen Quellen und Hilfsmittel benutzt habe (vgl. Art. 64 Abs. 1 Satz 6 BayHSchG).

(§ 9 Satz 2 Nr. 3 PromO BayNAT)

Hiermit erkläre ich, dass ich die Dissertation nicht bereits zur Erlangung eines akademischen Grades eingereicht habe und dass ich nicht bereits diese oder eine gleichartige Doktorprüfung endgültig nicht bestanden habe.

(§ 9 Satz 2 Nr. 4 PromO BayNAT)

Hiermit erkläre ich, dass ich Hilfe von gewerblichen Promotionsberatern bzw. -vermittlern oder ähnlichen Dienstleistern weder bisher in Anspruch genommen habe noch künftig in Anspruch nehmen werde.

(§ 9 Satz 2 Nr. 7 PromO BayNAT)

Hiermit erkläre ich mein Einverständnis, dass die elektronische Fassung meiner Dissertation unter Wahrung meiner Urheberrechte und des Datenschutzes einer gesonderten Überprüfung unterzogen werden kann.

(§ 9 Satz 2 Nr. 8 PromO BayNAT)

Hiermit erkläre ich mein Einverständnis, dass bei Verdacht wissenschaftlichen Fehlverhaltens Ermittlungen durch universitätsinterne Organe der wissenschaftlichen Selbstkontrolle stattfinden können.

....

Ort, Datum, Unterschrift